PULSE-DISCHARGE TECHNIQUE FOR ENHANCED BATTERY PERFORMANCE IN A HYBRID ENERGY STORAGE SYSTEM WITH SUPERCAPACITOR IN ELECTRIC VEHICLE POWERTRAIN

HSU MYAT NAING

A THESIS SUBMITTED IN PARTIAL FULFILLMENT

OF THE REQUIREMENT FOR THE DEGREE OF

MASTER OF ENGINEERING IN AUTOMOTIVE AND ADVANCED TRANSPORTATION ENGINEERING

SCHOOL OF ENGINEERING

KING MONGKUT'S INSTITUTE OF TECHNOLOGY LADKRABANG

2023

KMITL-2024-EN-M- 277-183

TITLE	Pulse-discharge technique for enhanced battery performance in a hybrid energy storage system with supercapacitor in electric vehicle powertrain
NAME	Ms.Hsu Myat Naing
STUDENT ID	64601176
DEGREE	Master of Engineering
PROGRAM	Automotive and Advanced Transportation Engineering
ACADEMIC YEAR	2023
THESIS ADVISOR	Asst.Prof. Dr. Chinda Charoenphonphanich
THESIS CO-ADVISOR	Prof. Dr. Masaki Yamakita

ABSTRACT

Electric vehicles (EVs) need energy storage with the highest energy density for long-term use. When accelerating, the battery pack is not able to handle the sudden energy consumption and performs worse because of peak utilization. Therefore, adding additional storage devices like supercapacitors can offer the necessary quick dynamic response. A Hybrid Energy Storage System (HESS) is a power system that utilizes two or more energy storage device by utilizing supercapacitors as energy support when there is a surge in current both during charge and discharge and the battery as the primary energy storage provider can optimize energy utilization on electric vehicles. In this work, the proposed method of pulse discharging at different frequencies was analyzed to control the energy management between battery and supercapacitor. To analyze the discharge energy and capacity of batteries by using pulse current method and to analysis characteristics at various switching frequencies, an experimental approach was first performed. Furthermore, to design the Hybrid Energy Storage System, pulse current algorithm was applied for power sharing algorithm. That system was designed in MATLAB/Simulink as validation and the system was tested at NEDC and WLTC driving cycle with switching frequencies ranging from 200Hz to 1000Hz. Both the experimental and simulation results show that pulse current discharging produced higher discharge energy due to the recovery of energy during the rest, and it is observed that lower switching frequencies facilitate achieving higher discharge energy. Regarding the simulation model, it is observed that the hybrid energy storage system with pulse current algorithm generates power in accordance with the dynamic power demands by the load. It is also observed that high switching frequencies develop losses in some areas of supercapacitors and batteries power. The results also highlight that HESS with pulse current power sharing method at low switching frequency generated a higher output power than at high switching frequencies.

Keywords: Pulse discharging, switching frequencies, Hybrid energy storage system, regenerative energy, MATLAB/SIMULINK

ACKNOWLEDGEMENTS

This master thesis is financially supported by King Mongkut's Institute of Technology Ladkrabang and National Science and Technology Development Agency (NSTDA). Firstly, I would like to express my gratitude to National Science and Technology Development Agency (NSTDA) for selecting me as a full scholarship recipient and enabling me to attend King Mongkut's Institute of Technology Ladkrabang to pursue a Master of Automotive Engineering degree.

My heartfelt appreciation goes to my dedicated supervisor, Asst. Prof. Dr. Chinda Charoenphonphanich from King Mongkut's Institute of Technology Ladkrabang, whose unwavering support and guidance have been the driving force behind this journey of my graduate study. I am also deeply grateful to Dr.-Ing. Manop Masomtob from National Science and Technology Development Agency, Thailand, for giving me invaluable advice and guidance throughout my research.

Furthermore, I wish to extend my thanks to Prof. Dr. Masaki Yamakita from Tokyo Institute of Technology, Japan, for his advice and support.

Moreover, I am thankful to my seniors, Mr. Pera Tanateerapong who supported and helped me a lot in performing experiments through my research journey. I also express my thanks to my friend, Lwin Yamon Phyo for sharing useful information and helping me in the research.

Finally, I am thankful to the committee members who assessed my master's thesis during the defense. Your expert questions and comments added important technical and scientific dimensions to this work.

Hsu Myat Naing

TABLE OF CONTENTS

LIST OF FIGURES

LIST OF TABLES

ABBREVIATIONS

EVs	Electric vehicles
Li-ion	lithium-ion
HEVs	Hybrid Electric Vehicles
SCs	Supercapacitors
HESS	Hybrid Energy Storage System
SOC	State of Charge
OCV	Open Circuit Voltage
CC	Constant Current
CV	Constant Voltage
CCCV	Constant Current Constant Voltage

Chapter 1 Introduction

1.1 Research Background

One of the biggest issues that the world's environment is currently facing is energy conservation. It is believed that transportation will be crucial to preserving energy in the future. Future transportation options include electric vehicles (EVs), which have the potential to reduce the usage of petroleum fuels that release large amounts of carbon dioxide [1]. Electric vehicles (EVs) need energy storage with the highest energy density for long-term use and due to their huge energy storage capacity, batteries are largely employed as an energy storage unit in electric vehicles. Since lithium-ion (Li-ion) batteries have quick charging times, minimal self-discharge, and a relatively high energy density, they are commonly utilized as an energy source in hybrid electric vehicles (HEVs) and EVs. The power of the battery is the most crucial component of an electric vehicle. As battery capacity directly relates to the driving range, customers are worried about getting stuck somewhere as charging stations are hard to find [2]. Using only batteries for EV can result in reduction in battery life in certain applications. When accelerating, the battery pack is not able to handle the sudden energy consumption and performs worse because of peak utilization. Large currents are also produced via regenerative breaking, which could shorten the battery lifespan. Due to such matters, the performance of the batteries degrades over time and face the problem of aging [3]. Therefore, adding additional storage devices like supercapacitors (SCs) can offer the necessary quick dynamic response when power is suddenly required due to extreme driving conditions. Furthermore, regenerative braking energy is stored in SCs to prevent the batteries from being exposed to peak current [4]. Because of the dynamic behavior of supercapacitors and their increased lifespan, power sharing between batteries and SCs is a potential solution for improving system performance and extending the lifespan of the batteries [5]. A hybrid energy storage system (HESS) is a power system that makes use of two or more energy storage mediums, in which the battery serves as the major energy storage source, while supercapacitors are used to support power during surges in current during both charge and discharge. According to the experiment, a hybrid power system can reduce the battery's required power and increase the efficiency of braking energy recovery as SCs has the capacity to charge with quick speed [6].

Batteries are recognized as a relatively high specific energy while supercapacitors are defined as lower specific energy and high-power density. A suitable energy management system should be used since the supercapacitor and battery operate differently when charging and discharging. Supercapacitors have a higher power density than batteries, which allows them to provide and receive sudden current surges. An efficient power distribution strategy that may modify the parameters of energy storage media and electric vehicle is necessary to achieve optimized energy consumption. As a result, it requires a system that can consider the starting, normal, and

regenerative braking conditions of an electric vehicle, each of which has a unique current variation curve for energy distribution, and distribute the power supplied to the load by the hybrid energy storage system as efficiently as possible [7].

1.2 Objectives

This research aimed to achieve the following objectives.

- To analyze the discharge energy and capacity of batteries by using pulse current method
- To compare the discharge energy and capacity of batteries at various switching frequencies (200Hz,400Hz,600Hz,800hz,1000Hz) and also with constant current method
- To design the Hybrid Energy Storage System that use pulse current algorithm for power sharing
- To analyze the performance of Hybrid Energy Storage System by pulse method at various switching frequencies (200Hz,400Hz,600Hz,800hz,1000Hz)

1.3 Scope of the study

The main objective of this thesis is to analyze the hybrid energy storage between battery and supercapacitor utilized pulse discharging method for electric vehicles. The research was structured into three main components:

- Pulse discharging operation of the battery pack was performed as an experimental process in which transistor switch is controlled by an Arduino board and controls the current with pulse width modulation. To analyze the effect of different switching frequencies on characteristics of battery, several different switching frequencies and duty cycle were tested with battery pack and compare with the result with constant current discharging.
- Hybrid Energy Storage System (HESS) combining Lithium-ion batteries and supercapacitors was developed in MATLAB as validation process. Pulse discharge algorithm was developed in HESS as a power sharing method.
- The speed profile for energy consumption was based on the New European Driving Cycle (NEDC) and Worldwide Harmonized Light Vehicles Test Cycle (WLTC). The consumption energy of the transmission system and motor are neglected in this study. The power consumption rate of electric vehicles was calculated by the vehicle dynamics model considering resistance forces affecting the vehicle.

1.4 Thesis outlines

This thesis is categorized into five chapters. In Chapter 1, research background, objectives, scope of the study, and outlines of the thesis are discussed.

In Chapter 2, the related theories for this study are presented. First, the operation of lithium-ion battery and definitions of battery are explained. After that battery model and charging and discharging method of battery are explained in detail. Theories about supercapacitors and energy

consumption of electric vehicles are also presented in this chapter. The basics theories about hybrid energy storage systems are also expressed in the chapter.

In Chapter 3, the experimental setups and simulation for this study were discussed. This chapter presents the experimental setups for examining the impact of pulse discharging on lithium-ion batteries at different switching frequencies. In addition, the simulation of hybrid energy storage system in MATLAB/ SIMULINK is also presented in this chapter.

In Chapter 4, the results of conducted experiments are presented. The characteristics of batteries during pulse discharging at different switching frequencies are presented and the experimental results are compared. The results of simulation for hybrid energy storage system deployed pulse discharging are presented and compared the results tested at different switching frequencies.

In chapter 5, all the works included in this thesis are summarized and discussed the extended works in the future.

Chapter 2 Background theories

In this chapter, the background theories related to lithium-ion battery, supercapacitor, charging and discharging method and hybrid energy storage system are discussed.

2.1 Lithium-ion battery operation

Because of their great energy density, lithium-ion batteries are commonly employed in high energy applications. The functioning of the lithium-ion battery during the charging and discharging stages is covered in this section. Batteries are electrochemical devices that develop from oxidation-reduction electrochemical reactions at the electrodes of their constituent materials. Chemical energy is transformed into electrical energy by them [8]. As shown in Figure 2.1, a battery cell typically consists of two electrodes (positive and negative), a separator, electrolyte, and current collectors that are located on each side of the electrodes. The positive electrode of the battery, or cathode, is where positive ions (Li+) originate and where negative ions (e−) are accepted and the anode is considered as a negative electrode. The separator is placed between the cathode and the anode as a barrier to prevent short circuit and it should have enough porosity to let the electrolyte readily flow between two electrodes. Liquid electrolyte is filled at the space left between the electrode and separator [9].

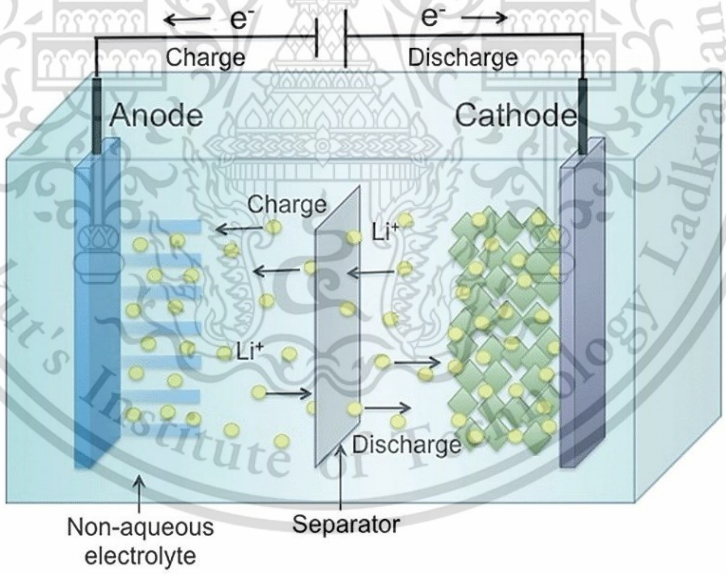

Figure 2.1 Operation of lithium-ion battery[10].

Electrons and lithium ions are excited by an external power source while Li-ion batteries are in the charging stage. The charging process can be regarded as an oxidation process. The power source speeds up the lithium ions to move from the cathode toward the anode during the charging process and the electrons move from the anode (negative electrode) to the cathode (positive electrode). As a result, electricity flows when lithium ions move between electrodes. The oxidation process is accomplished when the maximum storage capacity is achieved in the battery. When an electrical load is applied between the terminals of battery, the battery starts to deplete. Moving

the positively charged lithium ions (Li+) from a negative electrode (anode) to a positive electrode is the process of discharging (cathode). Therefore, electrons will move from the cathode to the anode [11].

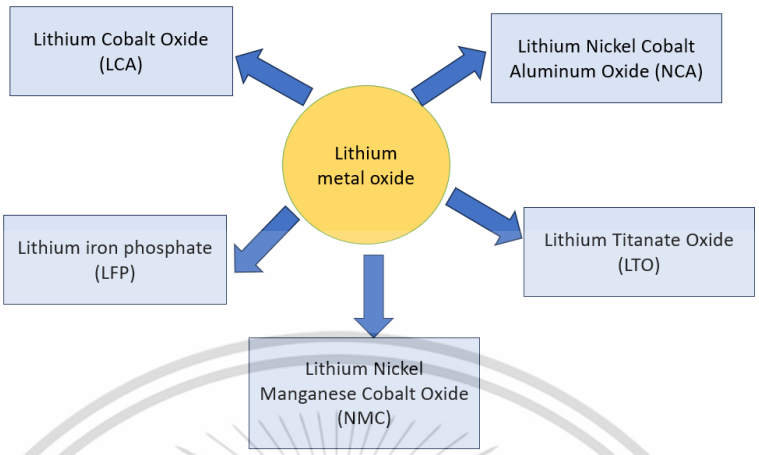

Figure 2.2 Different types of lithium metal oxide.

2.2 Definitions of battery

2.2.1 Battery capacity

The capacity of battery represents the amount of energy stored within the battery. The nominal rated capacity is defined by battery manufacturers. Battery capacity is measured in milliamps-hours (mAh). For example, if a battery has a capacity of 1000mAh, it can theoretically deliver a current of 1000mA for one hour or 500mA for two hours. The capacity of a battery is an important factor in determining how long a device or system will be able to operate on a single charge [3].

2.2.2 State of charge (SOC)

SOC indicates the amount of remaining energy or charge of battery. Using Coulomb counting method, SOC of the battery can be determined, and the range of SOC is described as from 0% (full discharge) to 100% (full charge). SOC is an important parameter for battery management system, and it is impacted by load current and temperature. Since SOC is the key factor in the safe operation of batteries, an accurate estimation of SOC is important. The calculation of SOC of the battery is presented in equation 2.1 [11],[12].

$$SOC = SOC_0 - \int_0^t \frac{I_b}{C_c} dt \qquad 2.1$$

where

SOC = State of Charge

SOC_0 = Initial state of charge

C_c = Capacity (Ah)

I_b = Current (+ discharge, - charge)

2.2.3 Battery voltage

Battery voltage is divided into two types: Open Circuit Voltage (OCV) and Closed-Circuit Voltage (CCV). Open circuit voltage is the terminal voltage of a battery cell at equilibrium condition or the voltage of a battery when there is no load connected to the battery, that is when the battery is in open circuit state. It is an important parameter to understand a battery's state of charge (SOC) and is used as a reference point to estimate the state of charge. The nonlinear relationship between SOC and OCV is determined by polynomial equation. CCV measures the battery voltage during charge and discharge conditions. The equation of the CCV is shown in equation 2.2 [13].

$$V_{cc} = V_{ocv} - i \cdot r_{int} \quad 2.2$$

where

V_{cc} = Close circuit voltage(V)
V_{ocv} = Open circuit voltage(V)
i = Electric current (A) (+ discharge, - charge)
r_{int} = Internal resistance(Ω)

2.2.4 Battery discharge or charge rate (C-rate)

C-rate is the most common way to express battery current. The C-rate of a battery is a measure used to express the rate at which a battery is charged or discharged relative to its capacity. For example, the battery current normalized to the rated capacity (C) of the battery. A C-rate of 1C for a battery with 1 Ah indicates a current of 1A; a current of 0.5A is represented by a 0.5C rate [14]. Thus, it will take approximately long hours to complete charging and discharging on a battery with a C rate of 0.5C than 1C rate [15].

2.2.5 Depth of discharge (DOD)

It is a measure that indicates the percentage of the capacity of a battery that has been discharged compared to its total capacity. In other terms, DOD indicates the charge removed from the battery. Depth of Discharge is a crucial factor in battery management and maintenance. Higher percentages of the capacity of battery being used during deeper discharge cycles can have an effect on the battery's overall longevity. As DOD inverses the SOC, DOD can be calculated from SOC in equation 2.3 [16].

$$DOD = 1 - SOC \quad 2.3$$

where

DOD = Depth of discharge
SOC = State of charge

2.3 Battery model

The initial stage in designing, controlling, and optimizing a battery management system is often to create a suitable model. Battery modeling is essential for both design and estimating better performance. Battery modelling can be categorized into three main types: battery electric model, battery thermal model and battery coupled model. The most prevalent kinds of battery electric models include data-driven, equivalent circuit, reduced-order, and electrochemical models. Although the electrochemical model needed a large amount of computing during model simulation, it offered very accurate prediction performance. For analogous circuit models, the electric behaviors of batteries have been represented by a combination of circuit elements, including voltage sources, capacities, and resistances. Because of their straightforward model structure and limited number of model parameters, equivalent circuit models have found widespread application in real-time battery applications. Neural networks and support vector machines are two examples of data-driven models that have been used to describe battery electric characteristics in the absence of prior knowledge. The classification of the battery modelling is presented in Figure 2.3 [17].

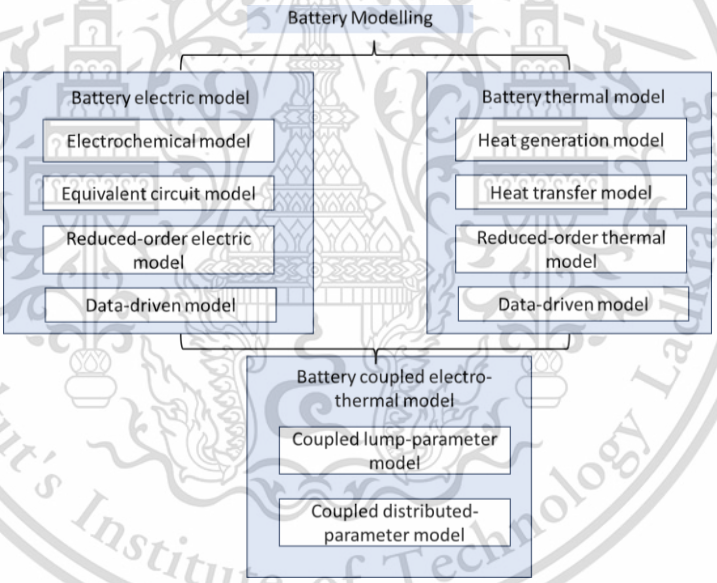

Figure 2.3 Classifications of battery modelling.

2.3.1 Equivalent circuit model

2.3.1.1 Simple or linear battery model

The simple model or internal resistance model, R_{int}, is the simplest equivalent circuit model, and it consists of an ideal voltage source and the internal resistance. The resistance R_{int} is defined as the energy losses that make batteries heat up. Only when the circuit is open, the terminal voltage V_T is the same with open circuit voltage V_{oc}. However, when a load is attached, this voltage is determined by equation 2.4 [18]

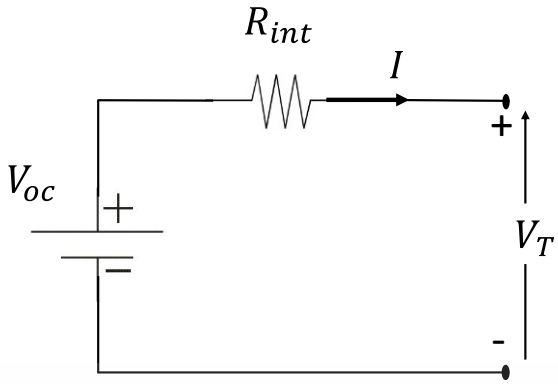

Figure 2.4 Schematic of Rint model.

$$U_t = U_{OCV} - I \cdot R_0 \quad (2.4)$$

where

U_t = Terminal voltage

R_0 = Internal resistance

U_{ocv} = Ideal voltage source

However, the R_{int} model has its disadvantages in describing the dynamic behavior of Lithium-ion batteries [17]. As a result, this model is able to simulate the voltage drop that occurs when the circuit is connected to the load, which is directly proportional to the circulating current.

2.3.1.2 Thevenin model

Thevenin-based models, which can simulate transient response, are organized using internal resistance, open circuit voltage (OCV), and RC networks. The present model parameters are connected in series with a parallel Resistance-Capacitance (RC) network to characterize the dynamic behavior of the lithium-ion battery.

As soon as the current is applied to a battery, the battery's voltage reduces immediately due to the resistance in the series. A DC voltage source is used to display a battery's open circuit voltage (OCV), which is influenced by the battery's state of charge (SOC)[18].

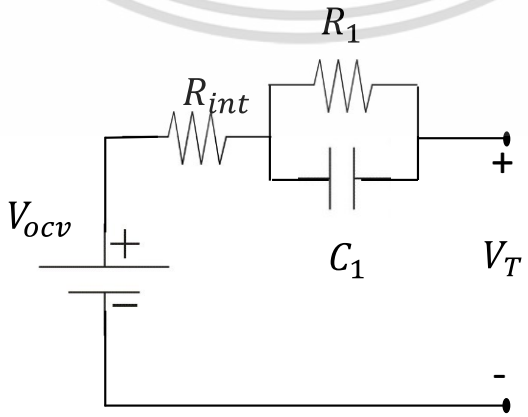

Figure 2.5 Second-order equivalent circuit model.

2.4 Charging and discharging method of battery

2.4.1 Constant current-constant voltage charging method

Constant current (CC) charging and constant voltage (CV) charging method are the two basic approaches of charging lithium-ion batteries. Because of its straightforward implementation, Constant Current-Constant Voltage (CC-CV) charging strategy combined the CC mode and CV mode, and it was defined as a useful way to recharge batteries. The battery is charged in two stages using the CC-CV charging strategy: first, a constant current is used to charge the battery and second, when the voltage reaches the switch voltage, a predefined voltage that is incredibly close to the full charge voltage, CV stage charging begins. In CV stage charging, the current decreases until the threshold value of current to prevent the battery from harm. The CV mode, which comes after the CC mode, can lengthen the charging time, and increase charging capacity while reducing the overvoltage stress on the battery cells. The charging duration can be greatly increased if the steady charging current is less than 0.5C.The CC-CV strategy is usually a reference when assessing experimental charging strategies [19],[20].

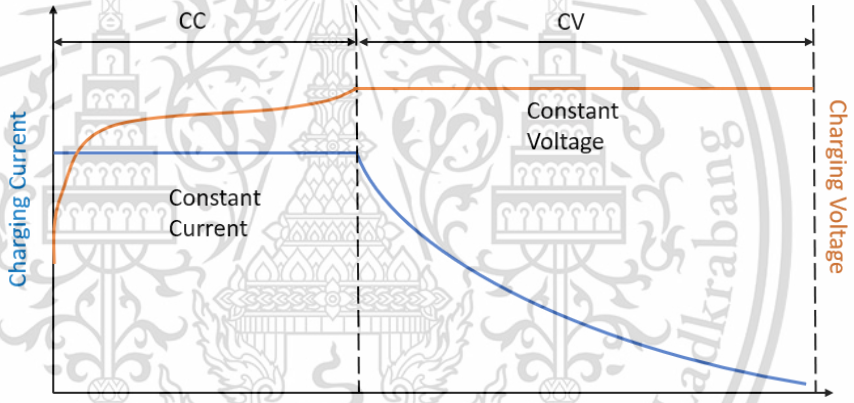

Figure 2.6 CC-CV (Constant Current- Constant Voltage) charging strategy.

2.4.2 Pulse current mode

Instead of employing a continuous charging current, the idea of pulse charging depends on gradual changes in current rate and/or direction. Essentially, the current can be replaced with a transient discharge pulse or terminated, leading to a shortened rest period. Short rest intervals may promote relaxation, and brief current inversions may facilitate both quick relaxation and the battery's electrochemical processes to revers [21]. The two basic pulsed current modes are Standard Positive Pulse Current (PPC) mode and standard Negative Pulse Current (NPC) mode. The standard PPC mode consists of using periodic relaxation time with positive constant current. Based on this concept, extended PPC modes are proposed which are Pulsed Current with Constant Current (PCCC) mode, Constant Current-Pulsed Current (CC-PC) mode, Pulse Modulation (PM) mode, and Pulsed Current-Constant Voltage (PC-CV) mode. The extended NPC modes are Constant Current-Constant Voltage with Negative Pulse (CC-CVNP) mode, Alternating Current Pulse (ACP) mode, Multi-Stage Constant Current-Constant Voltage with Negative Pulse (MCC-CVNP) mode [22].

The standard PPC mode consists of the constant current with periodical rest time. While the current is zero during the rest period, the positive pulse's current has a constant value, I_p . Toal period of positive and negative pulse is regarded as *T*, and the frequency *f* of current pulse is equal to $^1/_T$. In a period as shown in Figure 2.7, the width of the pulse current is considered as t_p, and the rest time t_r. Calculation of duty cycle for the positive pulsed current is expressed in equation. Magnitude of pulse current, I_p , Period T, and duty cycle D_p are the main parameters of the standard PPC mode. The duty cycle of the pulse current can be calculated by equation 2.5 and 2.6 [23].

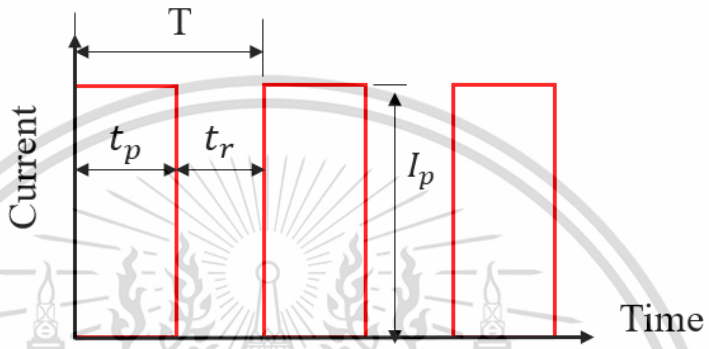

Figure 2.7 Standard PPC mode.

$$T = t_p + t_r \quad (2.5)$$

$$D_p = \frac{t_p}{T} \quad (2.6)$$

2.5 Supercapacitor operation

A supercapacitor, often referred to as an ultracapacitor, is an electrochemical device that can improve capacitance compared to ordinary capacitors. Supercapacitors are also electrical energy storage systems that have a high energy storage capacity and a rapid energy discharge rate. It consists of two porous electrodes submerged in electrolyte with a separator between the electrodes. Because supercapacitors use a separator rather than a dielectric between two electrodes, they can store more energy than conventional capacitors. Supercapacitors (SCs) have considerable specific power, strong charging and discharging currents, and a noteworthy efficiency because of their high capacitance and low series-resistance. Typical regular capacitors consist of two electrodes spaced by an insulating dielectric, like paper, mica, or ceramic. Although the supercapacitors have different structures from regular capacitors, they operate on the same principle. Based on various methods of charge storage, three types of supercapacitors can be identified. One type is an electric double layer capacitor which creates an electric double layer (Helmholtz layer) at the point where an electrode with a high specific surface area meets the electrolyte to store the energy. Another one is Pseudocapacitors which use Faradaic redox reactions

or quick reversible chemical desorption and adsorption to store energy. Hybrid supercapacitors, which combine Helmholtz layers and Faradaic redox processes, is the third type [24],[25]. The equivalent circuit model of supercapacitor is described in Figure 2.8 [26].

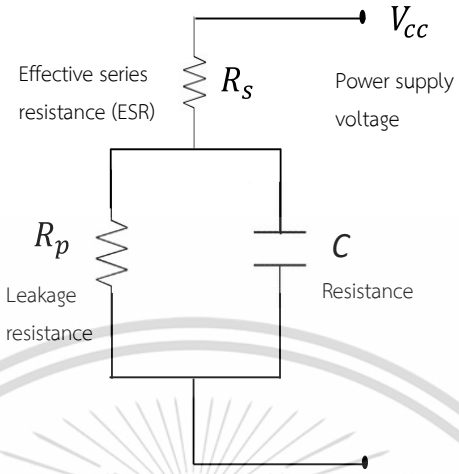

Figure 2.8 Equivalent circuit model of supercapacitor.

2.6 Definition of supercapacitor

2.6.1 Capacitance

The capacitance of the supercapacitor is described as the ratio of stored charges to the applied voltage and the unit of the capacitance is called in Farad. The calculation of the capacitance of supercapacitor is presented in equation 2.7.

$$C = \frac{Q}{V} \tag{2.7}$$

where

C = Capacitance (F)

Q = Quantity electric charge (C)

V = Voltage (V)

Supercapacitors are connected in parallel or series to increase the voltage and the capacitance of the supercapacitor. The capacitance of the supercapacitor is calculated by the equation 2.7 and the voltage of the supercapacitor is calculated by the equation 2.8 and the total voltage after series connection is calculated by equation 2.9.

$$C = C_{cell} \cdot \frac{n_p}{n_s} \tag{2.8}$$

where

C_{cell} = Capacitance of cell (F)

n_p = Number of cells in parallel

n_s = Number of cells in series

$$V = V_{cell} \cdot n_s \quad (2.9)$$

where

V_{cell} = Voltage of cell (V)

n_s = Number of cells in series

2.6.2 State of charge (SOC)

The state of charge of the supercapacitor is calculated as the same calculation as SOC of the battery and presented in equation 2.10 [15].

$$SOC(t) = SOC(t-1)\frac{\int i(t)dt}{Q} \quad (2.10)$$

where

SOC = State of charge

Q = Quantity electric charge

i = electric current (A) (+ discharge, - charge)

t = Time (s)

2.6.3 Equivalent series resistance

The internal resistance of the supercapacitor can be regarded as an ideal capacitor in series with a resistor. It is defined as the equivalent series resistance and expressed by equation 2.11 [27].

$$R_s = \frac{\Delta V}{i} \quad (2.11)$$

where

R_s = Equivalent series resistance (Ω)

V = Voltage (V)

i = Electric current (A) (+discharging, -charging)

2.6.4 Supercapacitor voltage

There are two forms of voltage in supercapacitors: closed circuit voltage (CCV) and open circuit voltage (OCV). OCV is the voltage across a capacitor's terminals when no load is attached to it and no current is passing through it. The voltage across a supercapacitor's terminals when it is attached to a load and current is flowing is known as the CCV. The calculation of OCV and CCV is defined in equation 2.12.

$$V_{cc} = V_{OC} - i \cdot R_s \quad (2.12)$$

where

V_{cc} = Close circuit voltage(V)

V_{oc} = Open circuit voltage(V)

i = Electric current (A) (+discharging, -charging)

R_s = Equivalent series resistance (Ω)

2.6.5 Energy of supercapacitor

The energy of the supercapacitor is proportional to the squared of voltage and expressed by the equation 2.13 [27].

$$E = \frac{1}{2} \cdot C \cdot V^2 \qquad 2.13$$

where

E = Energy (J)

C = Capacitance (F),

V = Voltage (V)

2.7 Hybrid energy storage system

A hybrid energy storage system (HESS) is a power system that combines two or more energy storage sources, and it is used in electric vehicles. The battery, which can optimize energy consumption in electric vehicles, serves as the main energy storage source in HESS. Supercapacitors are used to provide energy support during current surges during both charge and discharge. There are two types of hybrid energy storage systems: active and passive. In the passive configuration, the battery and supercapacitor are linked in parallel and have the same voltage levels. An ideal power distribution strategy that modifies the operating parameters of electrical vehicles and energy storage media is necessary to achieve optimal energy consumption. Thus, it requires a system that can both operate an electric vehicle and distribute the power supplied to the load by the hybrid energy storage. Batteries, supercapacitors, a bidirectional DC-DC converter, 3-phase inverters, a permanent magnet synchronous motor, and an energy management system are all components of a hybrid energy storage system[8]. Energy management system and a DC-DC converter regulate how power is distributed in HESS. The same DC-link is connected to two DC-DC converters, one of which controls the power flow from the batteries and the other the power flow from the SCs, as indicated in Figure 2.9.

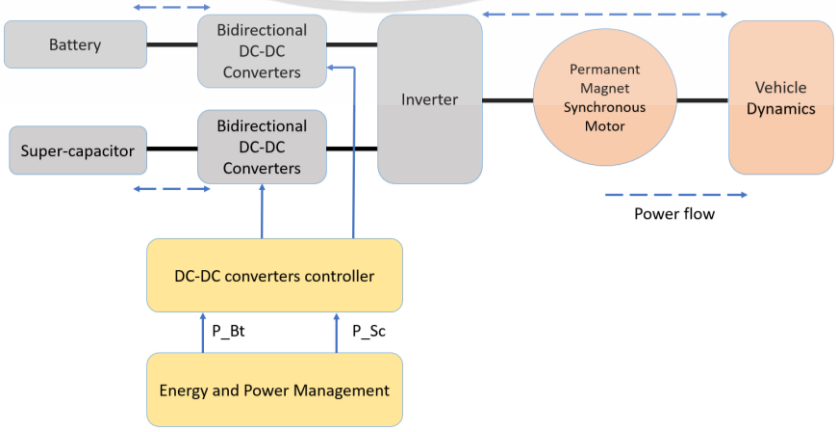

Figure 2.9 Hybrid energy storage system in Electric vehicle.

2.7.1 Battery-SC HESS Topologies

Using the proper energy management systems (EMSs) and topologies for HESSs, the distribution of electricity among various power sources is coordinated. A separate DC-AC converter is used to connect the HESS to either the DC bus or the AC bus. HESS is often created by coupling the supercapacitor and battery using a bidirectional DC-DC converter to maximize their benefits and minimize their downsides. Interconnection topologies come in three types: passive, semi-active, and active [8]. The most straightforward way to combine a battery and supercapacitor is with a passive hybrid architecture. One advantage of this design is that power electronic converters are not needed. As the battery maintains the DC bus's voltage, the supercapacitor's stored energy cannot be fully utilized. The type of system that has a bidirectional DC-DC converter connecting it to a DC bus is considered as a semi-active system. In the supercapacitor semi-active topology, the battery is connected directly to the DC bus, and to benefit from its wide voltage range, the SC is coupled in series with a bidirectional DC-DC converter. Active HESS is used when two storage devices are linked to a DC bus via a bidirectional DC-DC converter. This configuration is known as active HESS if the hybrid energy storage system is linked to the DC bus via a controller or energy management system for two bidirectional DC-DC converters. The DC bus's voltage is stable because the battery is directly connected [42].[43]

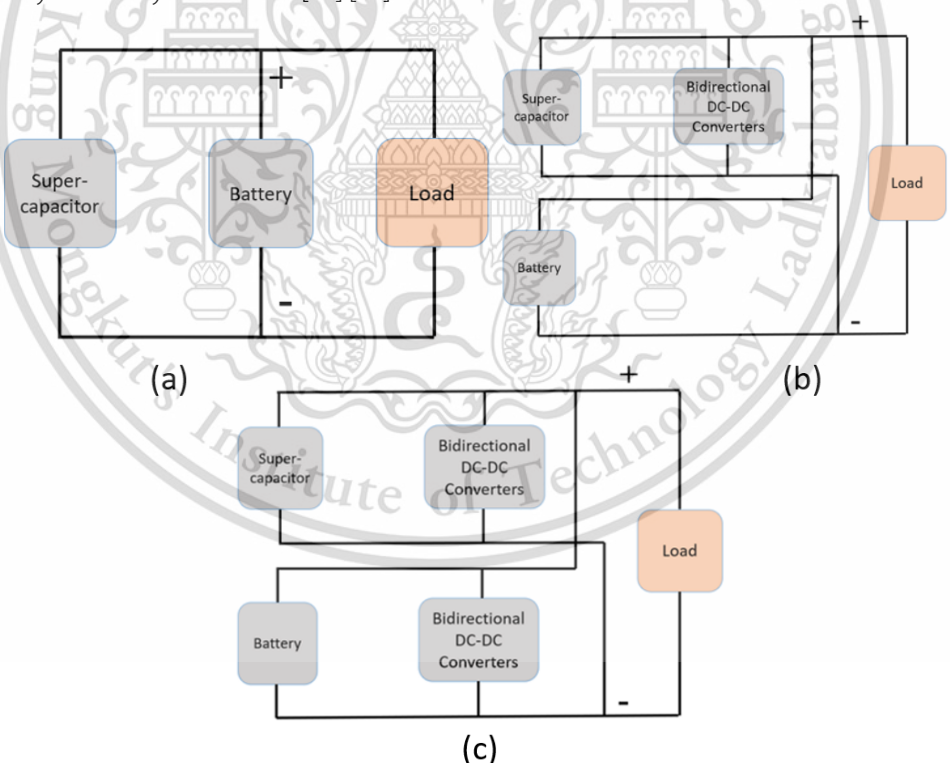

Figure 2.10 Topologies for HESS (a) passive, (b) semi-active (c) active configuration

Energy conversion law is used as a base for all enrgy management system that the load power needed is to be supplied by available power sources and the equation for the energy storage system is shown in equation 2.14.

$$P_{Load} = P_{sour} = P_{Bat} + P_{SC} \quad 2.14$$

At a particular instant of time, the power of EV can be defined as in equation [44] and the power load for the system is calculated by equation 2.15 and 2.16.

$$P_{EV} = P_{Bat} + P_{SC} \quad 2.15$$

$$P_{Load} = V_{DC} \cdot I_{DC} = \frac{1}{\eta} F_{te} \cdot v \quad 2.16$$

2.8 Energy consumption of vehicle

Total energy consumption can be calculated in this study by using total force and vehicle speed as shown in equation2.17 [28].

$$P = F \cdot v \quad 2.17$$

where

P = Electrical power (W)
F = Tractive force (N)
v = Vehicle speed (km/hr)

2.8.1 Vehicle dynamic

Determining the force components that influence the dynamics of the vehicle is the initial stage in vehicle modeling. According to Newton's second law, the acceleration of an object is inversely proportional to the net force acting on it. In other words, an object accelerates when the net force acting on it is nonzero. A moving vehicle is affected by the drag force, rolling resistance force, slope force, and acceleration force. A precise estimation of normal forces could significantly enhance vehicle handling and safety as they are important to vehicle dynamic control systems. The power delivered to the wheel by the powertrain, the condition of the roadway, the curb mass of the vehicles (including all components and passengers), and the aerodynamics of the vehicle determines the acceleration and speed of the vehicle [29],[30].

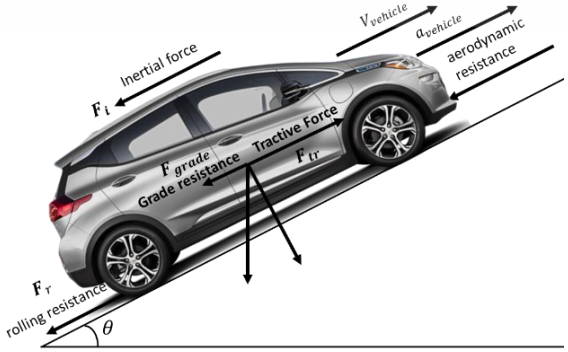

Figure 2.11 The external forces acting on a vehicle.

Tractive force (F_{tr}) is the force that make the movement to the vehicle, and in order to drive the vehicle, this force must outweigh the resistance force. These resistant forces are described as “road load force” and the calculation of total forces is presented in equation 2.18 [31].

$$F_{tr} = F_a + F_{aero} + F_r + F_{grade} \quad 2.18$$

2.7.1.1 Aerodynamic resistance force

The air's resistance to a vehicle's motion when it is moving through the atmosphere is known as the aerodynamic drag force. There are 2 types of aerodynamic drag force: drag due to frontal area and skin friction at the surface of the body. The resistance force increases with the square of the vehicle’s speed and is influenced by various factors, including vehicle’s shape, size, and the aerodynamic drag coefficient. The mathematical equation of the aerodynamic drag force is represented as

$$F_{aero} = 0.5 \cdot \rho \cdot C_d \cdot A \cdot v^2 \quad 2.19$$

where ρ is the density of the air, C_d is drag coefficient,A is the frontal area of the vehicles and v is the velocity of the vehicle.

The drag coefficient is a value that quantifies the aerodynamic drag and a vehicle experience as it moves through the air. It is a crucial parameter in vehicle design that has an impact on fuel efficiency, performance, and stability. The shape of the vehicle body has a significant effect on drag coefficient such as reducing the frontal area decreases the impact of air on the vehicle’s surface and thus lowers drag [30],[32].

2.7.1.2 Grade resistance force

When a vehicle is moving on an incline or gradient, it needs to overcome the force of gravity pulling it back down the slope. The grade resistance force, a type of gravitational force, is what tends to pull a vehicle back when it is climbing an inclined surface. The grade resistance force is influenced by the slope of the road or terrain and the weight of the vehicle. Grade resistance is a crucial factor to consider in vehicle dynamics, especially for fuel efficiency and performance calculations. The grade resistance acting on the vehicle can be calculated by equation 2.20 [33].

$$F_g = m \cdot g \cdot \sin(\theta) \quad 2.20$$

where m is the mass of the vehicle, g is gravitational acceleration and θ is the road grade in degree.

2.7.1.3 Rolling resistance force

Rolling resistance force is the force that opposes the motion of a vehicle’s tires as they roll over a surface. The friction between the tires of the vehicle and the road generates the rolling

resistance force. Roling resistance can vary depending on the type of road surface such as smooth pavement, gravel, or rough terrain. The calculation of rolling resistance force is presented in equation 2.21 .

$$F_r = \mu \cdot m \cdot g \cdot \cos(\theta) \quad 2.21$$

where μ is rolling resistance coefficient, m is the mass of the vehicle, g is gravitational acceleration and θ is the road grade in degree [33],[34].

Table 2.1 Rolling resistance coefficient on various types of roads [29]

Conditions	Rolling resistance coefficient
Car tires on concrete or asphalt	0.013
Car tires on rolled gravel	0.02
Unpaved road	0.05
Field	0.1–0.35

2.7.1.4 Inertial resistance force [35]

A part of the overall resistance that a moving vehicle encounters is called inertial resistance force, or inertial force. This force is associated with the vehicle's mass and its resistance to changes in motion and that helps a vehicle accelerate from rest to a predetermined speed in a given amount of time is known as the acceleration force [36]. The calculation of rolling resistance force is presented in equation 2.22.

$$F_a = m \cdot \frac{dv}{dt} \quad 2.22$$

where m is the mass of the vehicle and v is the speed of the vehicle.

2.8.2 Driving Cycle

Driving cycles are speed-time measurements that are used to calculate how much fuel and pollution a car emits, and to simulate the driving system and forecast its performance [37]. Vehicle driving simulations and tests are carried out to support the design process and help assess whether the design is appropriate for the desired use. The driving cycle process upgrades to a computer simulation or dynamometer from a road simulation. There are several different standard driving cycles [38]such as extra urban driving cycle (EUDC), ECE 15, New European driving cycle (NEDC), the world harmonized light vehicles test procedures (WLTC) and others. Depending on the kind of driving cycles profile mentioned above, these cycles include several accelerations and braking events over a specific period of time.

2.7.2.1 New European driving cycle (NEDC)

NEDC, or the New European Driving Cycle, is the testing protocol. The European Union Urban Driving Cycle (ECE) and the Extra-Urban Driving Cycle are combined to form NEDC driving cycle.

Testing EV energy consumption and regenerative braking performance has made extensive use of it. A full NEDC cycle has four repeating ECEs that follow an EUDC section to display a highway driving speed pattern, with a maximum speed of 120 km/h [39].

Table 2.2 Parameters of NEDC drive cycle [37].

Parameters	WLTP
Duration (s)	1800
Distance (km)	23.266
Average speed (with stops)(km/h)	46.5
Average speed (without stops) (km/h)	53.5
Maximum speed (km/h)	131.3

2.7.2.2 World harmonized light vehicles test procedures (WLTC)

The World harmonized Light-duty vehicles Test Procedure (WLTP) is globally harmonized standard for determining levels of pollutants such as CO_2 and it is used to calculate the fuel consumption of internal combustion engines (ICE) and the range of electric vehicles[40]. This cycle enables the efficiency of fuel economy of vehicle and the range. Based on the power to mass ratio of the test vehicle, this driving cycle is classified into three classes: Class 1 is for urban driving, Class 2 is for combined driving which includes both high-speed and low-speed sectors, and Class 3 is for extra urban driving.

Table 2.3 Parameters of WLTC drive cycle [41]

Parameters	NEDC
Duration (s)	1180
Distance (km)	11.016
Average speed (with stops)(km/h)	33.62
Average speed (without stops) (km/h)	44.08
Maximum speed (km/h)	120
Average positive acceleration (m/s^2)	0.59
Average negative acceleration (m/s^2)	-0.8

Chapter 3 Methodology

This chapter provides the experimental method and simulation method to build the battery and supercapacitor models for hybrid energy storage system with pulse current method. This research studies the effect of pulse discharging method on lithium-ion batteries in electric vehicles. Firstly, the pulse discharging method was performed with battery pack as experimentation, and then pulse discharging method was applied in hybrid energy storage system containing Lithium-ion battery pack and supercapacitor with simulation in MATLAB/Simulink.

In the first part of the experimental process, we employed the pulse current method to analyze the discharge energy and capacity of batteries. This involved subjecting the batteries to varied switching frequencies, specifically at 200Hz, 400Hz, 600Hz, 800Hz, and 1000Hz. In the second part of simulation phase, a hybrid energy storage system was designed by applying a pulse current algorithm for optimized power distribution. The system's performance was evaluated using the pulse method at varying switching frequencies (200Hz, 400Hz, 600Hz, 800Hz, and 1000Hz).

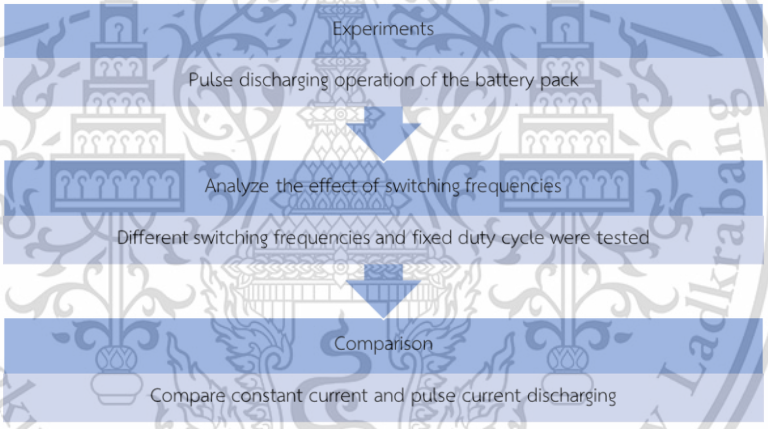

Figure 3.1 Methodology for experiments.

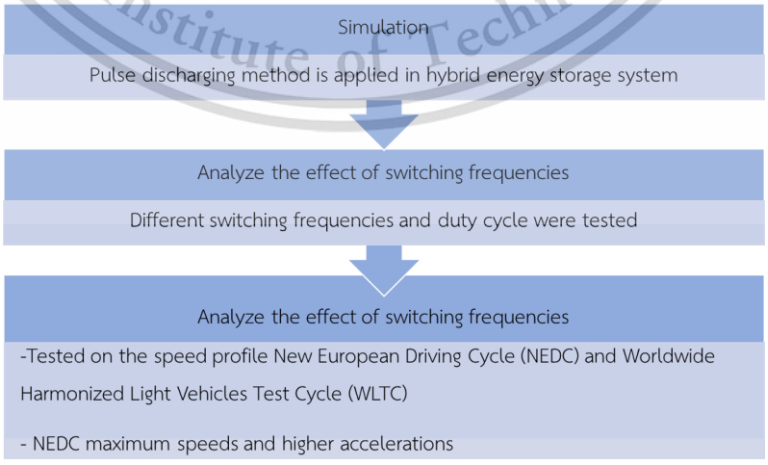

Figure 3.2 Methodology for simulation.

3.1 Experimental setup for pulse discharging

3.1.1 Experimental setup for Lithium-ion battery

In this study, the experimental setup was performed to analyze the effect of pulse discharge for battery. The apparatus used in the experiments are shown in Table 3.1.

Table 3.1 Experimental apparatus used in the experiments.

No	Equipment	Purpose	Remark
1	Arduino	Generate PWM signal	Uno
2	Lithium-ion Battery	Voltage source	Panasonic
3	Programmable power supply	Supply electrical power	Charge batteries, Provide power to optocoupler
4	Electronic load	Discharge batteries	Constant current
5	Data logger	Collect current and voltage data	Sampling rate 200ms
6	Clamp meter	Measure electrical current	0-200A
7	Oscilloscope	Measure signals	Frequency
8	Transistor	On/Off switching	Fuji electric
9	Optocoupler	Isolating high voltage circuit from low voltage circuit	PC 817

Figure 3.3 Optocoupler and power transistor.

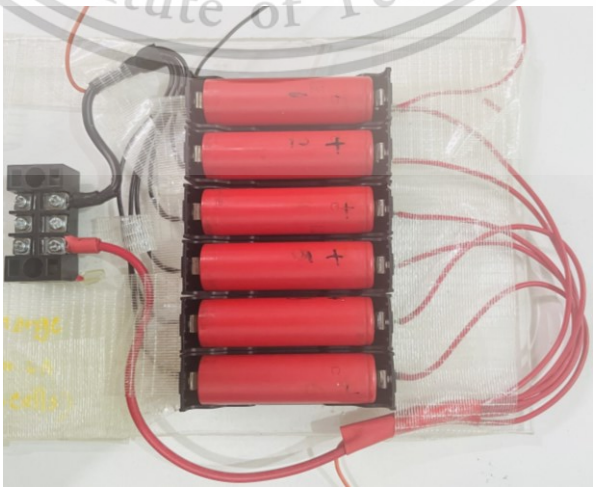

Figure 3.4 Battery pack for charging.

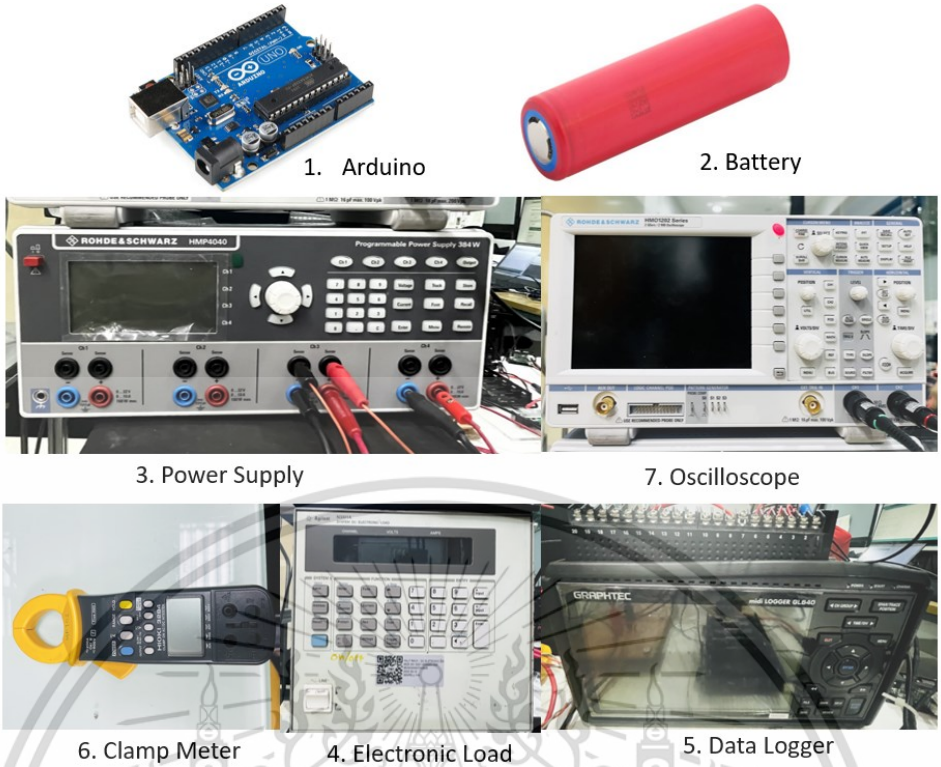

Figure 3.5 Experimental apparatus.

The specifications of the battery cell used in this experiment are described in Table 3.2. The lithium-ion cells in this study have a nominal capacity rating of 3450mAHh. Firstly, the initial characterization tests were performed to obtain the baseline results. All the cells were charged with constant current-constant method (CC-CV) until the maximum charging voltage of 4.2V. Arduino microcontroller was used to generate the Pulse Width Modulation (PWM) signals to control the discharging of batteries. In this experiment, direct current passage from the high voltage battery pack to the Arduino microcontroller was inhibited by placing an optocoupler between the Arduino and the transistor. Optocouplers serve as a crucial component for isolating high voltage circuits from low voltage circuits in electronic systems. The optocoupler effectively transmits electrical signals between two isolated circuits, ensuring that there is no direct electrical connection between them. Optocoupler contains two sides; input and output side in which high-voltage input can activate the LED on the input side, which emits light. This light is then detected by the light-sensitive component on the output side, which is electrically isolated from the input side. The output side can be connected to the low voltage circuit, ensuring that high voltage and low voltage sections remain completely separated. To execute switching in the discharging state, an electronic power switch known as a power transistor module was utilized. To investigate the effects of different frequencies of pulse discharging on lithium-ion batteries, six Panasonic NCR18650GA cells (designated as cell A, B, C, D, E, F, and G) were chosen. Parallel connection design was used for charging batteries as battery management system was not used and parallel charging is easy to control to reach maximum charging voltage, and series connection is used for discharging.

Table 3.2 Specification of Panasonic battery cell

Parameters	Value
Cell type	NCR18650GA
Rated capacity	3450mAh
Nominal voltage	3.6V
Maximum discharge voltage	2.5V
Maximum charging voltage	4.2V
Maximum discharge current	10A
Standard charging current	1.675A
Energy density	224Wh/kg

The lithium-ion battery pack was connected to the electronic load and the power transistor switch is controlled by Arduino microcontroller for the pulse discharge. Power supply was used to supply the voltage to optocoupler and power transistor. The voltage and current data of batteries was recorded using a data logger, and the clamp meter was used to monitor the current during discharge. Oscilloscope was used to check the switching frequency rate and to record the frequency data. The lithium-ion battery pack was discharged within the boundary conditions to obtain the voltage behavior.

The experimental setup of the battery pack during discharging state is shown in Figure 3.6. By connecting the PWM output pin from Arduino to the gate of a transistor, the switching behavior was controlled and as a result, the power delivered to a load was regulated. PWM facilitates precise control of the duty cycle, enabling modulation of the average voltage applied to the load.

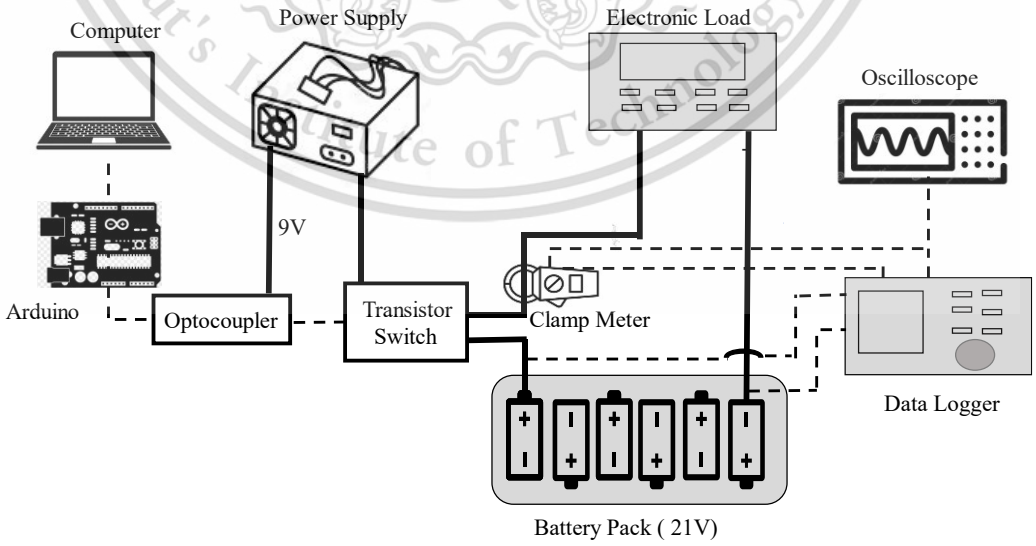

Figure 3.6 Experimental setup schematic for voltage behavior of Lithium-ion battery.

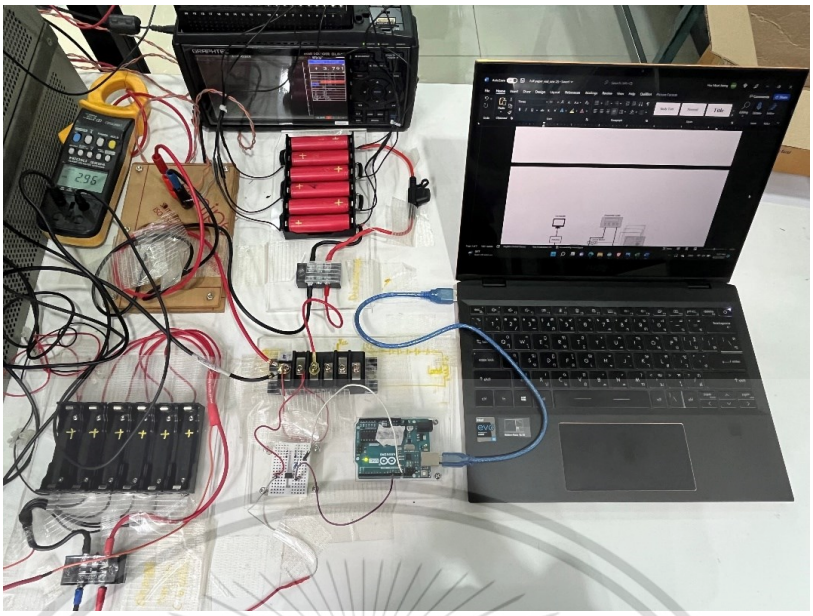

Figure 3.7 Charging and discharging experiment of Lithium-ion batteries.

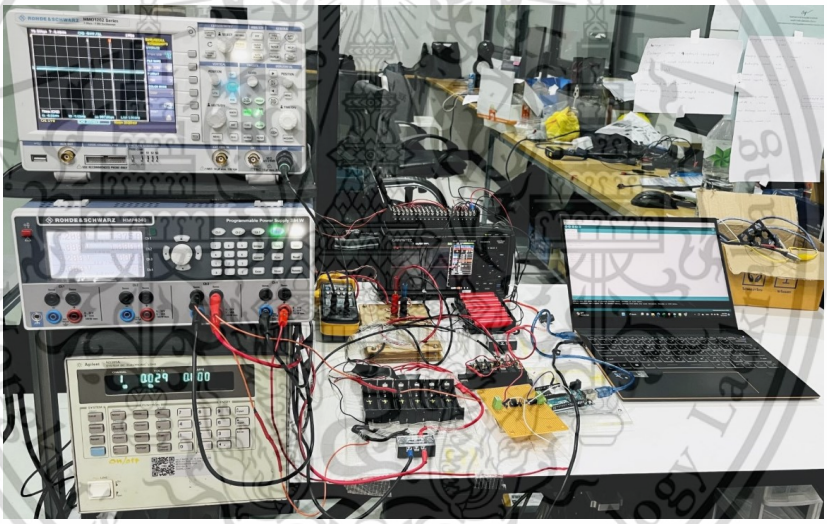

Figure 3.8 Charging and discharging experiment of Lithium-ion batteries.

Applying the suitable duty cycle for pulse discharging is important for achieving the desired performance and reliability. In the pulse discharging application, as longer on-time allows for more energy to be transferred to the output and to step up the input voltage to a higher output voltage, high duty cycle of 75% was selected. 75% duty cycle allows for a slightly shorter ON time compared to an 80% duty cycle. However, this reduces stress on the transistor switch and associated components and shorter ON time (75% duty cycle) results in lower heat generation during each pulse. Moreover, longer Off time results in achieving higher energy restoration and recovery. That means 75% duty cycle have longer Off time than 80% duty cycle. A duty cycle of 75% means that the discharging current is active for 75% of the time and switched off for the remaining 25%. The procedure of the experiment is shown as flow chart in Figure 3.9.

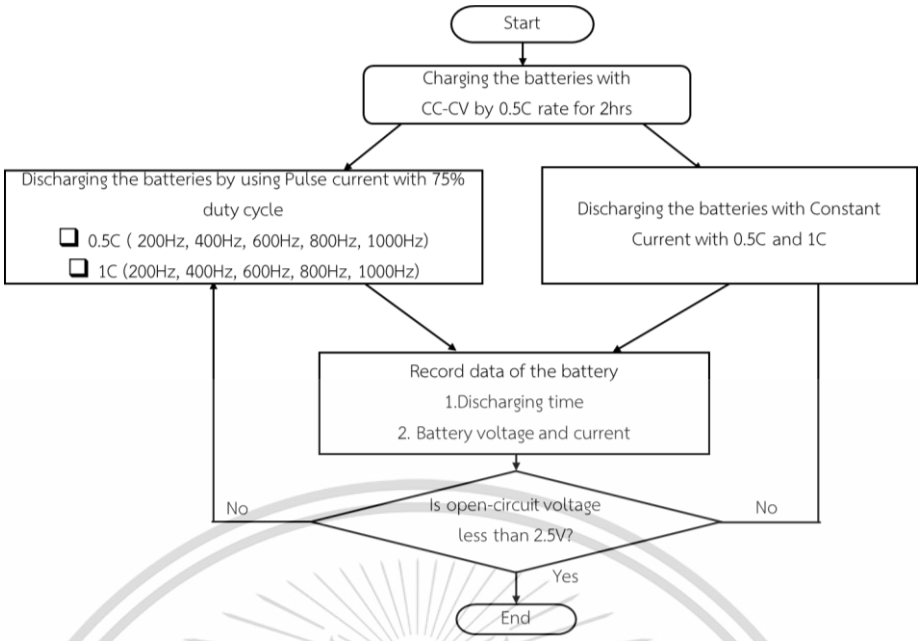

Figure 3.9 Flowchart for experimental operation of Lithium-ion battery pack.

3.1.2 Constant Current - Constant Voltage Charging Method

The battery pack was charged under constant current conditions to cut-off voltage (4.2V) with 0.5C, and then charged under constant voltage condition until the current dropped to a predetermined value.

Table 3.3 Experimental conditions for charging of battery pack.

Topic	Parameters	Values
Conditions	Charging Current	1.75A (0.5C)
Battery cell	Cut-off voltage	4.2V
	Charging time	2 hours

3.1.3 Pulse current discharging

Table 3.4 Experimental conditions for pulse discharge of battery pack

Topic	Parameters	Values
Conditions	Discharging Current	1.75A (0.5C)
		3.5A (1C)
Battery cell	Operating voltage	2.5V – 4.2V
	Capacity	3500mAh

After charging the battery with CC-CV method, discharging of battery with constant current and pulse discharging method was performed. In discharging a battery cell, two discharging currents were chosen during the test: 1.75A (0.5C) and 3.5A (1C). The selection of the discharging current depends on the specific application's power requirements and desired discharge duration. A simplified procedure for battery discharging experiments with varying switch frequencies is shown in Table 3.5. Firstly, after the charging step of battery, the battery discharging experiment was

started by setting the discharging current to a constant 3.5A, which is equivalent to a 1C rate. The duty cycle and frequency of the switch was controlled through the Arduino. The first test was conducted at a switch frequency of 200Hz with 75% duty cycle. The battery's performance data for each test was recorded by a data logger and oscilloscope. Discharging of battery was stopped when the cut-off voltage of battery reached 2.5V. After finishing the discharge step, all of the batteries were rested for about one hour and charged again with CC-CV method with 0.5C rate until fully charged cut-off voltage. The fully charged battery was discharged again for the pulse discharging at the same current and duty cycle by changing the switching frequency to 400Hz. When the pulse discharge at 400Hz was finished, all of the batteries were rested and charged again at full voltage. After that another subsequent test was performed by increasing the switching frequency to 600Hz, 800Hz, and 1000Hz. When the pulse discharge test was finished at 1000Hz, the test was prepared for the transition to 0.5C rate. The same procedures of pulse discharging tests by changing only the current rate of 0.5C at 200Hz, 400H, 600Hz, 800Hz and 1000Hz and 75% duty cycle were applied.

The constant current discharging method maintains a steady, moderate discharging rate without the on-and-off time. Battery pack was discharged with constant current method at 0.5C and 1C by recording voltage, current and frequency data for voltage fluctuations and fast discharge duration. The current wave form of battery pack during

Table 3.5 Frequencies and duty cycle parameters for pulse discharging

Parameters	Values	
Pulse Discharging	3.5A(1C) 75% (Duty Cycle)	200Hz,400Hz,600Hz,800Hz,1000Hz
Constant Current Discharging	3.5A (1C)	
Pulse Discharging	1.75A(0.5C) 75% (Duty Cycle)	200Hz,400Hz,600Hz,800Hz,1000Hz
Constant Current Discharging	1.75A (0.5C)	

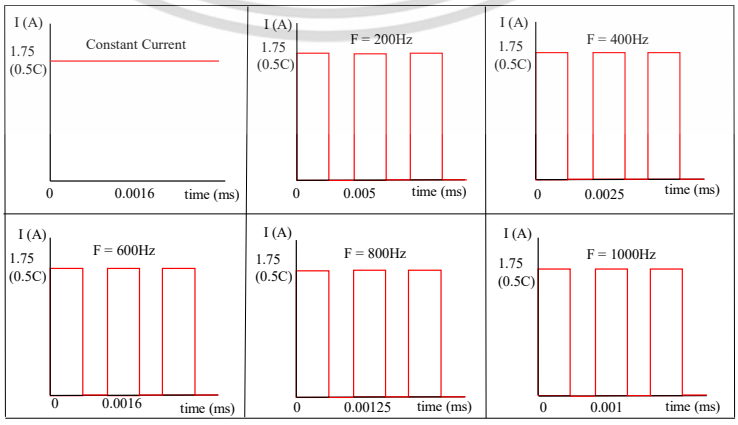

Figure 3.10 Constant current and pulse discharging at different frequencies for 0.5C.

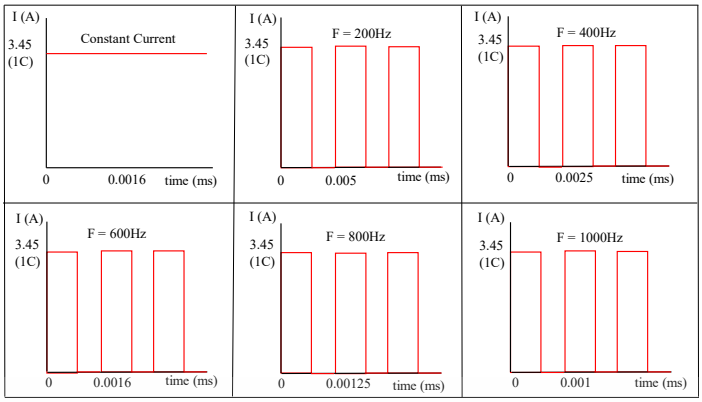

Figure 3.11 Constant current and pulse discharging at different frequencies for 1C.

3.2 Simulation of Hybrid Energy Storage System(HESS) with pulse discharging

3.2.1 Applying Pulse Width Modulation (PWM) method in HESS

The main purpose of this research is to apply the pulse current method in hybrid energy storage systems. Power management between battery and supercapacitor is controlled by using the duty cycle to control the power sharing between two energy sources. Adjusting duty cycle value between battery and supercapacitor is based on the power requirement. When more power is required, the duty cycle is adjusted to allow a larger portion of the energy to flow from the batteries or supercapacitors to the load. During periods of high load demand, the duty cycle will be varied based on the voltage difference of battery and supercapacitor, allowing one energy source to contribute 80% of the power and another will contribute 20% of the power. For power sharing of 20% duty cycle, battery provides 20% of the power for the load and supercapacitor provides the remaining 80% of the power for the load. For power sharing of 80% duty cycle, battery provides 80% of the power for the load and supercapacitor provides the remaining 20% of the power for the load. The power sharing with duty cycle ratio is shown in Figure 3.12 - Figure 3.15. For the case when both energy storage is needed, battery and supercapacitor simultaneously provide power to the load known as parallel operation.

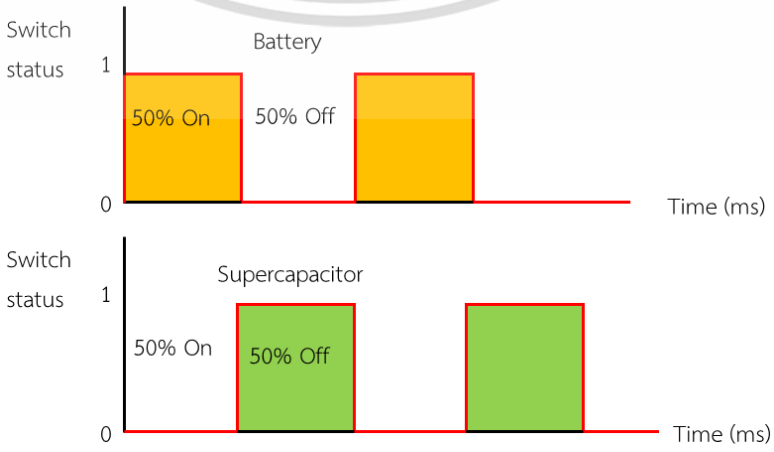

Figure 3.12 50% duty cycle for power sharing.

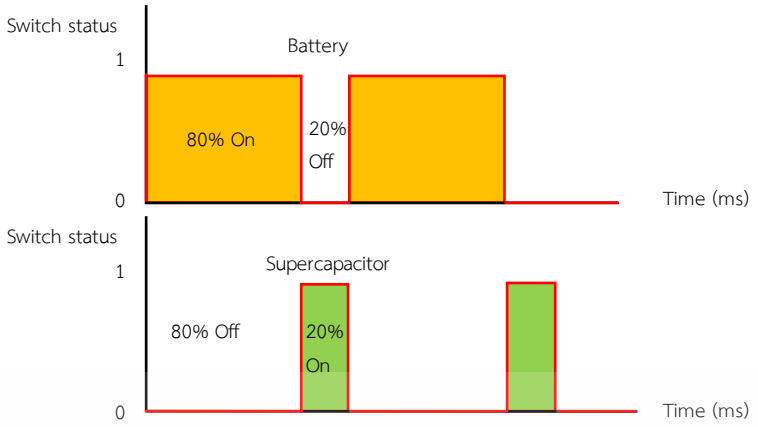

Figure 3.13 80% duty cycle for power sharing.

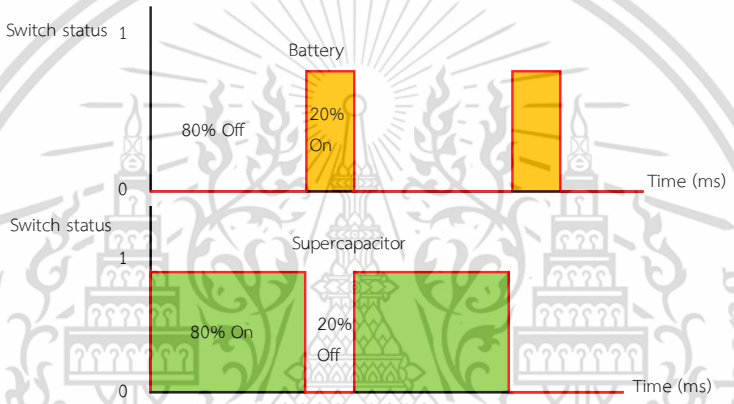

Figure 3.14 20% duty cycle for power sharing.

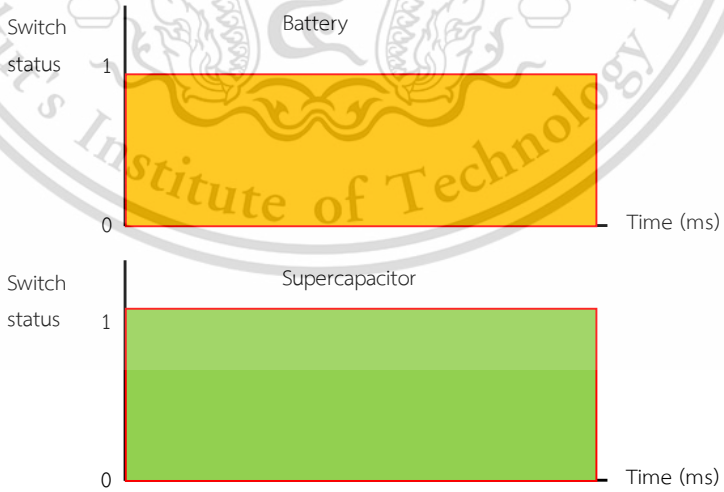

Figure 3.15 100% duty cycle for battery and supercapacitor at the same time.

3.2.2 Methodology for Hybrid Energy Storage System

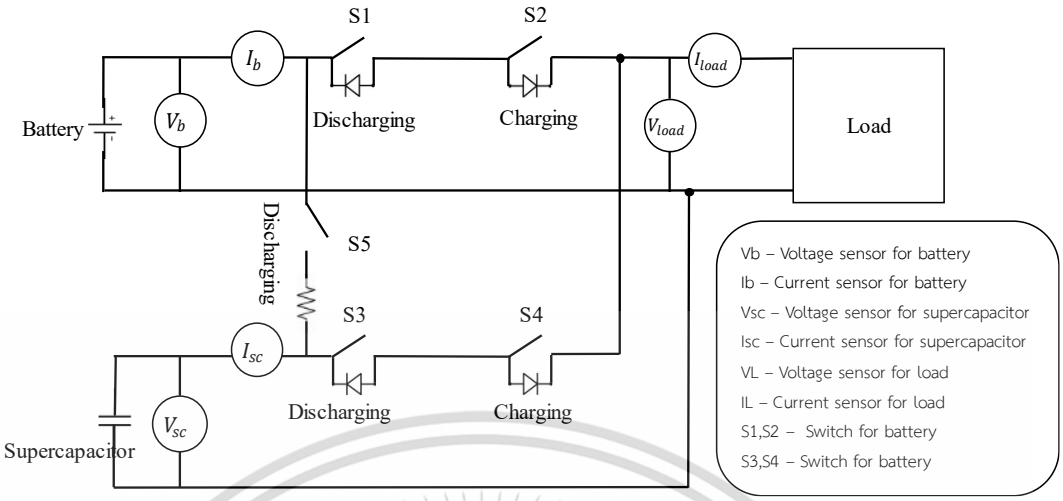

Figure 3.16 Electrical diagram of Hybrid Energy Storage system.

The hybrid energy storage system (HESS) consisting of batteries, supercapacitors, five switches and diodes was developed with the proposed energy management system. HESS, comprising five switches, offers an efficient solution for managing energy storage and distribution in electric vehicles. This method was aimed to enhance the efficiency of HESS by adjusting the energy flow to varying load demands. Energy transfer is performed between sources and loads in back-and-forth direction as well as from one energy source to another. The ratio of battery and supercapacitor is calculated according to the demand of load power. The working principle of the five switches for power sharing is shown in Figure 3.27. The battery is the primary energy source when the vehicle runs under normal conditions and supercapacitor is used as energy support. Switch S1 and S5 are used for discharging of Battery. During normal load condition, S1 is activated to provide the power from battery to load and the current will flow through forward bias diode. During that condition, supercapacitors are also charged by battery by activating switch S5. Switch S2 is used for charging battery by regenerative braking, due to the current flow through the forward bias diode. The same strategy is also performed for supercapacitor. Switch S3 is used for discharging of supercapacitor and switch S4 is used for charging of supercapacitor by regenerative braking. The conditions of supercapacitor charging, discharging and battery charging, discharging are considered based on the duty cycle of 5 switches. The duty cycle and working states of the five switches are determined based on batteries voltage, supercapacitors voltage and power requirement. As shown in Figure 3.18, The main inputs of HESS algorithm are voltage of batteries and supercapacitors and power demand from load. Firstly, the capability to discharge each storage is determined by measuring the voltage difference between the battery and supercapacitor.

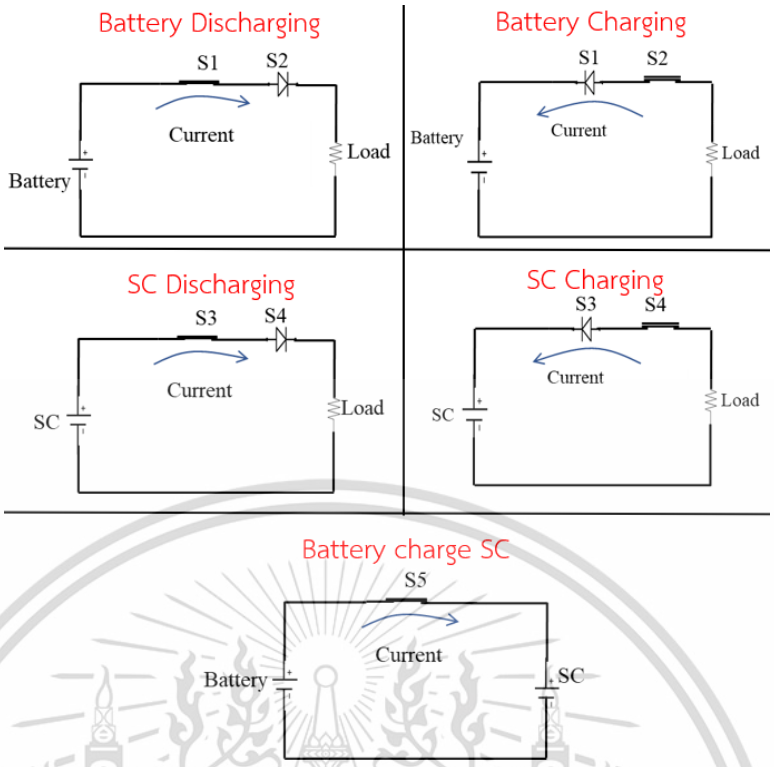

Figure 3.17 Activation of five switches for the operation of hybrid energy storage system.

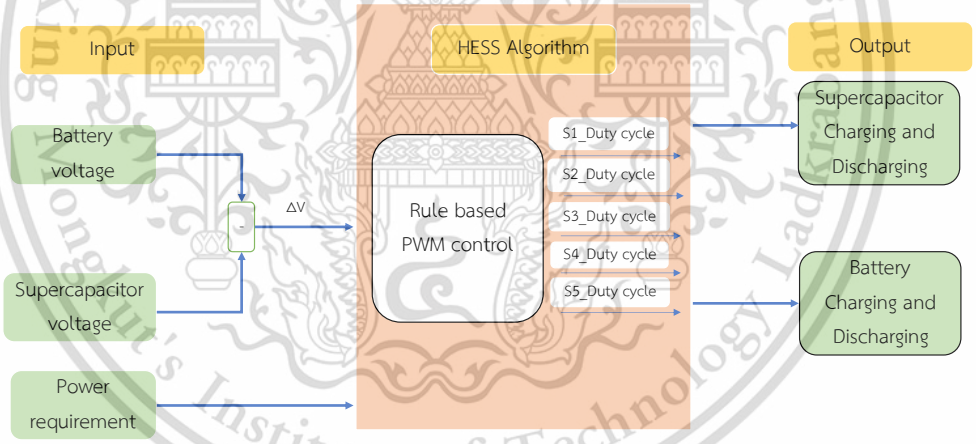

Figure 3.18 Power management for hybrid energy storage system.

According to the working principles of power sharing between battery and supercapacitor shown in Figure 3.19, when the power demand is less than zero, it is regarded as regenerative braking power and batteries and supercapacitors are charged by activating switch 2 and 4 based on the voltage difference of batteries and supercapacitors. When the power demand is greater than zero and below 3000W, switch 1 and 5 are ON. Switch 5 is on for transfer of energy from battery to supercapacitor to charge the supercapacitor, allowing it to store energy for rapid discharge during peak demand periods. Simultaneously, switch 1 is engaged to direct the battery's energy towards supplying power to the load as the primary source. When the power demand exceeds 3000, the HESS shares the power between batteries and supercapacitor. Switches 1 and 3 work together to meet the increased energy requirements. Switch 1 is activated for the direct

contribution of the battery's power to the load and switch 3 is simultaneously activated to allow the supercapacitor to supply additional power to the load.

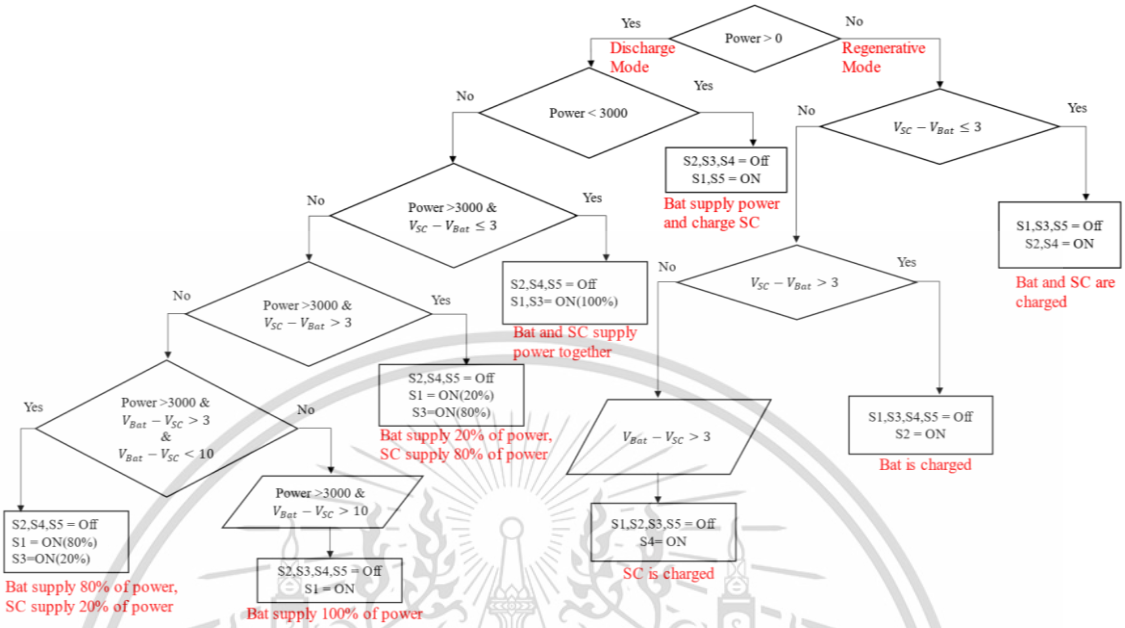

Figure 3.19 Flowchart for the power management between two energy sources.

When the voltage difference from supercapacitor to battery is minimal, both switch 1 and switch 3 are activated with 100% duty cycle. The function of performing switch 1 and 3 simultaneously addresses high-power demands effectively and optimizes the overall system performance. When the voltage difference from the supercapacitors to the batteries exceeds 3V, switch 1 is engaged with a 20% duty cycle, allowing the battery to contribute a controlled 20% of the power required to sustain the load and switch 3 operates with an 80% duty cycle, providing the majority of the power from the supercapacitor to the load demand. After delivering 20% of power from battery, switch 1 is off and switch 3 is on to supply 80% of power from supercapacitor. When the voltage difference from battery to supercapacitor is greater than 3 and less than 10, switch 1 is engaged with a 80% duty cycle, allowing the battery to contribute the majority of the power from the battery and switch 3 operates with only 20% duty cycle, only 20% of the power from supercapacitor. When the power demand surpasses 3000 and the voltage difference from battery to supercapacitor is greater than 10, the HESS employs a straightforward effective approach by activating only switch 1 to supply power from battery.

Specifying the voltage difference between batteries and supercapacitors depends on the various factors for the applications. With a lower threshold, the system transitions to the supercapacitors at a relatively small voltage difference, ensuring frequent and efficient utilization of the supercapacitor's rapid discharge capabilities. A lower voltage difference threshold enables the system to respond quickly to sudden changes in power demand.

3.2.3 Simulation of Hybrid Energy Storage System

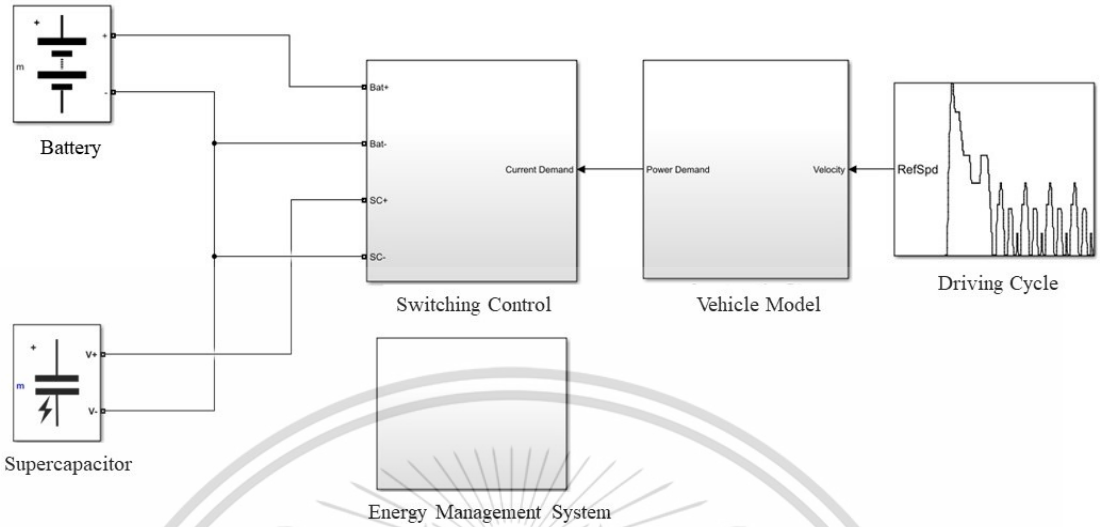

Figure 3.20 Simulation model of Hybrid Energy Storage System.

A Simulink model is developed to represent a hybrid energy storage system comprising a battery and supercapacitor block, a switching control block, a power demand block, an energy management block, and a driving cycle. The fundamental workflow of the model involves obtaining the power demand for a vehicle from the driving cycle Figure 3.21. The model incorporates a dynamic mechanism where the charging and discharging of the battery and supercapacitors are determined upon the sign of the power demand.

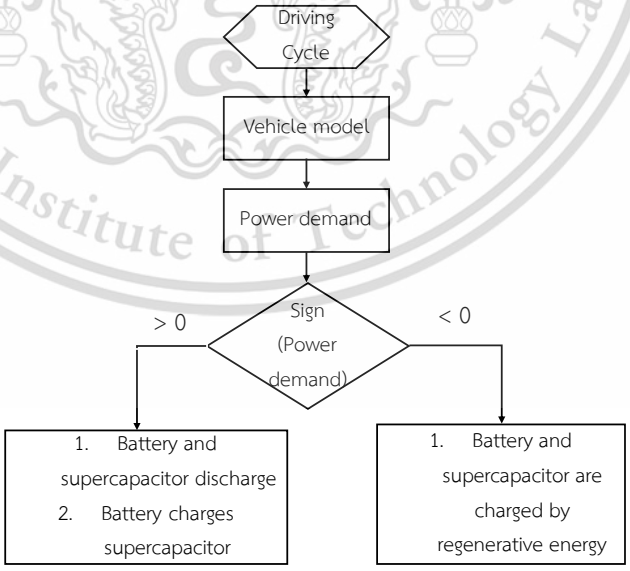

Figure 3.21 Flowchart for the overall working principle of HESS.

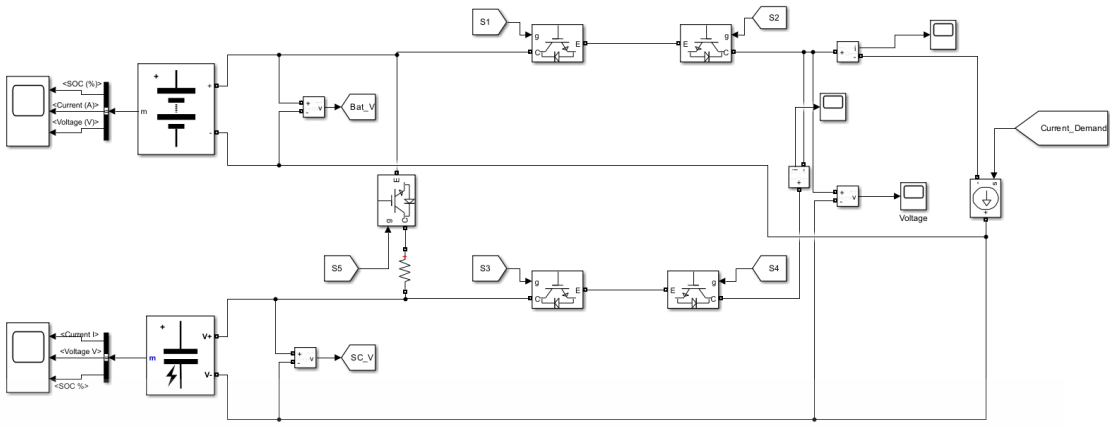

Figure 3.22 Switching control in Simulink.

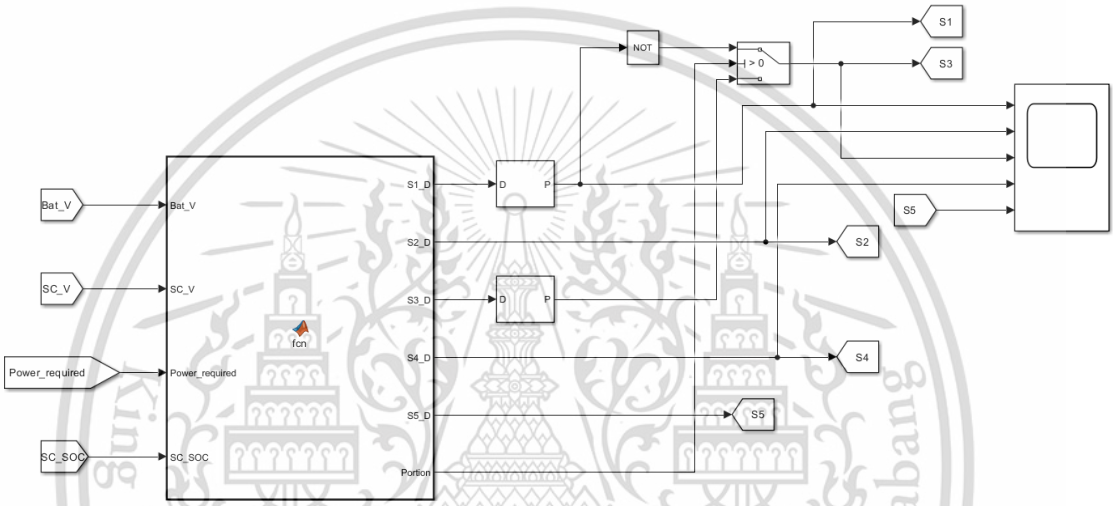

Figure 3.23 Energy management system.

The input sigals of the EMS are the SOC of the batteries (SOC_{Bat}), SOC of the supercapacitors (SOC_{SC}), voltage of the batteries (V_{Bat}), voltage of the supercapacitors (V_{SC}) and power demad of the electric vehicle and the output of the EMS the duty cycle for the switches to operate the switching between batteries and supercapacitors. When the the vehicle is stopped that is the power requirement of the vehicle is zero, the battery uses its rated power to charge supercapacitor if the SOC of supercapacitor is below the threshold value 90%.

If the speed of the vehicle is different from zero, the power requirement of vehicle become high and power variation from battery to supercapacitor is needed. The positive power requirement represents the fact that the vehicle is driving. In this situation, the battery or supercapacitor have to supply the required driving current to meet the vehicle driving demand. To separate the usage of battery only and together with battery and supercapacitor, power requirement is limited at 3000W. For the regenerative braking operation, if the SOC of the battery is less than 95%, it is directly charged by the load power.

3.2.4 Simulation of Lithium-ion battery model

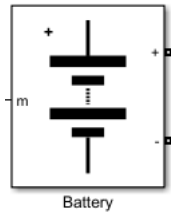

Figure 3.24 battery Block in Simulink.

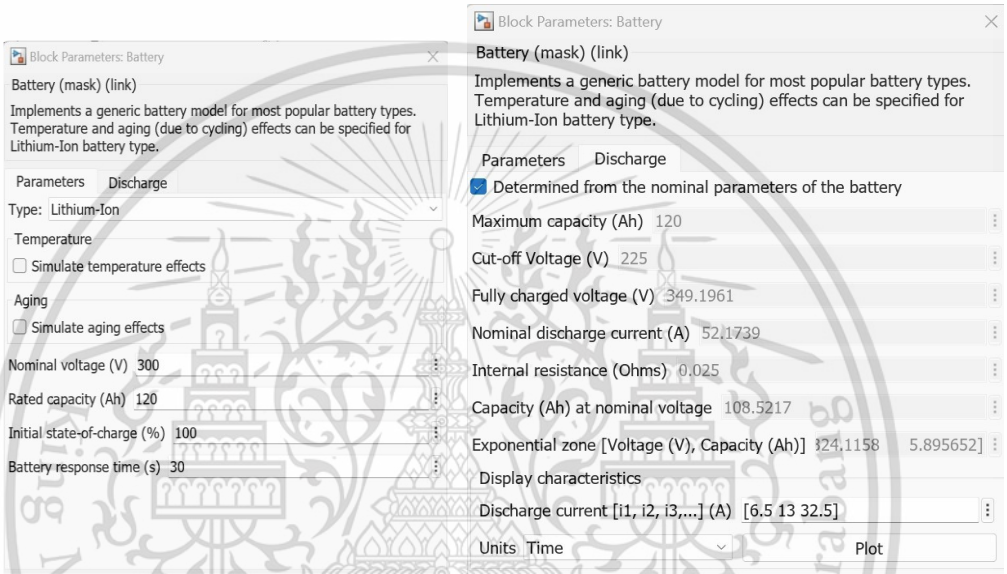

Figure 3.25 Parameters of batteries model block.

This section describes the dynamic discharge behaviors of battery pack in order to accurately identify its operational voltage and state of charge. By using battery model in MATLAB, many parameters such as nominal voltage, rated capacity and initial state-of-charge are defined, and this model represents the Lithium-ion battery pack model. To validate the experiment of the pulse discharge, the simulation was needed to confirm the experimental model behavior of the lithium-ion battery. To meet the vehicle power performance criteria, the battery pack for an electric car needs a higher power density. Total voltage, capacity energy, and battery numbers are considered for the choice of battery pack. It is assumed that the battery pack's nominal voltage (V_b) is 350V. When constructing a battery pack for an electric vehicle, capacity and power are the two most important factors to consider. The capacity of the battery is determined by calculating the electric power consumption of EV with the desired nominal voltage.

$$C_b = \frac{E_b}{V_b} \tag{3.1}$$

$$E_b = \frac{P_b}{v} \tag{3.2}$$

$$N_{series} = \frac{V_b}{V_c} \quad 3.3$$

$$N_{series} = \frac{C_b}{C_c} \quad 3.4$$

where N_{series} and $N_{parallel}$ are the number of cells in series and in parallel and V_{Cell} is the terminal voltage of single cell and V_{Bat_Pack} is the terminal voltage of battery pack and I_{Cell} is the current of single cell and I_{Bat_Pack} is the current of battery pack. The number of battery cells connected in series is calculated by dividing the nominal voltage of the whole battery pack (V_b) to the voltage of each cell (V_c). The number of cells linked in parallel is determined as the ratio of battery pack total capacity (C_b) and capacity of each battery cell (C_c) as shown in equation 3.3. Figure 3.10 shows the battery model that was created in MATLAB/Simulink.

Table 3.6 Specifications of battery pack in EV.

Specifications	Values
Nominal voltage	300V
Capacity	120Ah
Cut-off voltage	225V
Nominal discharge current	52.17
Internal resistance	0.025Ω

3.2.5 Simulation of supercapacitor model

The simulation of a supercapacitor model in Simulink is an important step in optimizing the performance of energy storage systems within electric vehicles (EVs). In this simulation, the chosen parameters were directly aligned with the design requirements for the desired power demand. By carefully selecting these parameters, including capacitance, voltage ratings, and equivalent series resistance (ESR), the simulation allows for a thorough evaluation of the supercapacitor's ability to efficiently capture, store, and deliver energy as needed, contributing to the overall performance and energy efficiency of the EV.

Table 3.7 Specifications of supercapacitor model

Specifications	Values
Rated capacitance	99.5F
Rated voltage	320V
Initial voltage	320V
Maximum ESR	0.0089

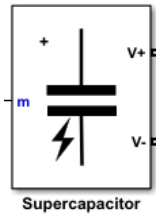

Figure 3.26 Supercapacitor block in Simulink.

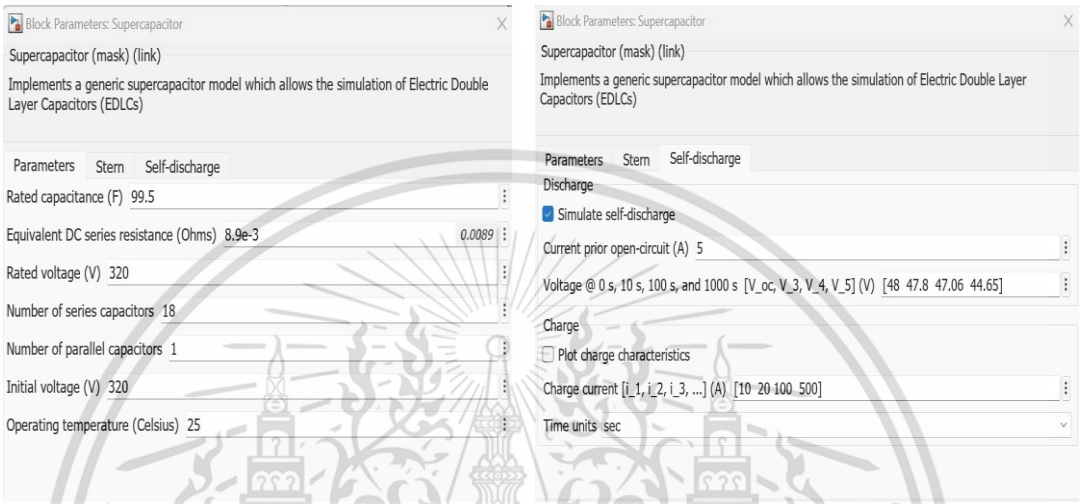

Figure 3.27 Parameters of supercapacitor model block in Simulink.

3.2.6 Methodology for power load

To demonstrate the operation of an EV, a vehicle dynamic model was implemented in MATLAB/Simulink. As driving cycle data simulates real-world driving situations by providing data at different speeds over time, standard drive cycle data will be used in this model. The design of vehicle dynamics is inspired from the specifications of a Chevrolet Bolt EV. The specifications of the electric vehicle used in this model are presented in table 3.8. To determine the amount of power needed from the energy storage system, the speed profile data is converted to a power profile data. Rolling resistance power, aerodynamic drag power, slope resistance power and acceleration resistance power are all considered for the total power demand. Drive cycle data is used to validate the modeling results and this model uses NEDC and WLTC driving cycle to calculate the power of an electric vehicle. The overview for finding the power demand from the resistance force was mentioned in

Figure 3.29. The required power demand is calculated by multiplication of the speed of the vehicle at a specific time and the aerodynamic, Inertia, rolling and gradient resistance forces. The overview for calculation of power from electric vehicle in MATLAB/Simulink software is represented in Figure 3.30.

Figure 3.28 Chevrolet Bolt EV model

Table 3.8 Specifications of electric vehicle.

Description	Values
Vehicle mass	1616.15 kg
Vehicle inertial mass	1678.30 kg
Air density	1.14kgm^{-3}
Aerodynamic drag coefficient	0.3
Rolling resistance coefficient	0.02
Gradient	0
Wheel radius	0.315(m)
Vehicle frontal area	2.1 m^2

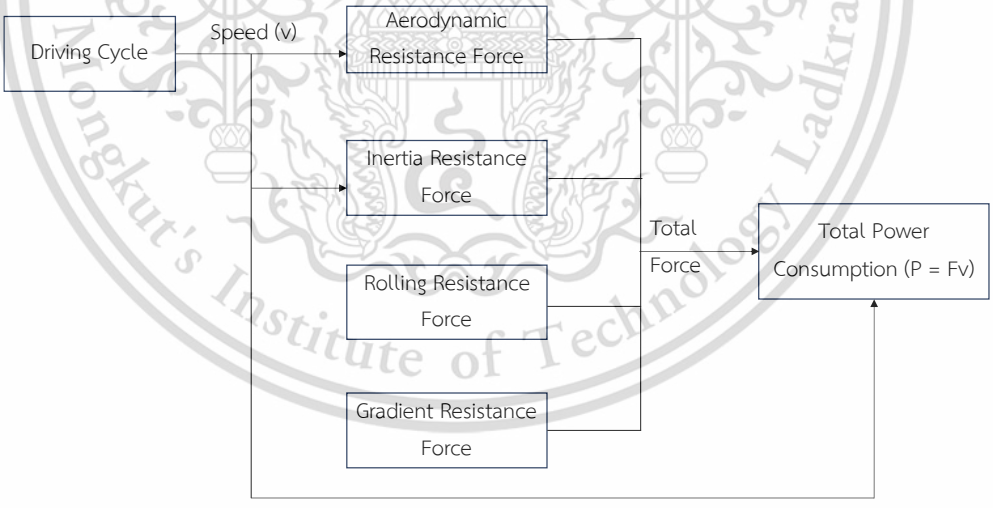

Figure 3.29 Power calculation for driving cycle.

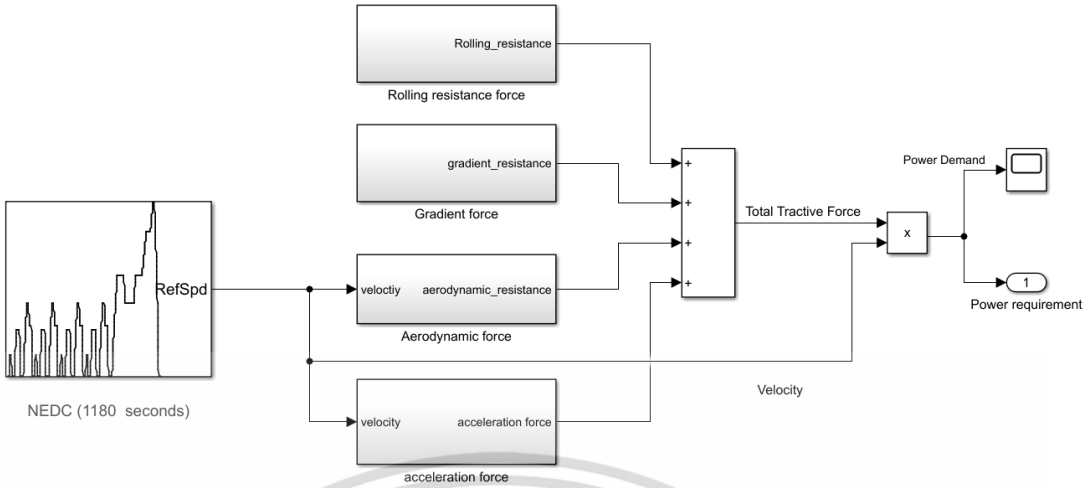

Figure 3.30 Energy consumption model in MATLAB/Simulink software.

According to the equation the total current demand for battery can be calculated by dividing the total power demand by the voltage of the bus voltage between battery and supercapacitor.

$$I_{load} = \frac{P_{veh}}{U_{bus}} \quad 3.5$$

where

U_{bus}=the bus voltage

P_{veh}=the power demand of electric vehicle

I_{load}=the current demand from load

Chapter 4 Results and Discussions

In this chapter, we will discuss the results of proposed experimental studies on effects of switching frequencies over characteristics of lithium-ion batteries. We will also discuss the performance of simulation model for validation of pulse discharging method in hybrid energy storage system tested at different switching frequencies.

4.1 Experimental results of Batteries pack

In this study, we analyze the impact of pulse discharging on lithium-ion batteries in accordance with the experimental procedures from Table 3.5. Two methods of discharging were used to analyze the study: pulse discharging and constant current discharge. The frequency (0Hz, 200Hz, 400H, 600Hz, 800Hz, 1000Hz), duty cycle (75%), and C rate (0.5C and 1C) are selected for the study. In this chapter, the experimental results of the Panasonic NCR18650GA battery pack is shown. The open circuit voltage (OCV) of the battery pack was not consistent throughout the testing despite maintaining a consistent OCV at the beginning of the test. This was because of a delay in connection induced by an error when connecting to the electronic load. The voltage behavior of battery pack during pulse discharge at 400Hz, 800Hz is shown in Figure 4.1 and Figure 4.2. The discharging curve of voltage of battery pack with constant current is presented in Figure 4.3. The total discharging time of battery pack tested with pulse discharging at switching frequencies of 200Hz, 400Hz, 600Hz, 800Hz and 1000Hz are compared with constant current discharging method to explore the effects of pulse discharging at various frequencies. The voltage curve of the battery pack at o.5C and 1C at various switching frequencies are shown in figure 4.4 and 4.5.

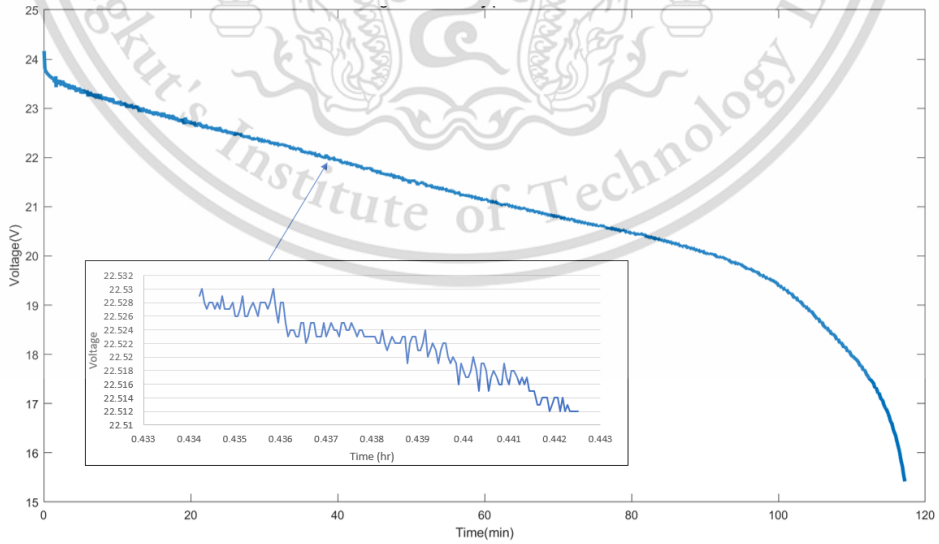

Figure 4.1 Voltage of battery pack during discharging at 400Hz 0.5C

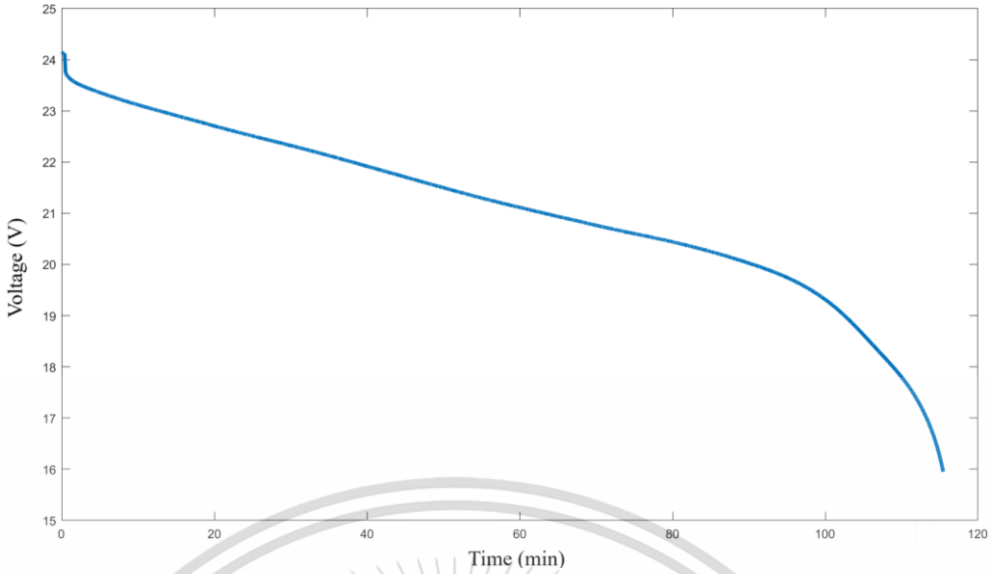

Figure 4.2 Voltage of battery pack during discharging at 800Hz 0.5C.

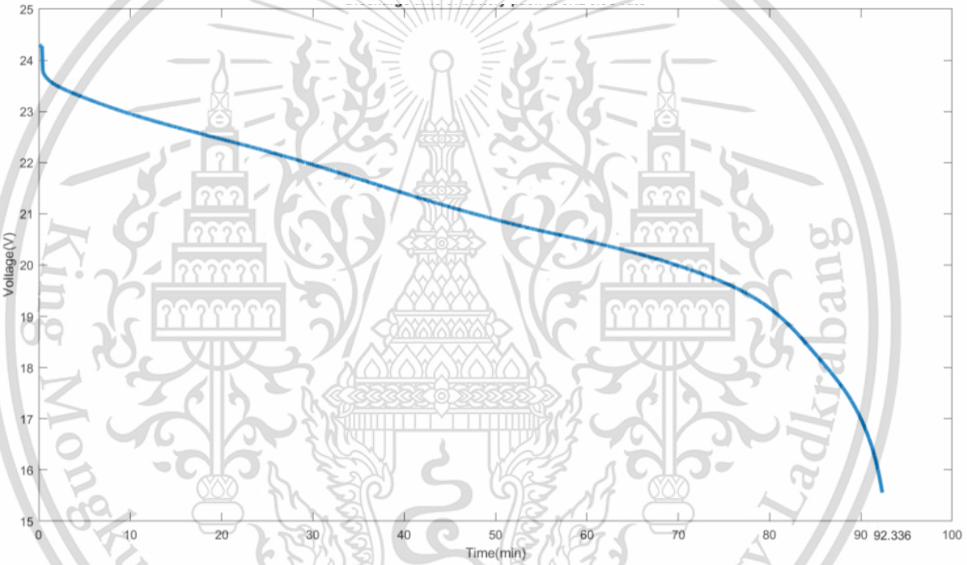

Figure 4.3 Voltage of battery pack with constant current discharging at 0.5C.

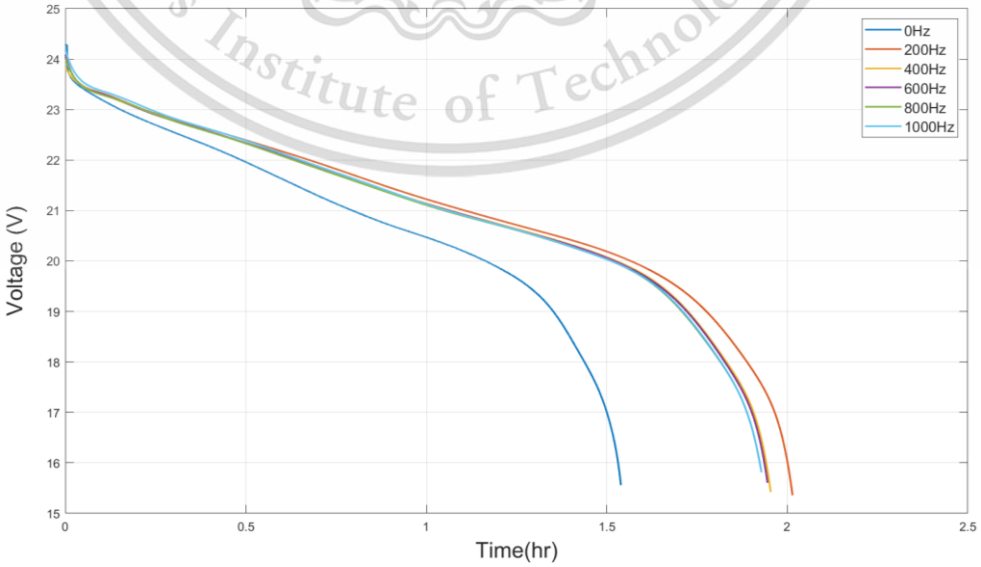

Figure 4.4 Total discharging time of battery pack at 0.5C.

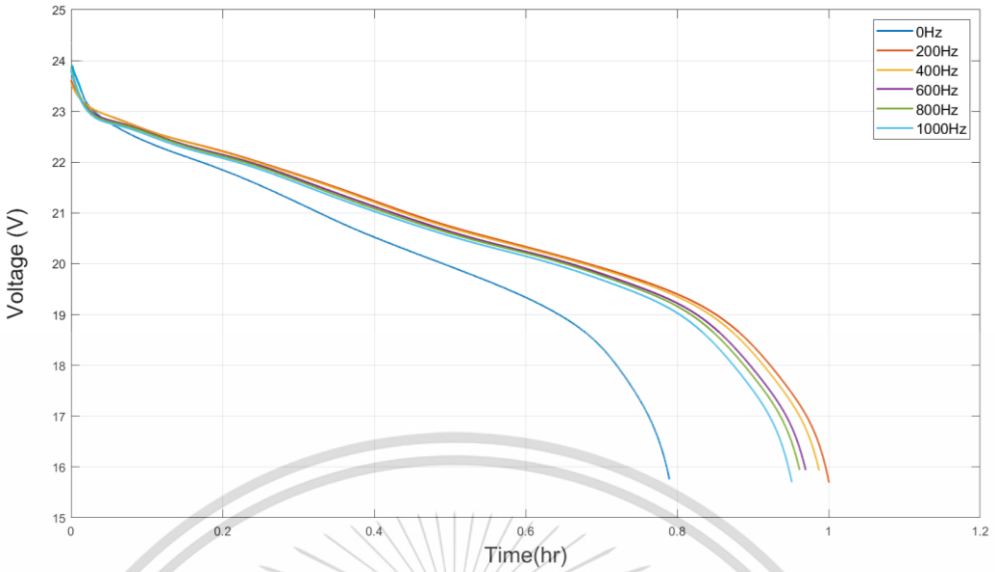

Figure 4.5 Total discharging time of battery pack at 1C.

The total discharging time of battery pack not only at 0.5C but also at 1C took long time at 200Hz. The battery took the longest time to discharge when it was discharged at 200 Hz as opposed to other frequencies. Discharging time with 400Hz frequency had the second longest duration and 1000Hz frequency generated the shortest discharge time among all the frequencies. Therefore, when switching frequencies are low, discharge time of battery is longer.

Figure 4.6 and Figure 4.7 illustrate the discharging capacity of battery pack test at 0.5C and 1C at different frequencies. From the results, it can be seen that in terms of discharging time, constant current discharging recorded a duration of approximately 1.7 hours, whereas pulse discharging recorded more than 2 hours due to relaxation time. The discharging time at low switching frequency generates longer duration than at high switching frequency.

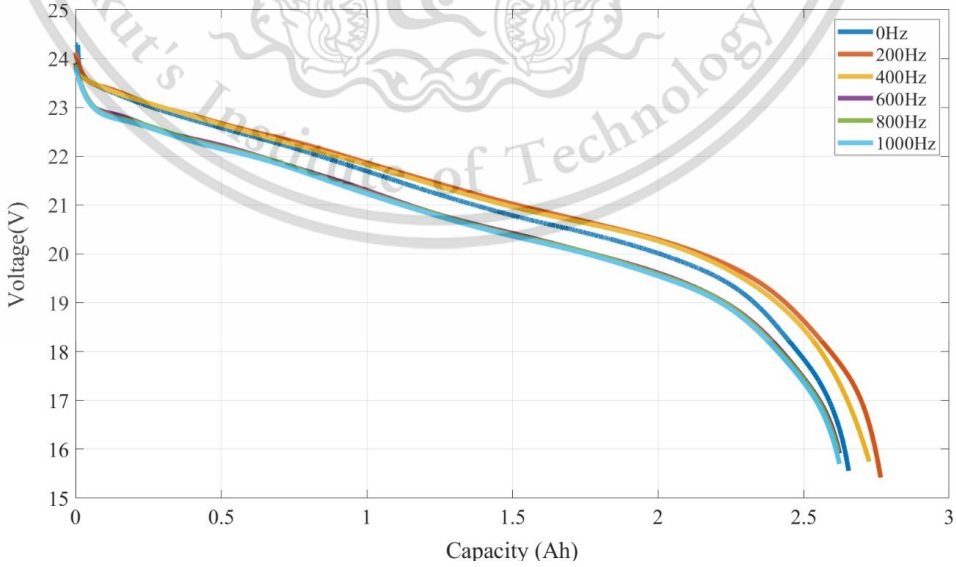

Figure 4.6 Comparison of Discharging capacity of pulse discharging and constant current discharging at 0.5C

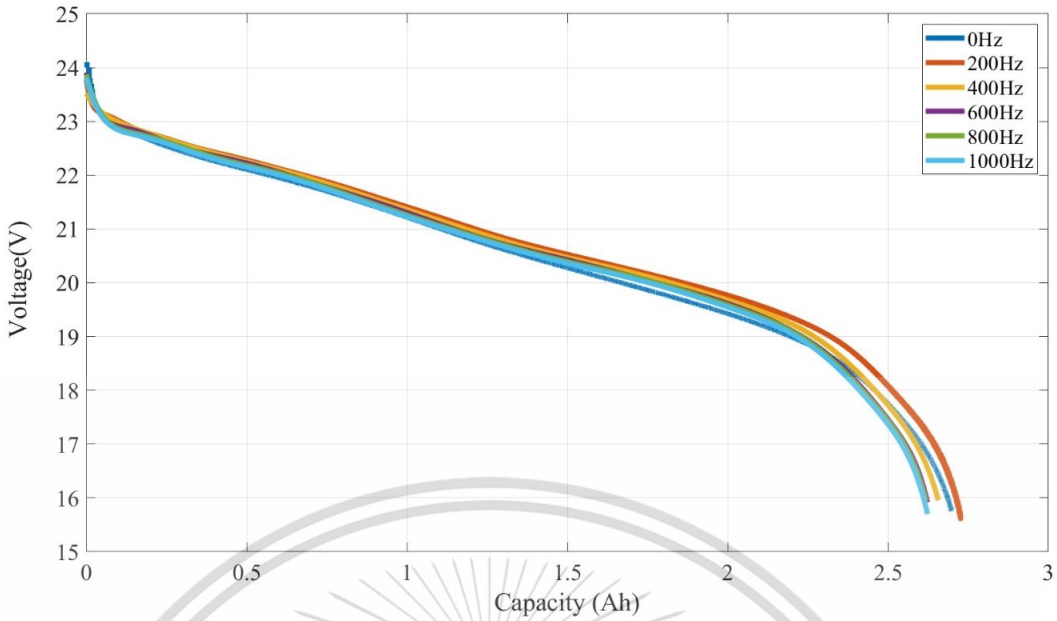

Figure 4.7 Comparison of Discharging capacity of pulse discharging and constant current discharging at 1C.

Figure 4.8 and figure 4.9 illustrate the energy of battery during discharging at 0.5C and 1C at different frequencies. From the results, it can be seen that pulse discharging at low frequency 200Hz offered a significant increase in energy compared to 400Hz, 600Hz,800Hz and 1000Hz. When compared to constant current and pulse current discharging, pulse current generates higher discharge energy according to the results.

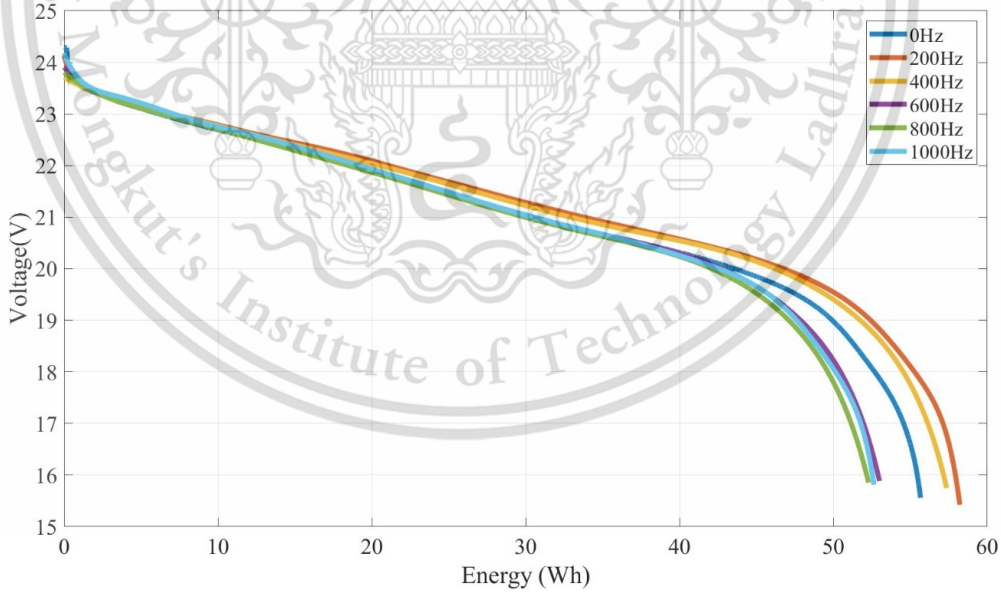

Figure 4.8 Comparison of energy of pulse discharging and constant current discharging at 0.5C

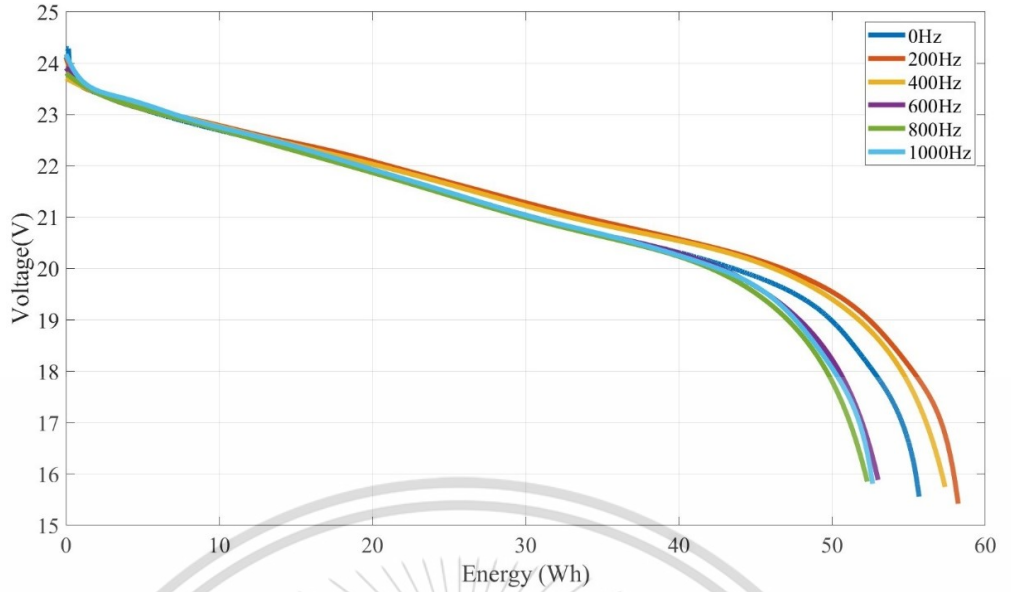

Figure 4.9 Comparison of energy of pulse discharging and constant current discharging at 1C.

Figure 4.10 Comparison of discharge energy at different frequencies at 1C.

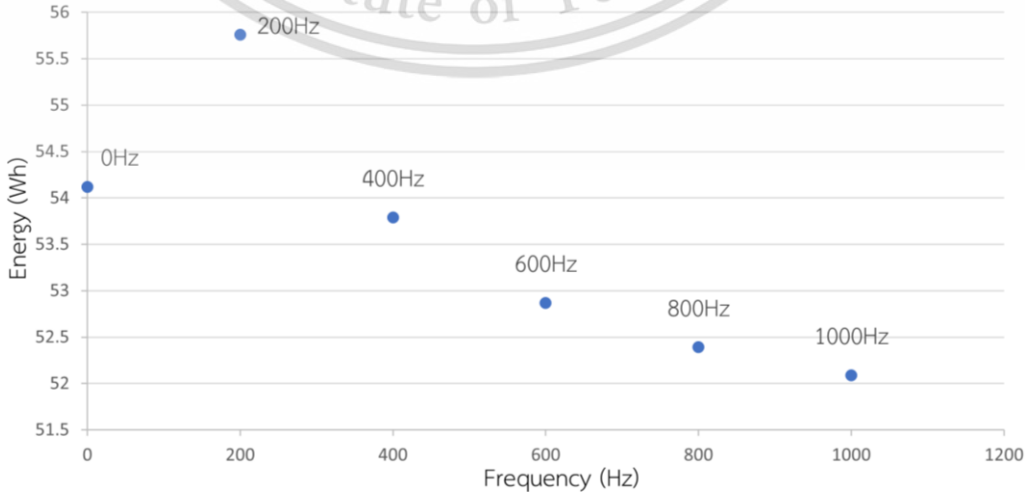

Figure 4.11 Comparison of discharge energy at different frequencies at 0.5C.

According to the results from Figure 4.10 and Figure 4.11, it can be seen that pulse discharging at low frequency 200Hz offered a significant increase in energy compared to 400Hz, 600Hz,800Hz and 1000Hz. Overall, in terms of discharging time, pulse current discharging generated longer discharging time than constant current discharging. The discharging time at low switching frequency generated longer duration than at high switching frequency. In terms of discharge energy, pulse current discharging produced higher discharge energy than constant current discharging due to the recovery of energy during rest. In terms of frequencies, discharging at low switching frequencies generates greater results than at high switching frequencies.

4.2 Simulation results of HESS with pulse discharging method in NEDC drive cycle

A simulation model was built on MATLAB/Simulink for the proposed energy management system utilizing pulse discharging. The simulation was carried out on New European Driving Cycle (NEDC) to test the control strategy of pulse discharging in HESS. Simulation results and comparisons of HESS outputs between various switching frequencies for NEDC driving cycle are shown in this section. The vehicle went in three phases: an acceleration phase, a constant speed phase and a deceleration phase and it was driven to a maximum speed of 120km/hr. The speed data and power demand of the vehicle are presented in figure 4.10 and figure 4.11.

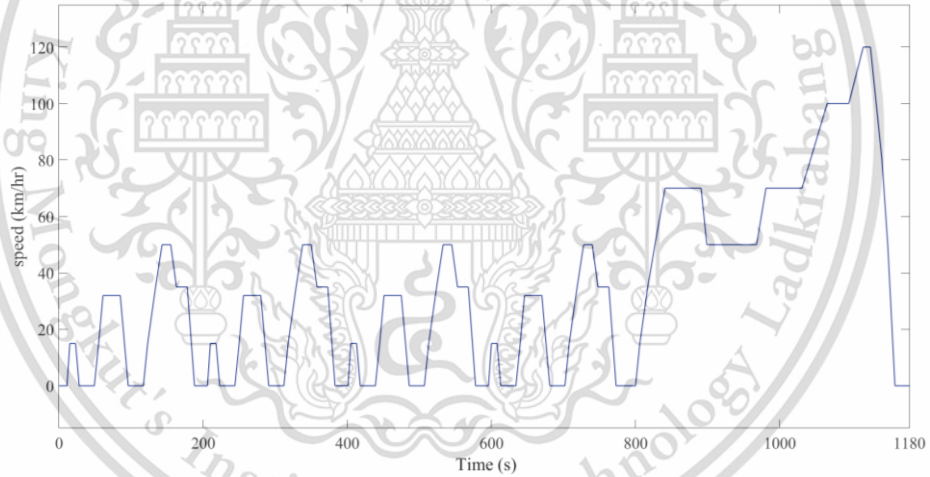

Figure 4.12 NEDC driving cycle profile.

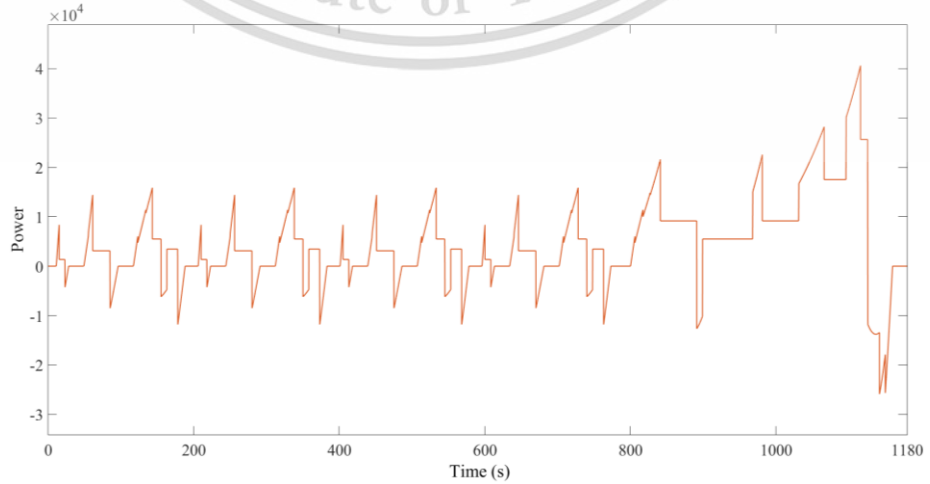

Figure 4.13 Power demand of electric vehicle.

4.2.1 Pulse discharging at 200Hz switching frequency

The first test of simulation is performed at 200Hz switching frequency with NEDC driving cycle in Simulink. In the first 11s, when the vehicle is stopped, the batteries charged the supercapacitors as the SOC of supercapacitor is less than 99%. It can be observed that the current of the supercapacitor becomes negative, and it receives some power from the battery. At 12s, only the batteries start to provide power as the demand of power is less than 3000W and supercapacitor is still charged by battery. At 12.439s, the power of electric vehicle starts higher than 3000W and the voltage difference of battery and supercapacitor is greater than 10, only battery generates the power for the electric vehicle and stops charging of supercapacitor. At t = 23s, the speed of electric vehicle decreases to its reference, enabling regenerative braking. However, as the voltage difference of battery and supercapacitor is greater than 3, which means the voltage of battery is greater than supercapacitor, the system only allows the supercapacitors to charge. It is observed that the sign of the supercapacitor power is negative, and it is charged by regenerative power during EV is moving. The energy management system is regarded as the power sharing when the load power is lower than 3000W, the battery supplies a full load power, and the supercapacitors is charged by battery. While the load power is greater than 3000W, battery and supercapacitors is discharged by pulse method with specified duty cycle and frequencies. The battery voltage, current and SOC data are presented in Figure 4.14 - Figure 4.16.

When the load power goes up above 3000W, the power sharing between battery and supercapacitor is performed and the sharing strategy is based on the voltage difference between battery and supercapacitor. At t = 710.13s, the energy management system is subjected to a rising power request from the load and energy sharing with pulse discharging of duty cycle 80% and 20% is conducted for supporting power to the vehicle. The switching frequencies of the HESS are changed and tested at various frequencies at 200Hz, 400Hz, 6000Hz, 800Hz and 1000Hz. The variation of characteristics of battery and supercapacitor is compared at different frequencies. The voltage, current and SOC of supercapacitor is shown in Figure 4.17 - Figure 4.19.

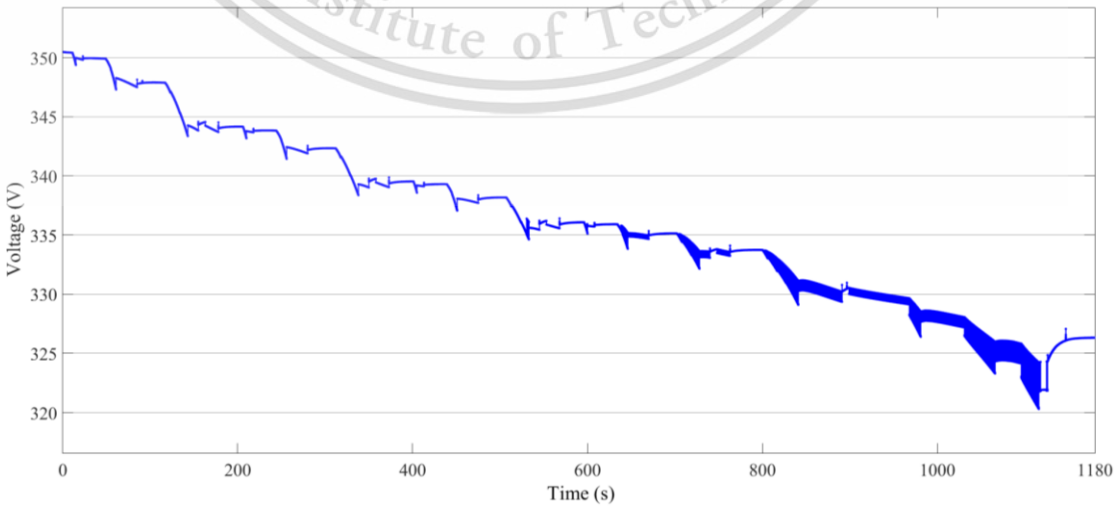

Figure 4.14 Battery Voltage at 200Hz frequency.

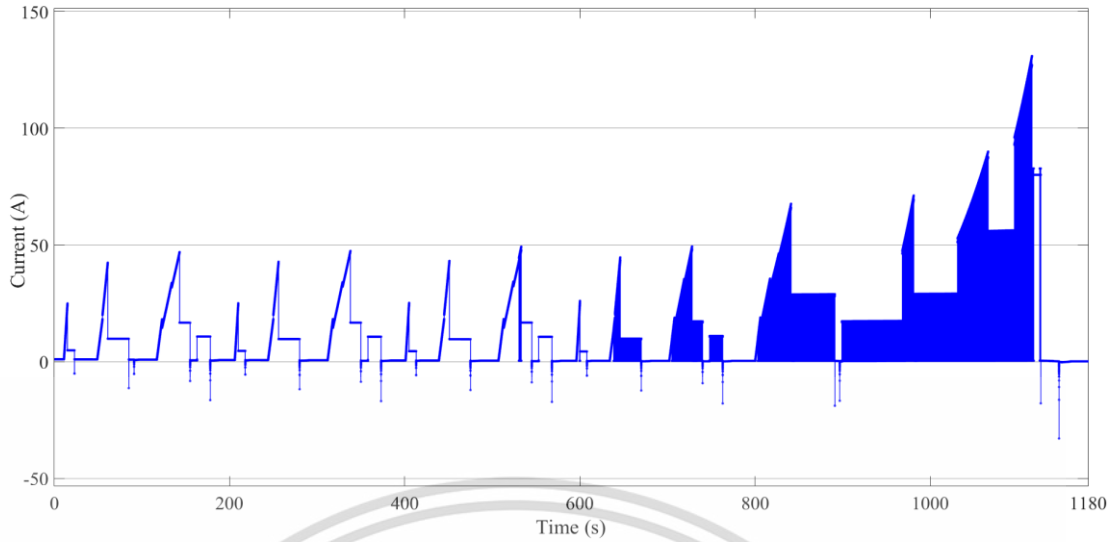

Figure 4.15 Battery current at 200Hz frequency.

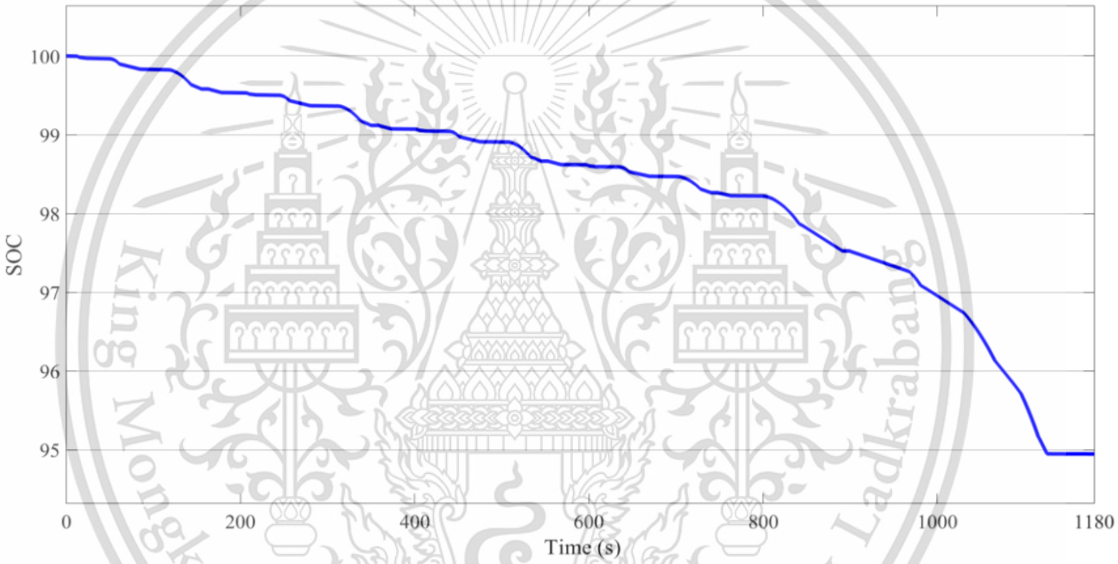

Figure 4.16 Battery SOC at 200Hz frequency.

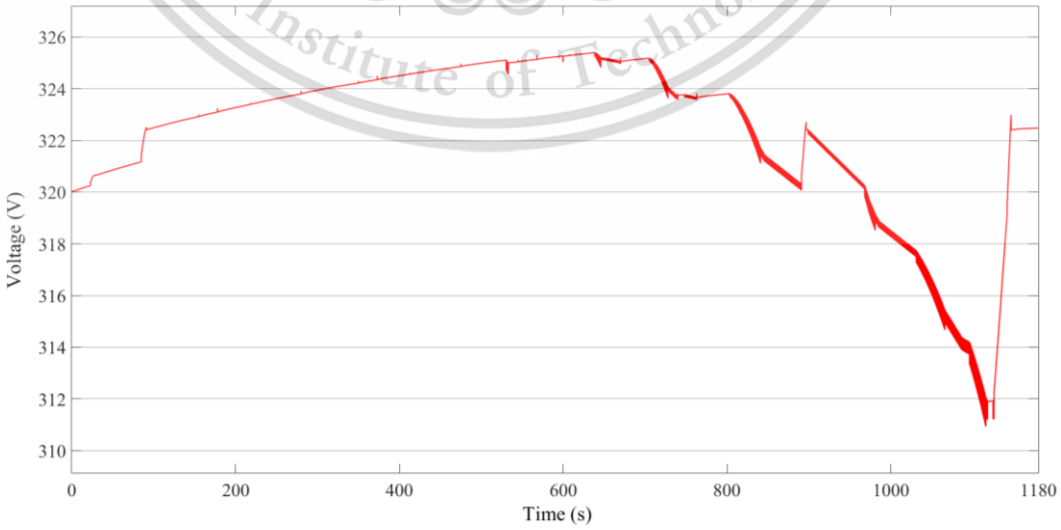

Figure 4.17 Supercapacitor voltage at 200Hz frequency.

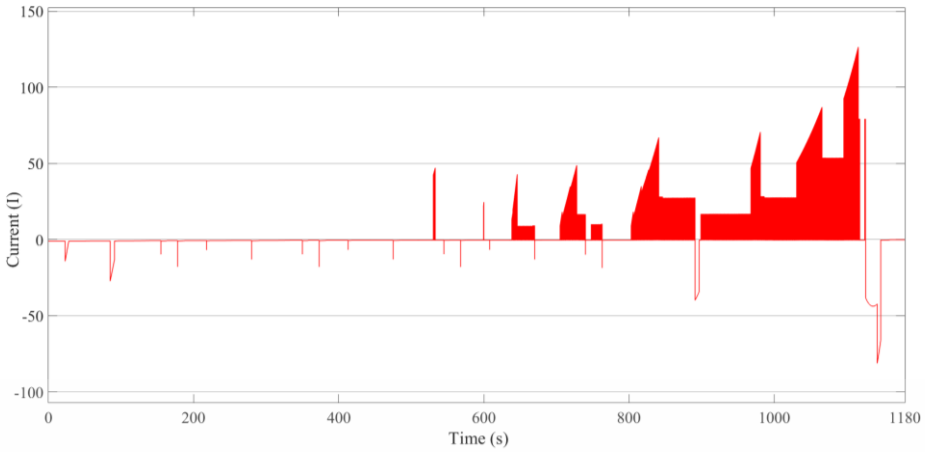

Figure 4.18 Supercapacitor current at 200Hz frequency.

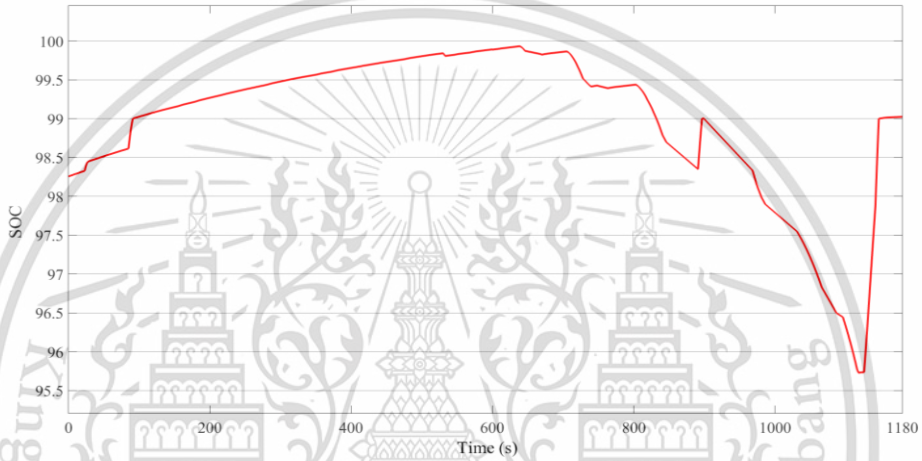

Figure 4.19 Supercapacitor SOC at 200Hz frequency.

Figure 4.18 and 4.19 shows charge and discharge state of battery and supercapacitor in which only batteries provide the average power required by the EV load, and during high acceleration and decelerations phase supercapacitors and batteries perform charging and discharging together. Additionally, supercapacitors draw energy from the batteries when the SOC falls below the minimum threshold, acceleration to restore the energy to help the batteries in the next accelerations and braking phases.

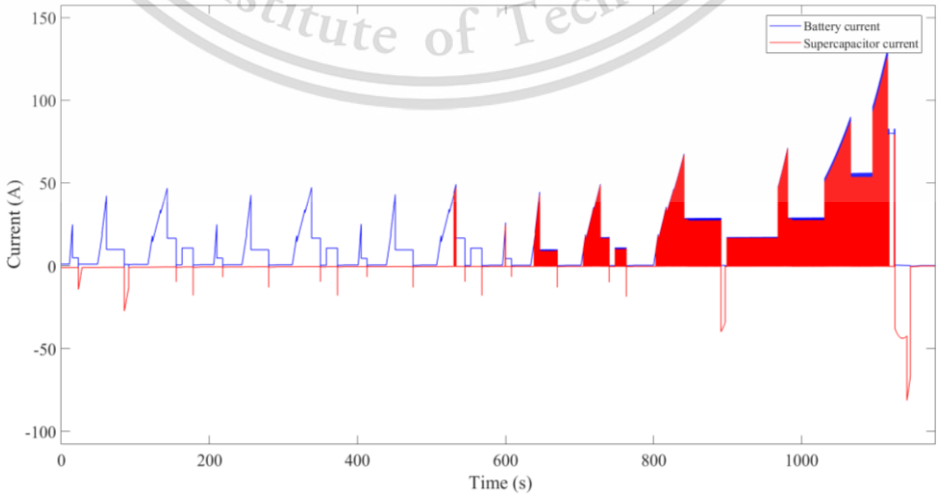

Figure 4.20 Battery current and supercapacitor current at 200Hz frequency.

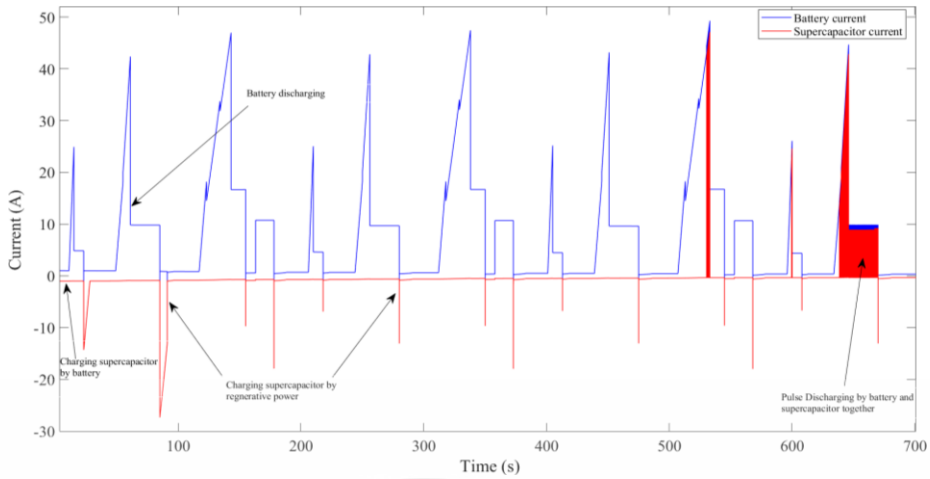

Figure 4.21 Charging and discharging current of battery and supercapacitor at 200Hz frequency.

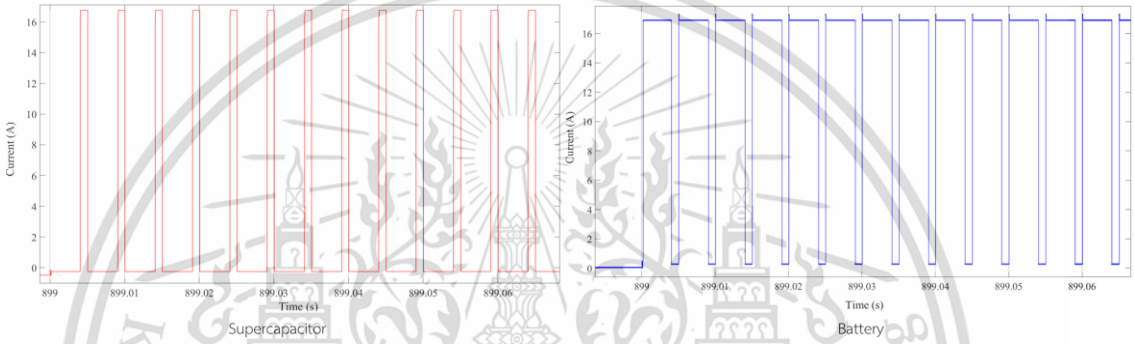

Figure 4.22 Supercapacitor and battery pulse current with 20% and 80% duty cycle.

4.2.2 Pulse discharging at 400Hz switching frequency

Another simulation of changing the switching frequency of switches is performed and tested with NEDC driving cycle. The voltage and current of batteries changed during the test with 400Hz switching frequency is shown in Figure 4.23-Figure 4.24. The characteristics of voltage and current of supercapacitor is shown in Figure 4.25-Figure 4.26 and the amount of power produced by supercapacitor during charging and discharging state is Figure 4.27Figure 4.27. Power demand from electric vehicle and total power output from batteries and supercapacitor is compared and the results from Figure 4.28 shows that battery and supercapacitor can generate the required output power and batteries and supercapacitors is charged according to the threshold value of SOC during regenerative braking.

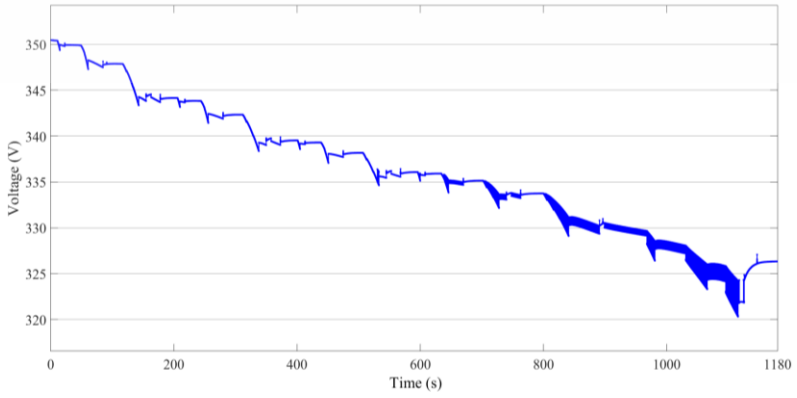

Figure 4.23 Battery voltage at 400Hz switching frequency.

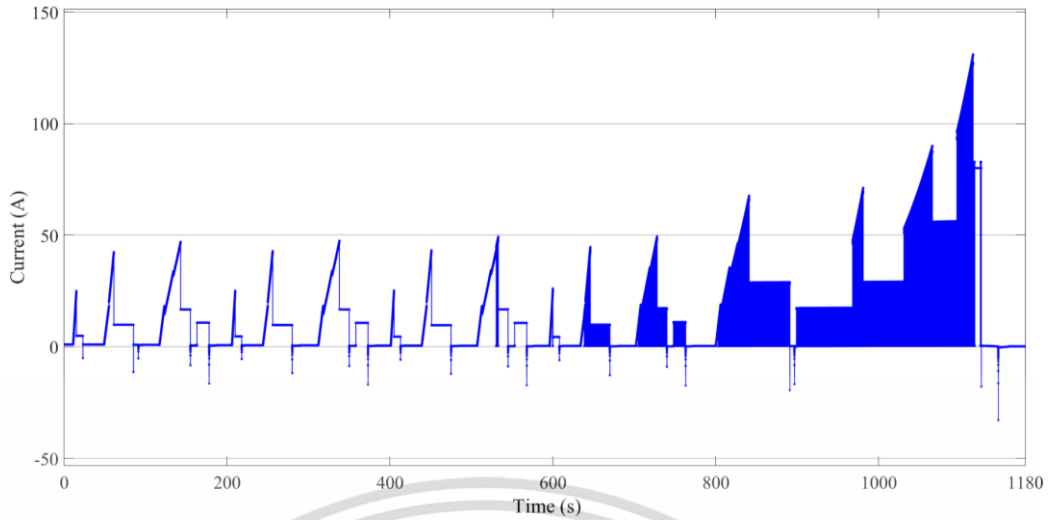

Figure 4.24 Battery current at 400Hz frequency.

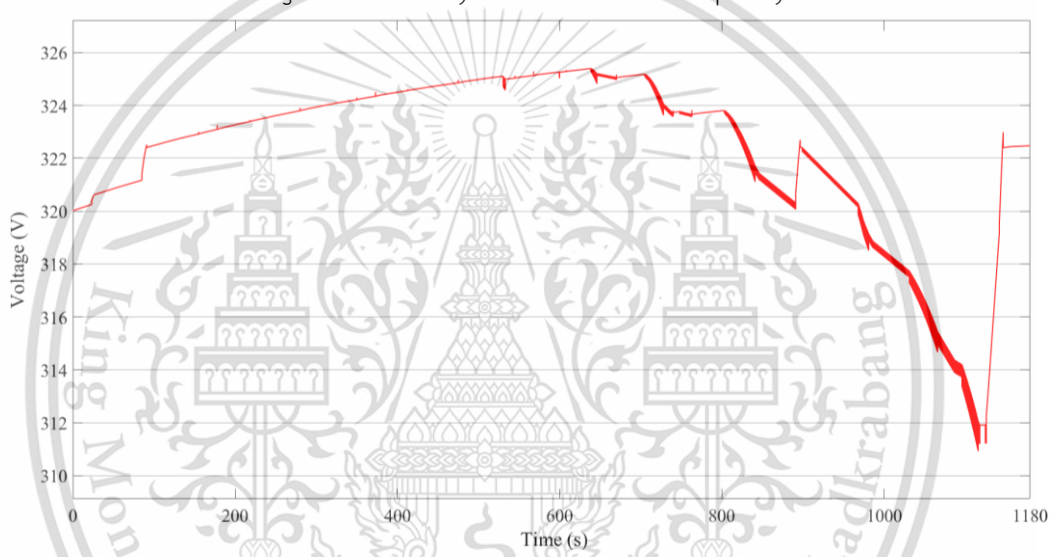

Figure 4.25 Supercapacitor voltage at 400Hz switching frequency.

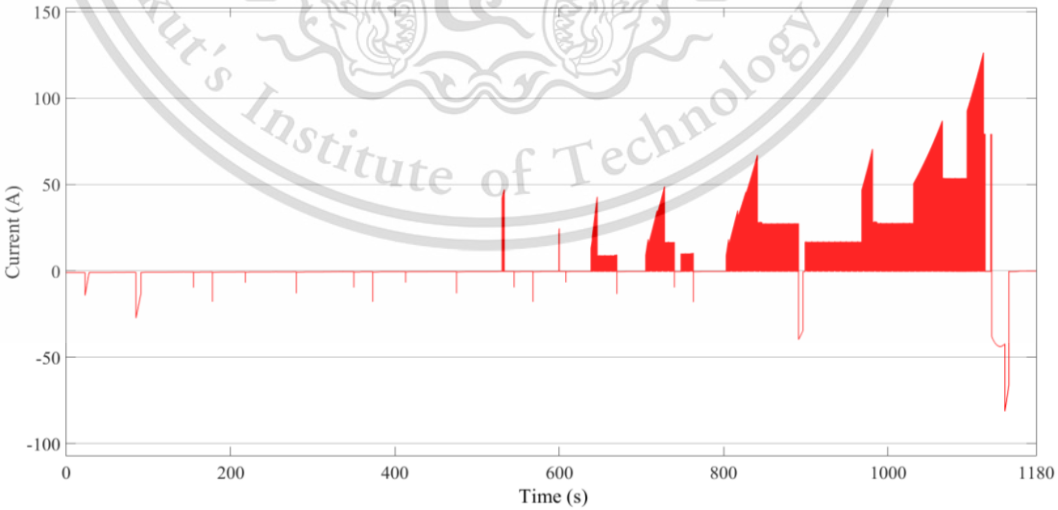

Figure 4.26 Supercapacitor current at 400Hz switching frequency.

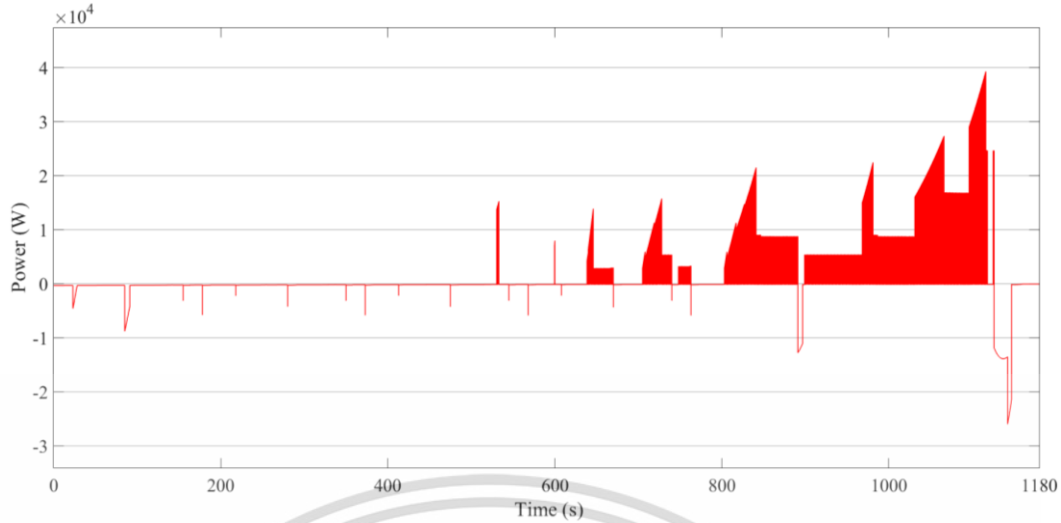

Figure 4.27 Supercapacitor power at 400Hz switching frequency.

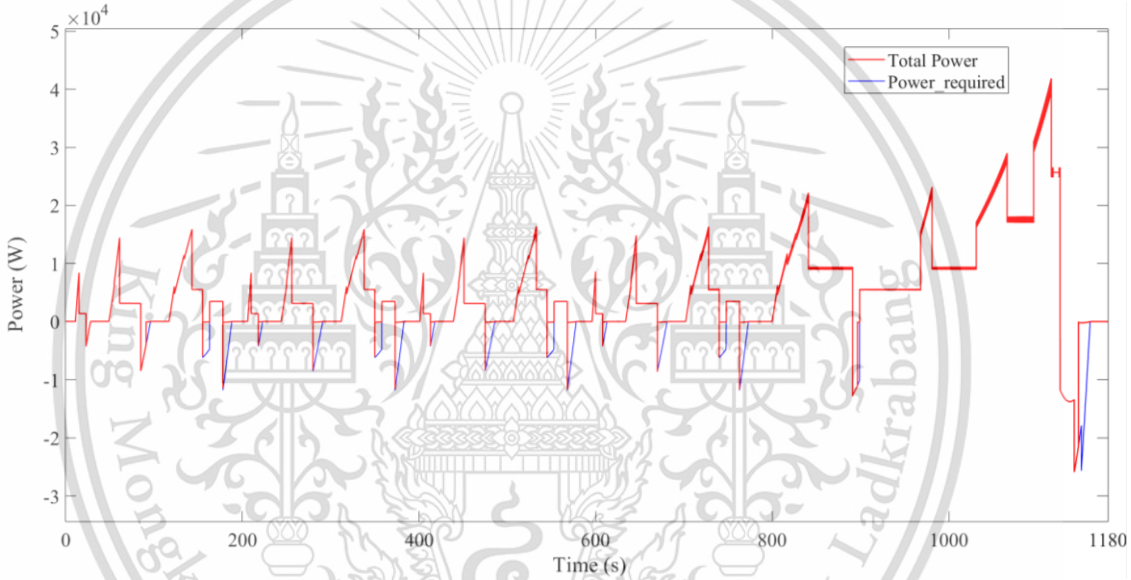

Figure 4.28 Comparison of power demand and total power from Battery and supercapacitor at 400Hz frequency.

4.2.3 Pulse discharging at 600Hz switching frequency

Simulation of hybrid energy storage system deployed pulse current method is tested at 600Hz switching frequency. The characteristics of batteries changed during the test with is shown in Figure 4.29-.Figure 4.30. The characteristics of supercapacitor changed during the test with is shown in Figure 4.31-Figure 4.32.

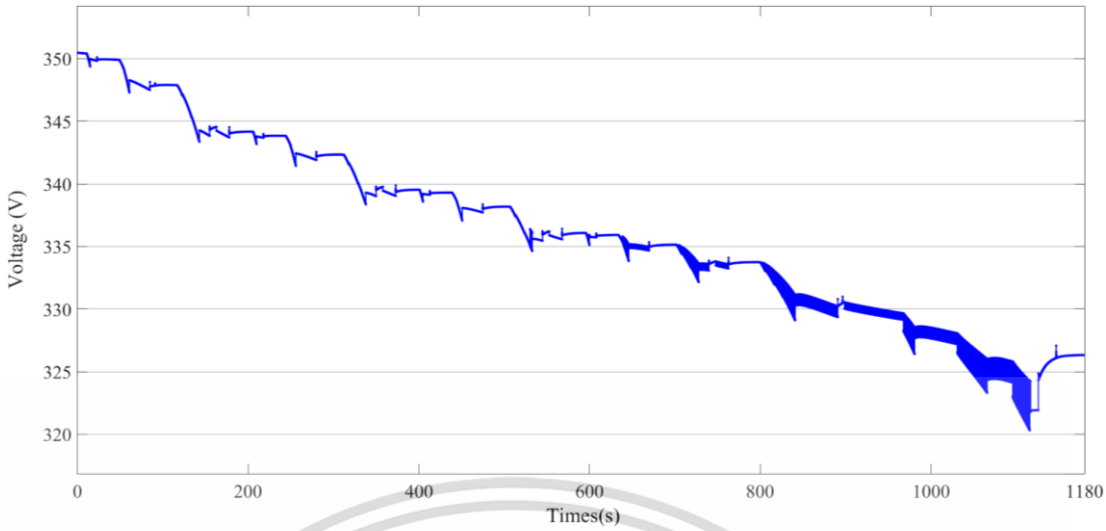

Figure 4.29 Battery voltage at 600Hz frequency.

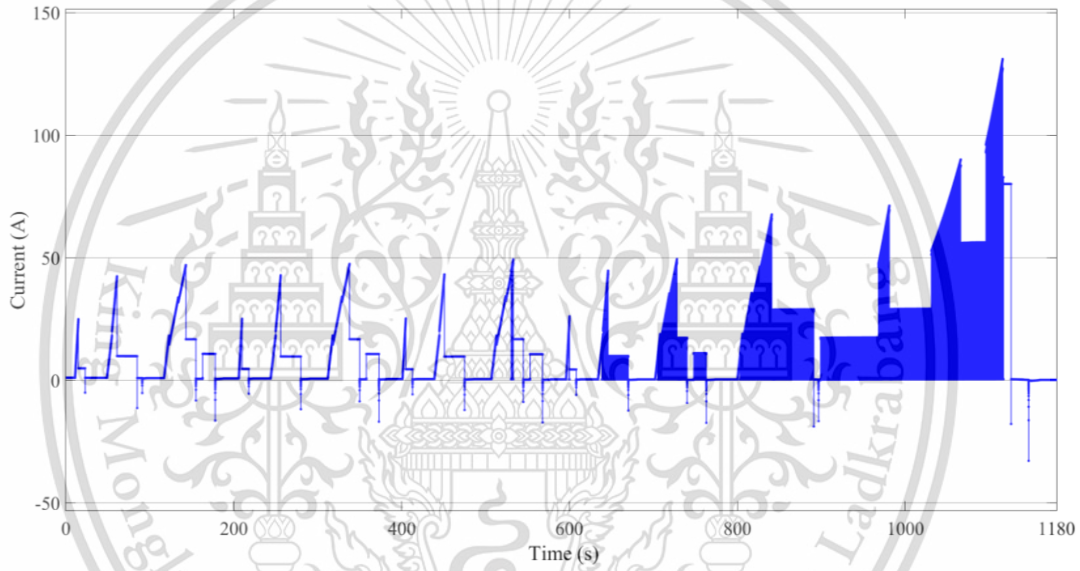

Figure 4.30 Battery current at 600Hz frequency.

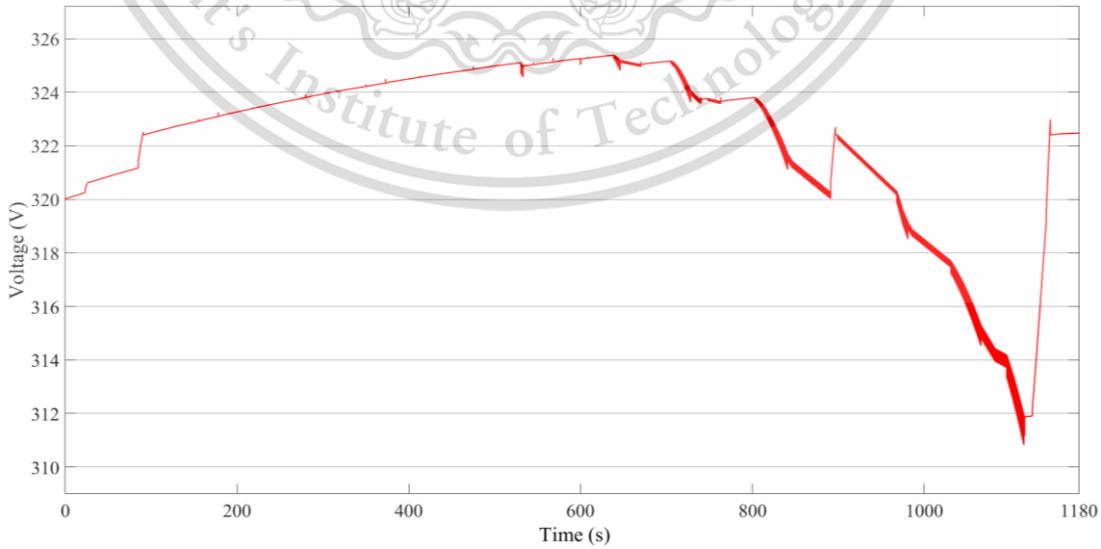

Figure 4.31 Supercapacitor voltage at 600Hz frequency.

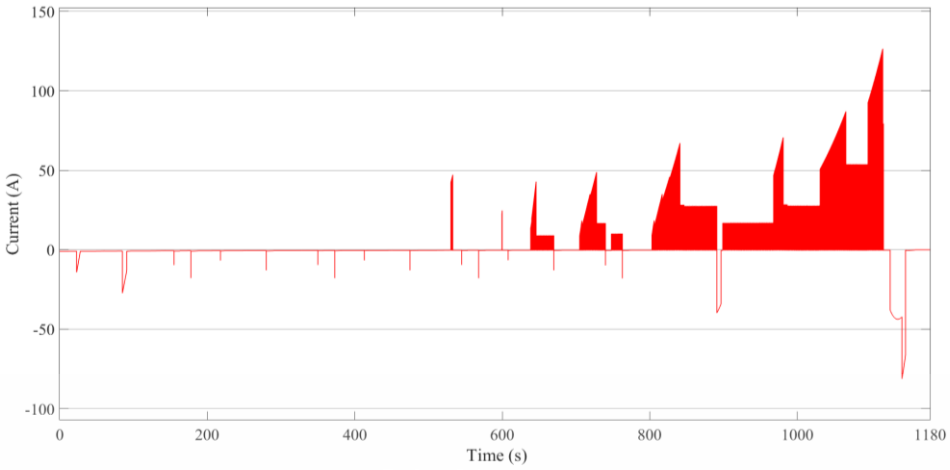

Figure 4.32 Supercapacitor current at 600Hz frequency.

4.2.4 Pulse discharging at 800Hz switching frequency

Simulation of hybrid energy storage system deployed pulse current method is tested at 800Hz switching frequency. The voltage, current and SOC of batteries changed during the test with is shown in Figure 4.33-Figure 4.35. The voltage, current and SOC of supercapacitor changed during the test with is shown in Figure 4.36-Figure 4.38. Comparison of total power from batteries and supercapacitors and power demand from electric vehicle is shown in Figure 4.39.

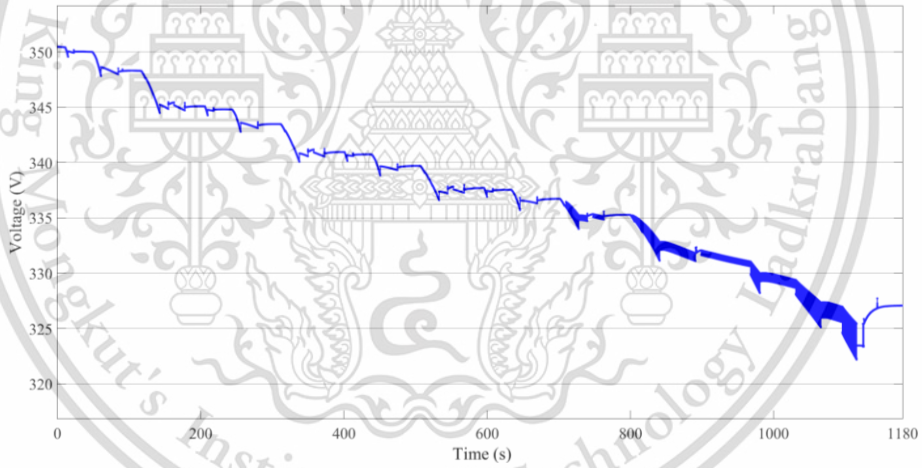

Figure 4.33 Battery voltage at 800Hz frequency.

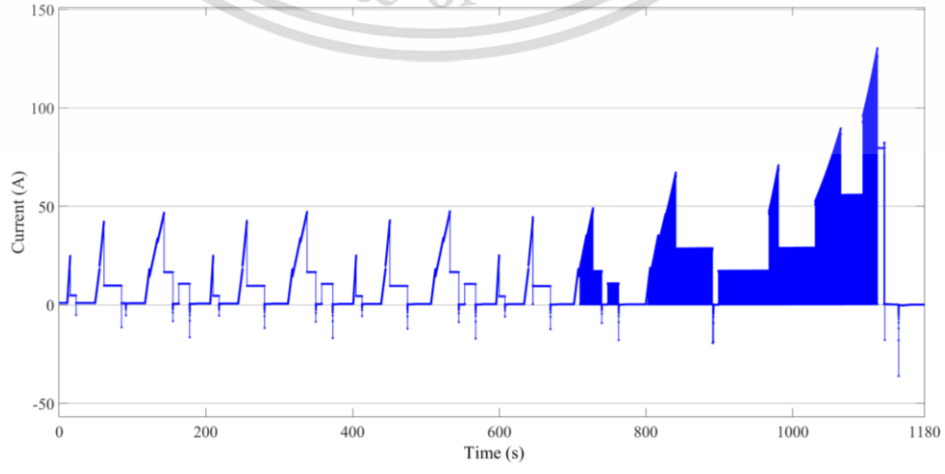

Figure 4.34 Battery current at 800Hz frequency.

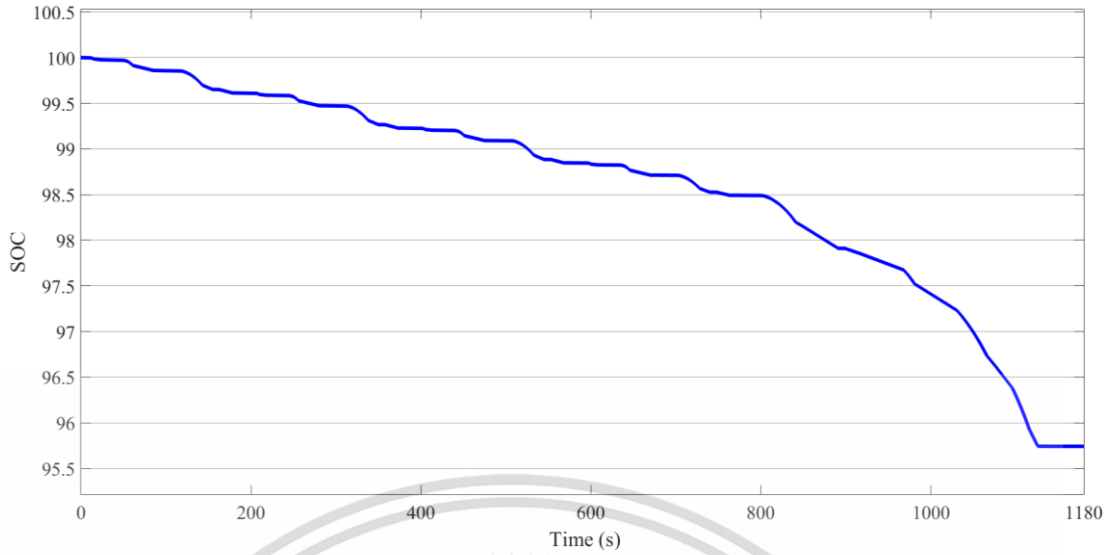

Figure 4.35 Battery SOC at 800Hz frequency

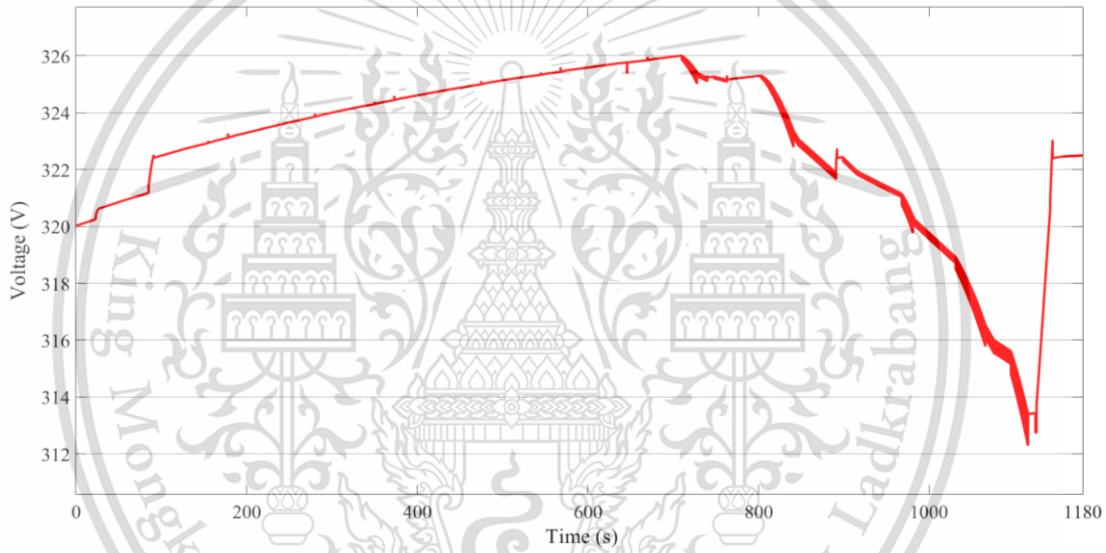

Figure 4.36 Supercapacitor voltage at 800Hz frequency

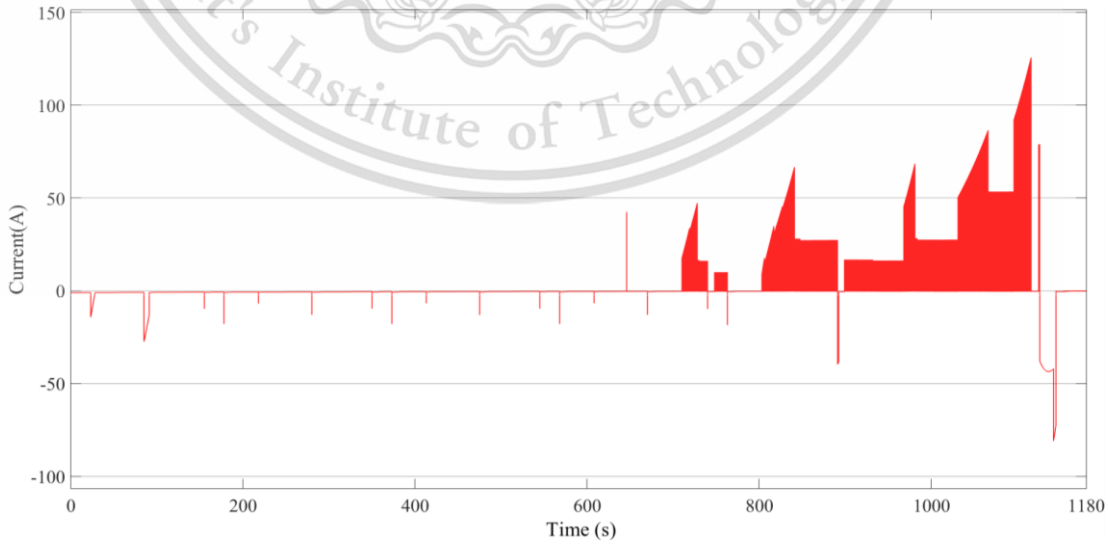

Figure 4.37 Supercapacitor current at 800Hz frequency

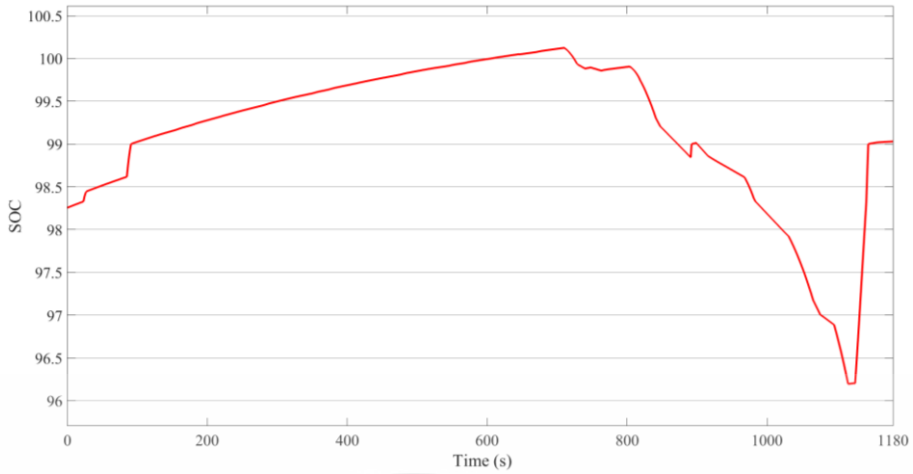

Figure 4.38 Supercapacitor SOC at 800Hz frequency.

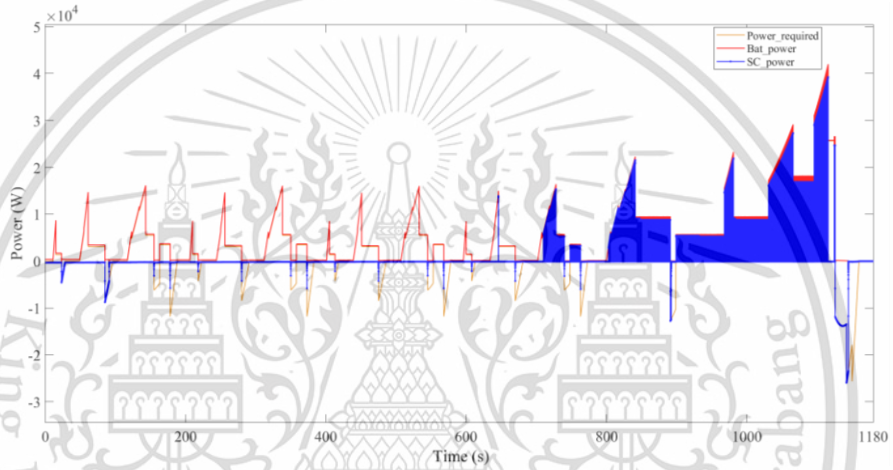

Figure 4.39 Comparison of total power and power demand at 800Hz frequency.

4.2.5 Pulse discharging at 1000Hz switching frequency

Simulation of applying pulse discharging method in HESS of electric vehicle model is tested at 100Hz switching frequency. The characteristics of batteries varied during the test is shown in Figure 4.40-Figure 4.41. The characteristics of voltage, current and SOC of battery varied during the test is shown in Figure 4.42-Figure 4.43.

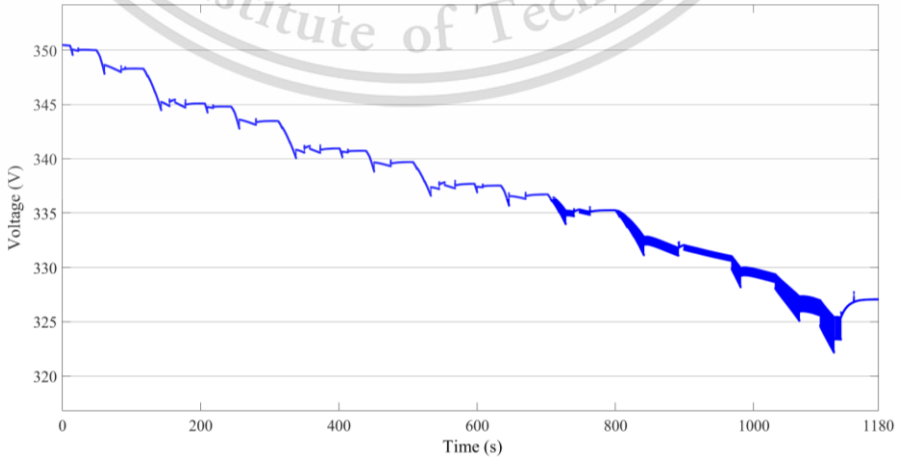

Figure 4.40 Battery voltage at 1000Hz frequency.

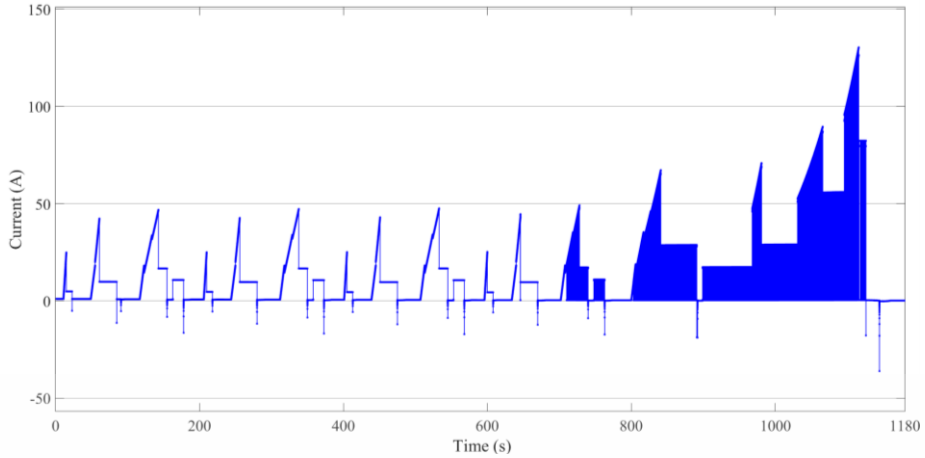

Figure 4.41 Battery current at 1000Hz frequency.

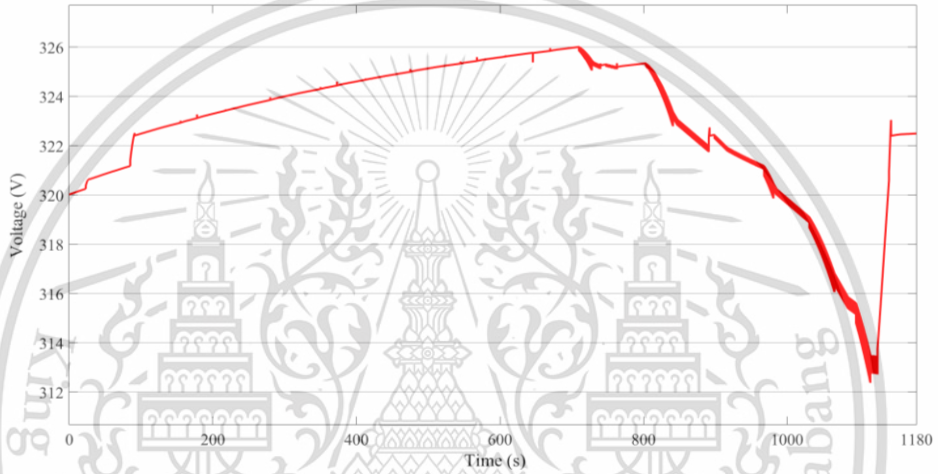

Figure 4.42 Supercapacitor voltage at 1000Hz frequency.

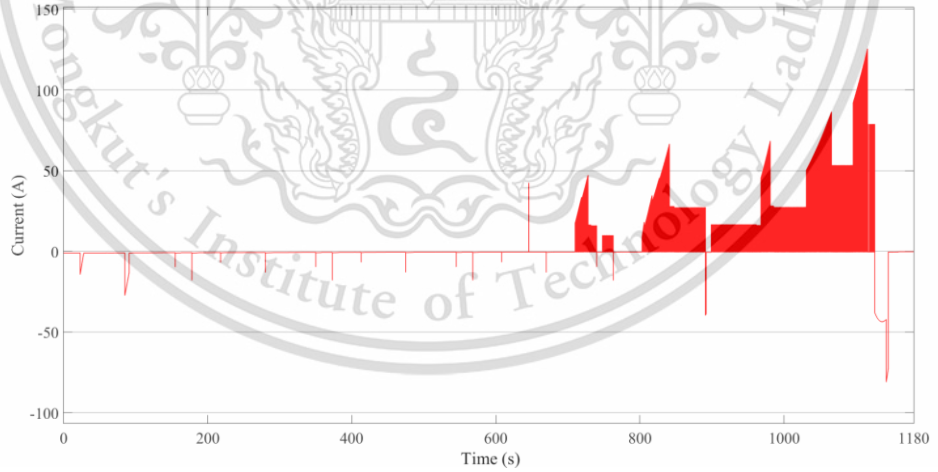

Figure 4.43 Supercapacitor current at 1000Hz frequency.

4.2.6 Comparison of characteristics of HESS at different switching frequencies

According to Figure 4.44, when the output power of HESS generated during pulse discharging is compared at different frequencies, the results show that high switching frequencies develop losses in some areas of battery power. It is observed that lower switching frequencies facilitate achieving higher power from battery power. Also, for supercapacitor power, high switching frequencies develop some losses in supercapacitors power.

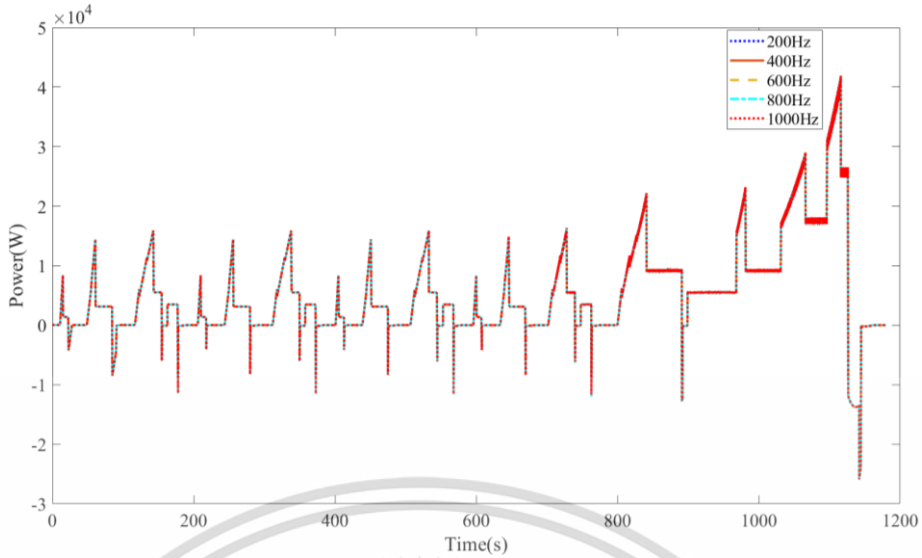

Figure 4.44 Comparison of total output power from HESS at different frequencies.

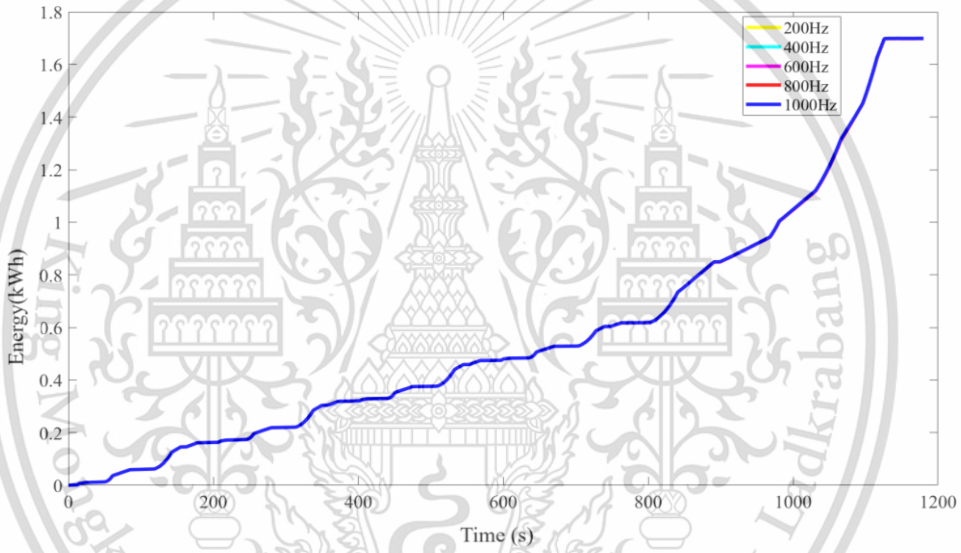

Figure 4.45 Comparison of total energy from hybrid energy storage system at different frequencies.

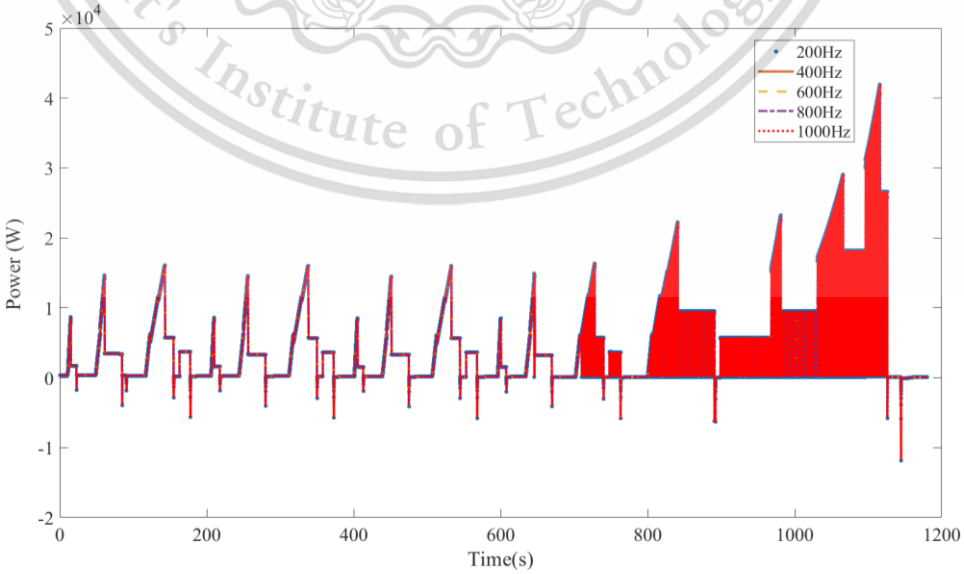

Figure 4.46 Comparison of batteries power at different frequencies.

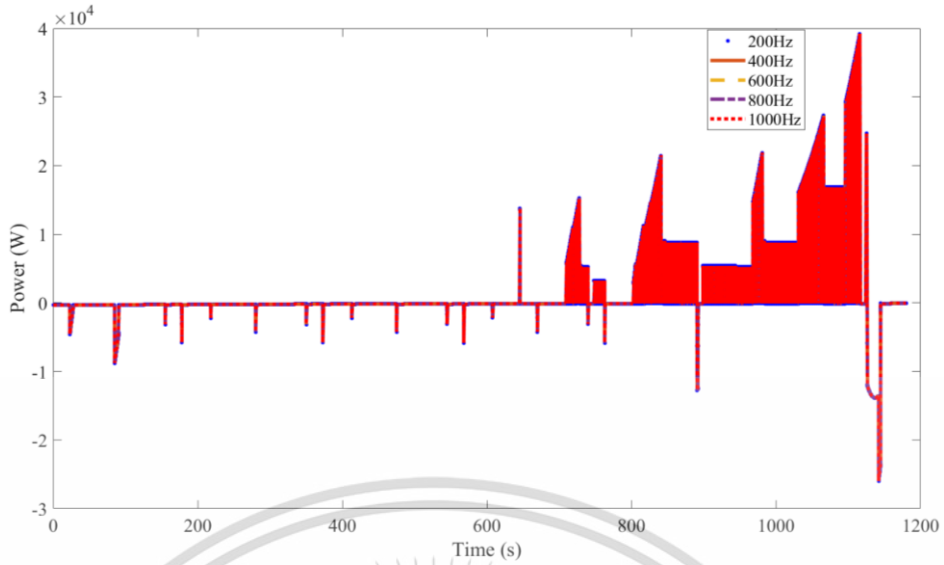

Figure 4.47 Comparison of supercapacitors power at different frequencies.

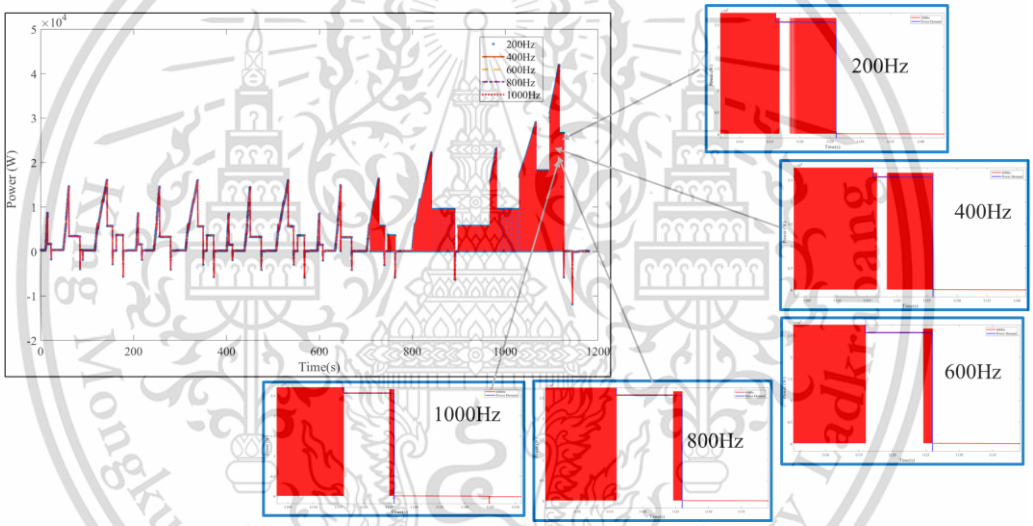

Figure 4.48 Battery power losses variation in different switching frequencies.

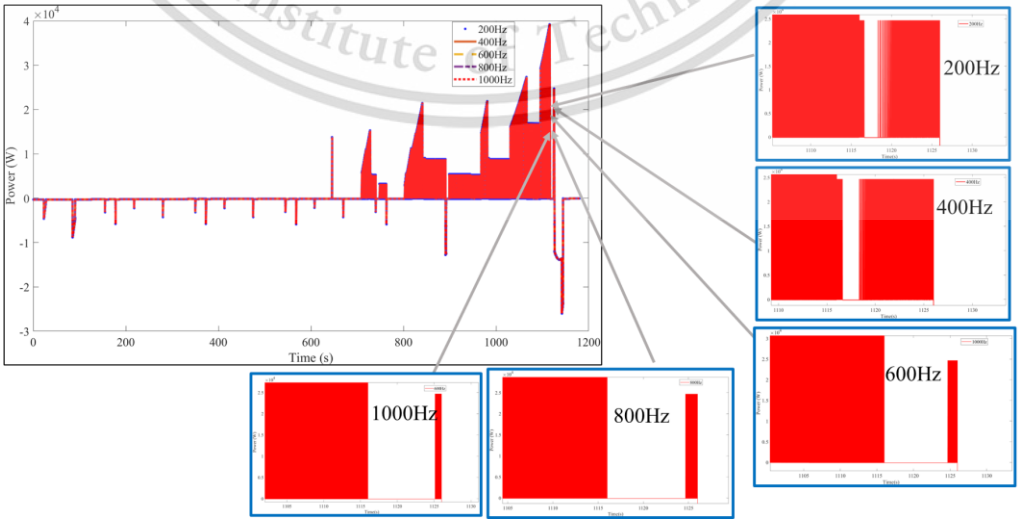

Figure 4.49 Battery power losses variation in different switching frequencies.

High switching frequencies in a hybrid energy storage system result in increased losses in both the supercapacitors and batteries power. Optimizing switching frequencies is crucial to minimize these losses and enhance the performance of the hybrid energy storage system.

4.3 Simulation results of HESS with pulse discharging method in WLTC drive cycle

The simulation was carried out on WLTC drive cycle to test the control strategy of pulse discharging in HESS. Simulation results and comparisons of HESS outputs between various switching frequencies for WLTC driving cycle are shown in this section. The switching frequencies of the HESS are changed and tested at various frequencies at 200Hz, 400Hz, 6000Hz, 800Hz and 1000Hz. The variation of characteristics of battery and supercapacitor is compared at different frequencies.

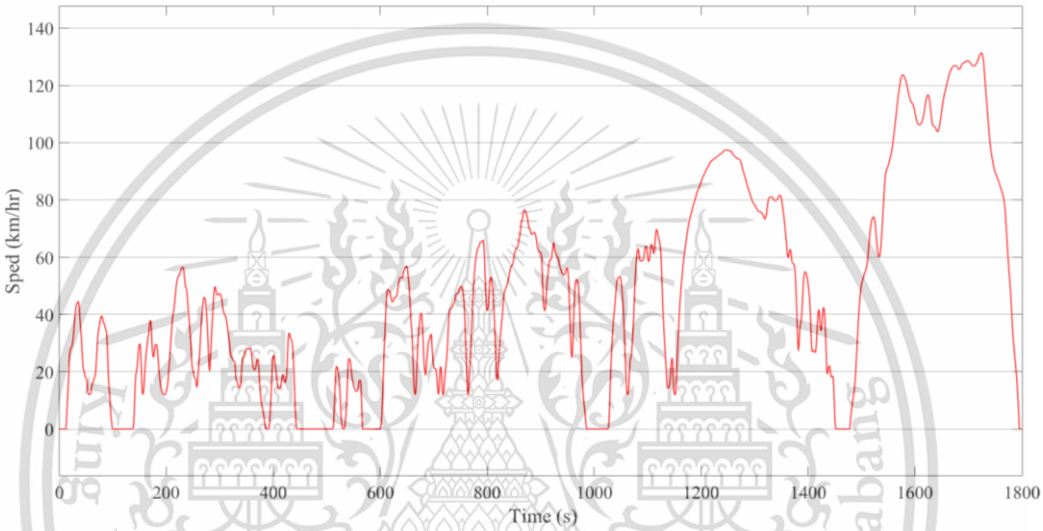

Figure 4.50 WLTC driving cycle profile.

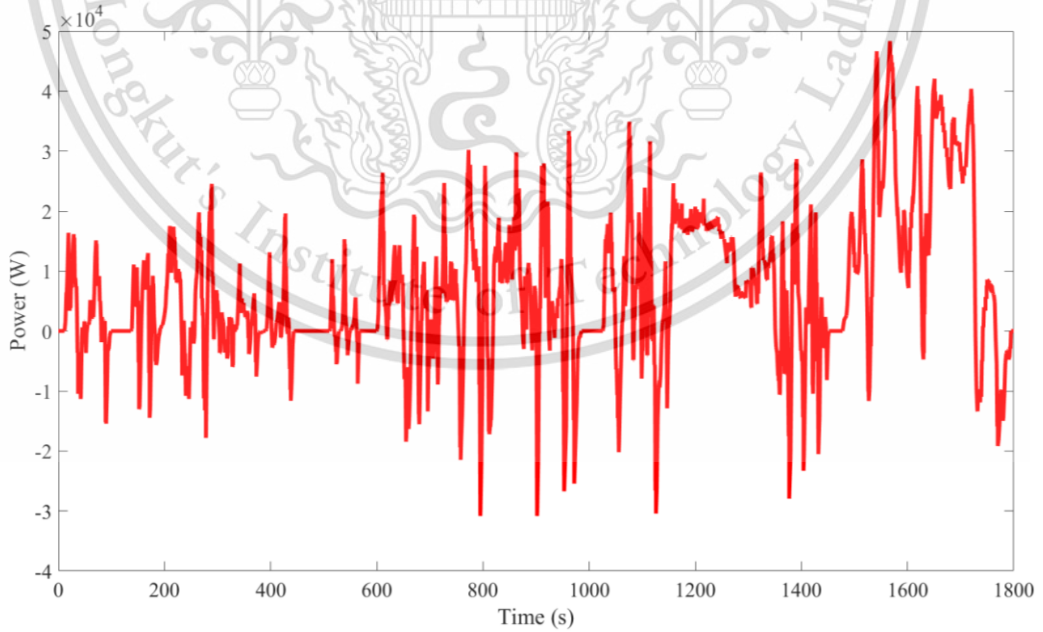

Figure 4.51 Power demand of electric vehicle.

4.3.1 Pulse discharging at 200Hz switching frequency

The test of simulation is performed at 200Hz switching frequency with WLTC driving cycle in Simulink. The battery voltage, current and SOC data are presented in Figure 4.52-Figure 4.53. The voltage, current and SOC of supercapacitor is shown in Figure 4.54-Figure 4.55 Figure 4.19.

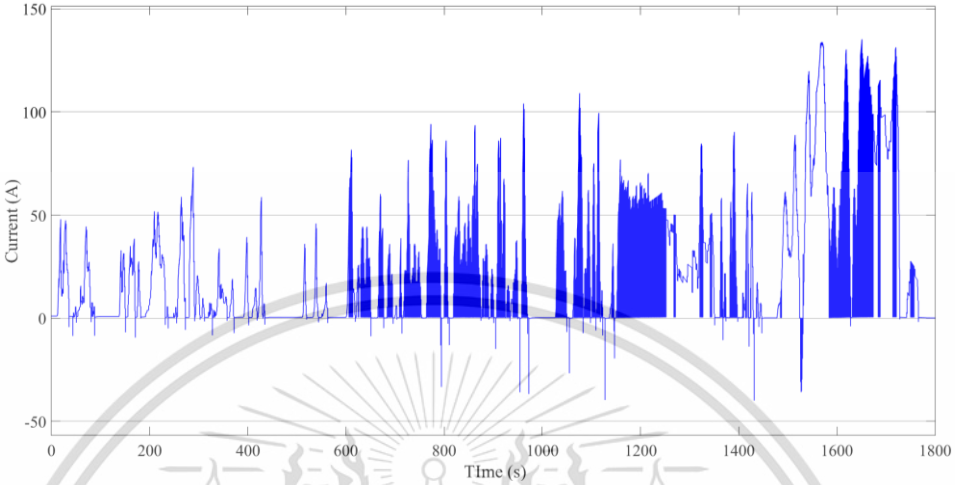

Figure 4.52 Battery current at 200Hz frequency.

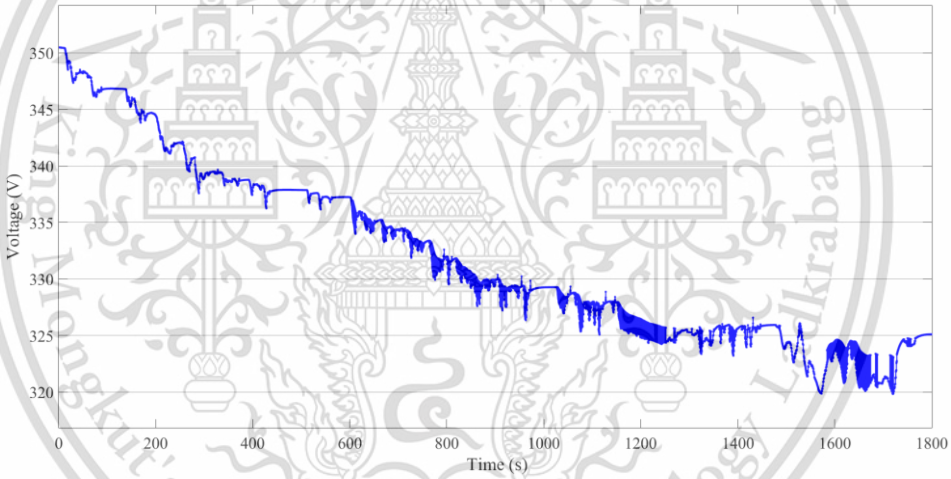

Figure 4.53 Battery voltage at 200Hz frequency.

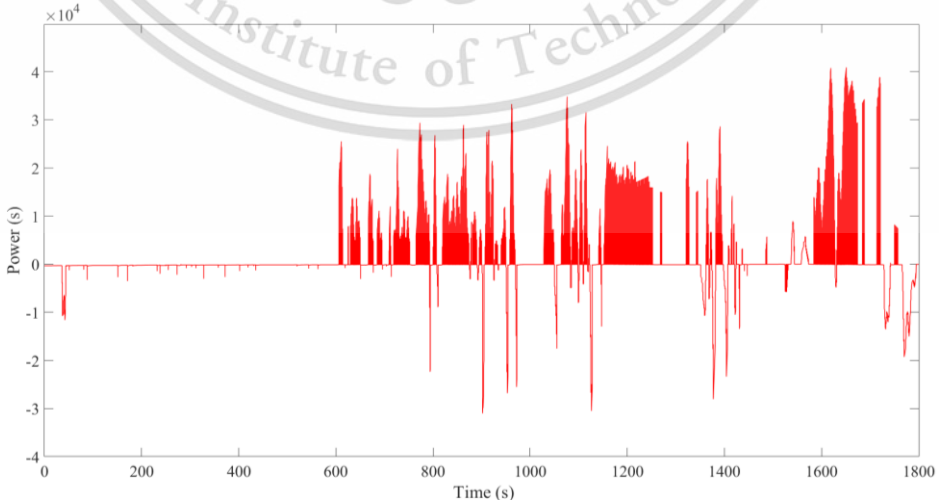

Figure 4.54 Supercapacitor current at 200Hz frequency.

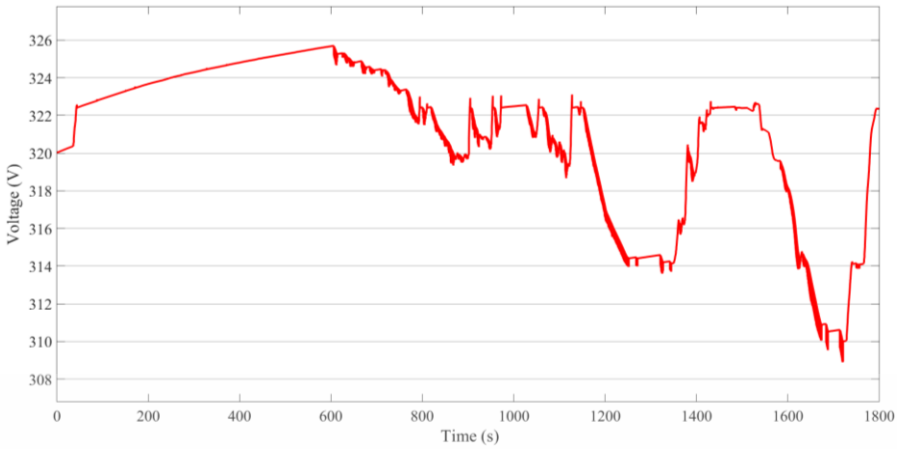

Figure 4.55 Supercapacitor voltage at 200Hz frequency.

4.3.2 Pulse discharging at 400Hz switching frequency

Another simulation of changing the switching frequency of switches is performed and tested with WLTC driving cycle. The power demand from EV and the output power from battery and supercapacitor is compared in Figure 4.56 and the current characteristics of batteries and supercapacitors changed during the test in shown in Figure 4.58 and Figure 4.59.

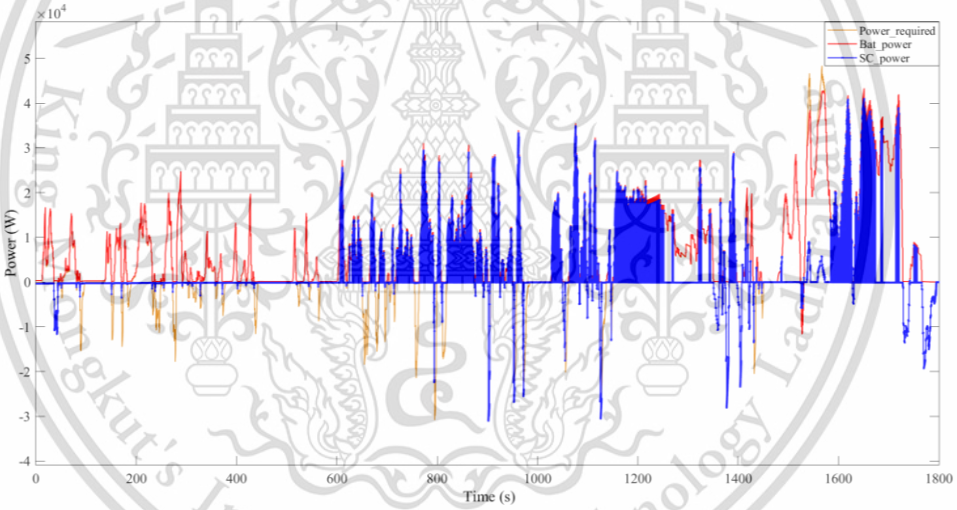

Figure 4.56 Comparing power demand and power from HESS.

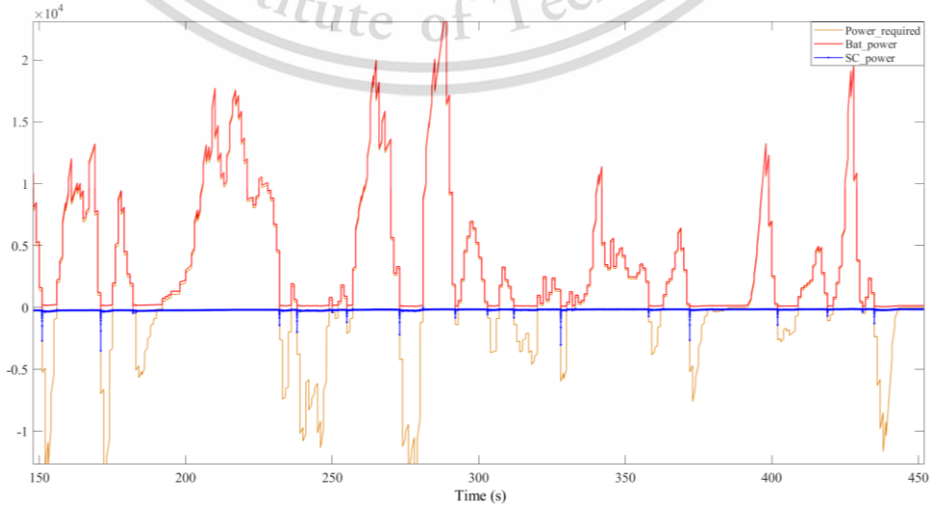

Figure 4.57 Comparing power demand and power from HESS.

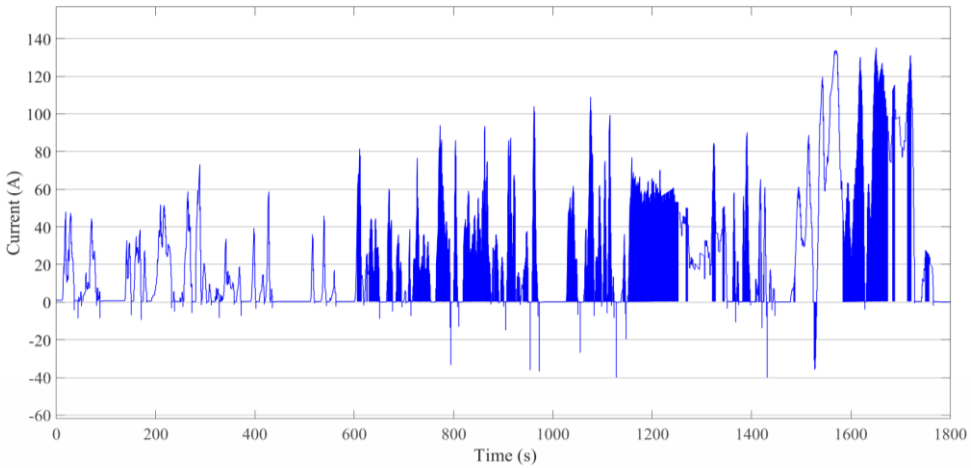

Figure 4.58 Battery current at 400Hz frequency.

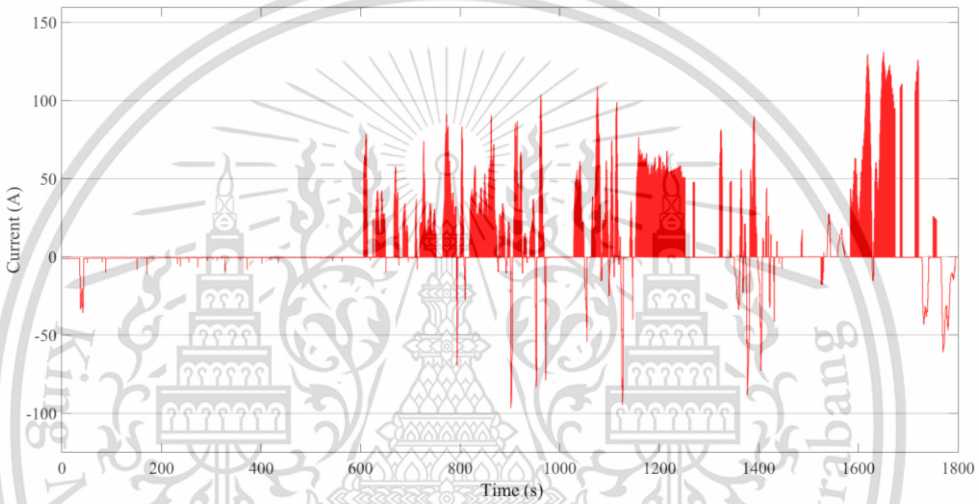

Figure 4.59 Supercapacitor current at 400Hz frequency.

4.3.3 Pulse discharging at 600Hz switching frequency

Another simulation of changing the switching frequency of switches at 600Hz is performed and tested with WLTC driving cycle. The current characteristics of batteries and supercapacitors changed during the test in shown in Figure 4.60-Figure 4.61.

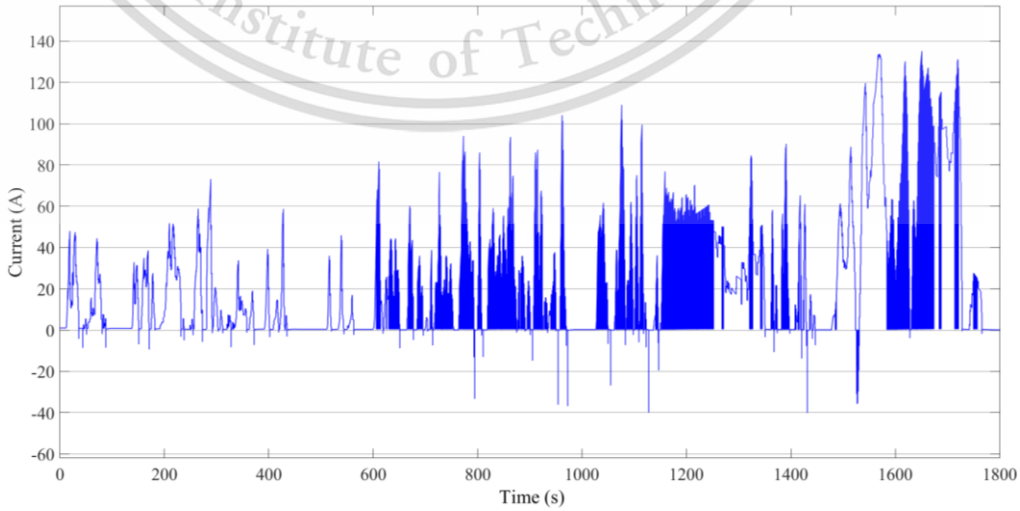

Figure 4.60 Batteries current at 600Hz frequency.

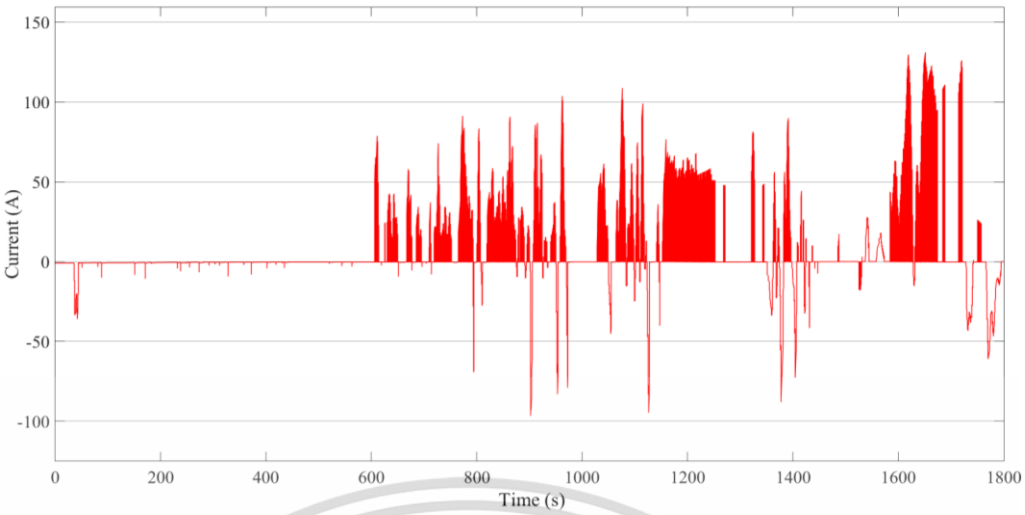

Figure 4.61 Supercapacitors current at 600Hz frequency.

4.3.4 Pulse discharging at 800Hz switching frequency

Another simulation of changing the switching frequency of switches at 800Hz is performed and tested with WLTC driving cycle. The voltage characteristics of batteries and supercapacitors changed during the test in shown in Figure 4.62-Figure 4.63.

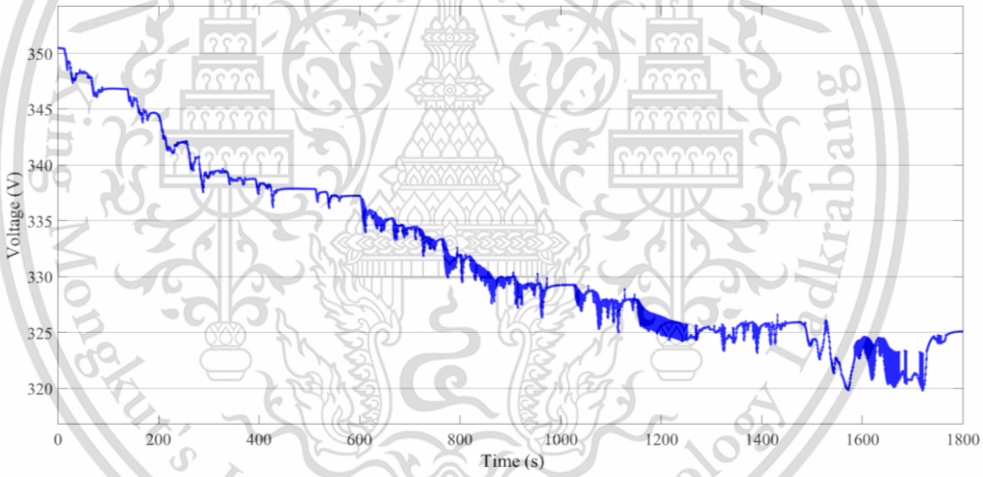

Figure 4.62 Battery voltage at 800Hz frequency.

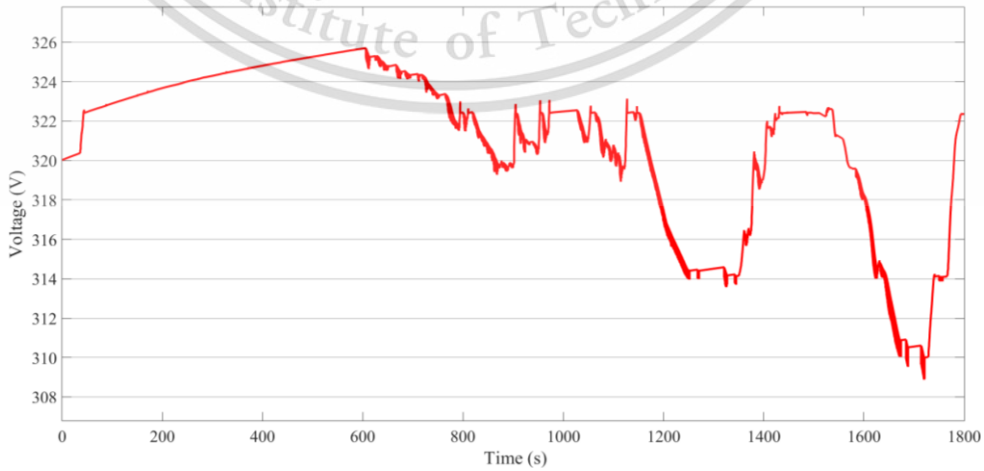

Figure 4.63 Supercapacitor voltage at 800Hz frequency.

4.3.5 Pulse discharging at 1000Hz switching frequency

Another simulation of changing the switching frequency of switches at 1000Hz is performed and tested with WLTC driving cycle. The voltage characteristics of batteries and supercapacitors changed during the test in shown in Figure 4.64-Figure 4.65.

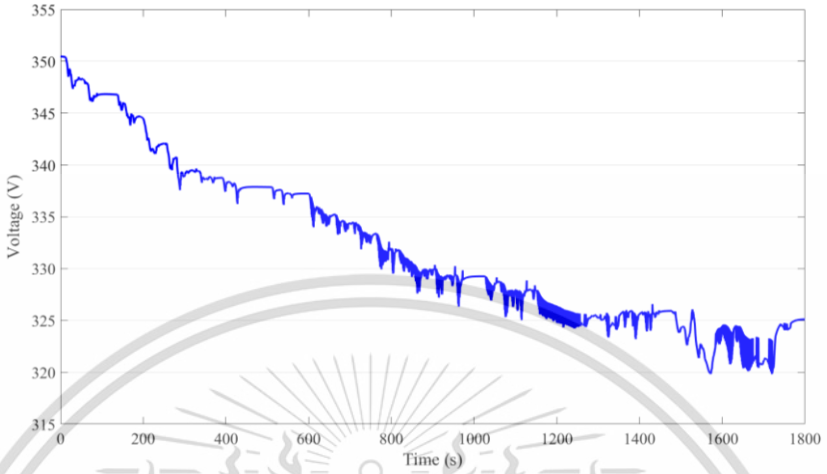

Figure 4.64 Batteries voltage at 1000Hz frequency.

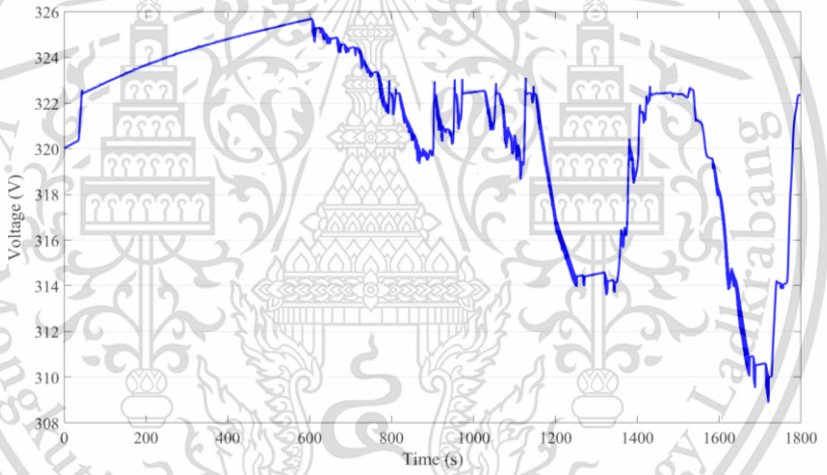

Figure 4.65 Supercapacitors voltage at 1000Hz frequency.

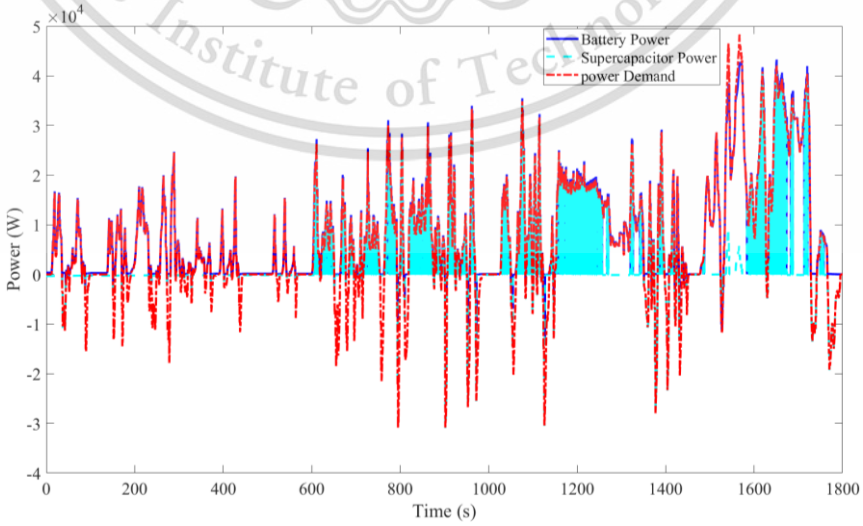

Figure 4.66 Comparison of power demand and power from batteries and supercapacitors.

4.3.6 Comparison of characteristics of HESS at different switching frequencies

According to the results when compared battery power, supercapacitors power and output power of HESS, it can be seen that high switching frequencies develop losses in some areas of batteries power and supercapacitor power. Although HESS could generate the required power by the load, it is observed that lower switching frequencies facilitate achieving higher power from both batteries and supercapacitors. Battery and supercapacitor produced the output power required by the vehicle and in the presence of switching losses, HESS demonstrates its proficiency in generating the required power demand by the load. It can be seen that by applying pulse discharging method, HESS generated output power required by the load.

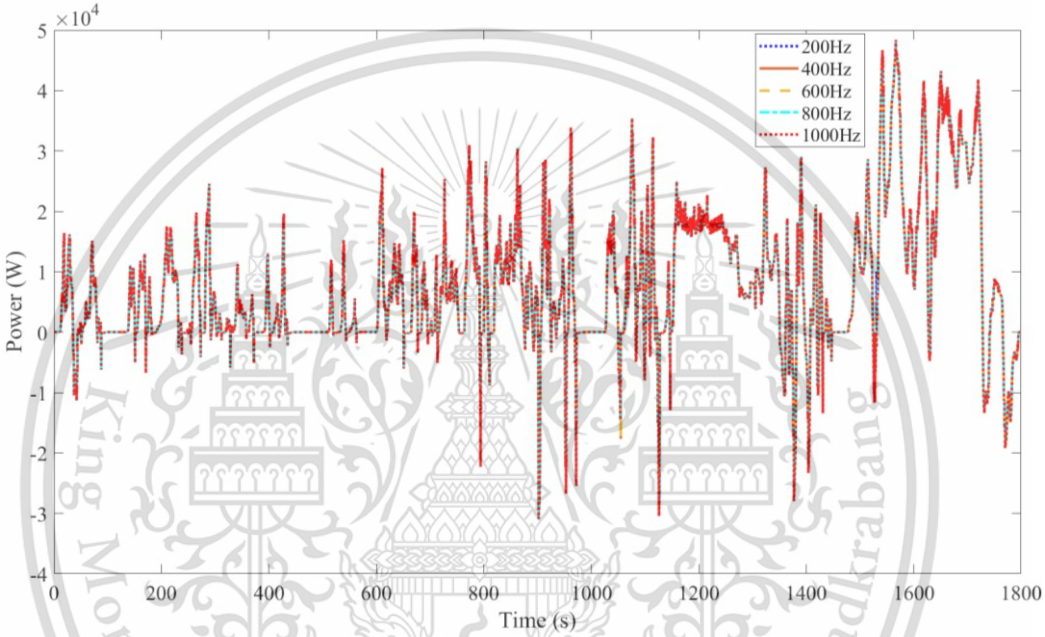

Figure 4.67 Comparison of total output power from HESS at different frequencies.

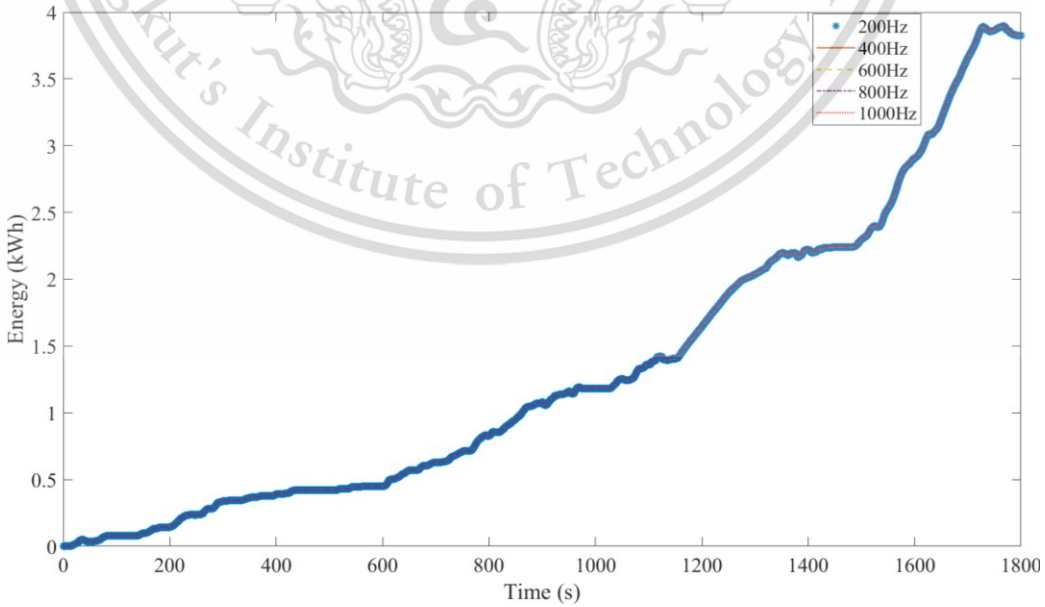

Figure 4.68 Comparison of total output energy from HESS at different frequencies.

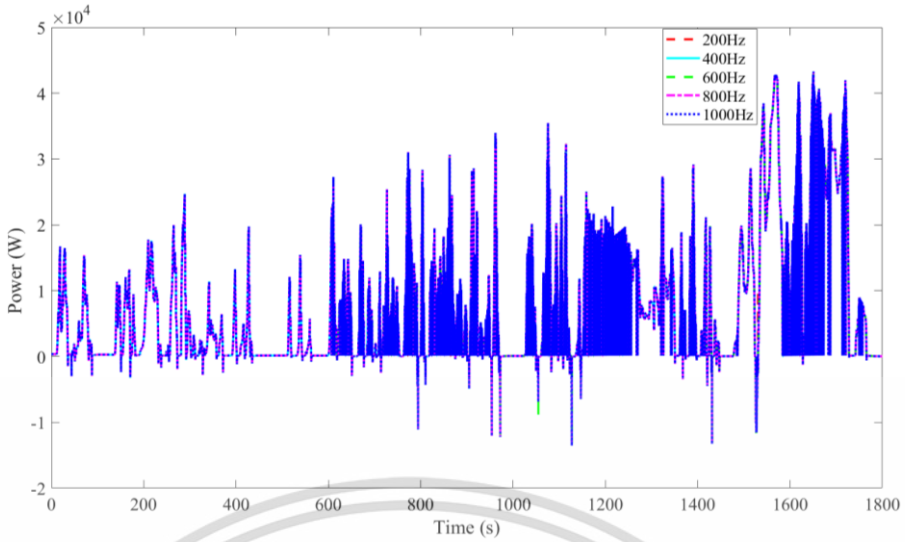

Figure 4.69 Comparison of battery power at different frequencies.

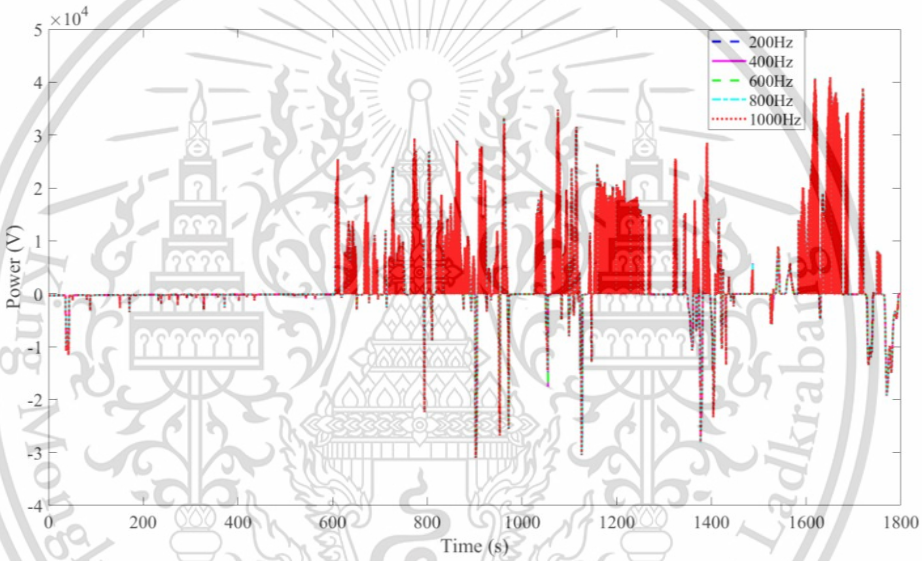

Figure 4.70 Comparison of supercapacitor power at different frequencies.

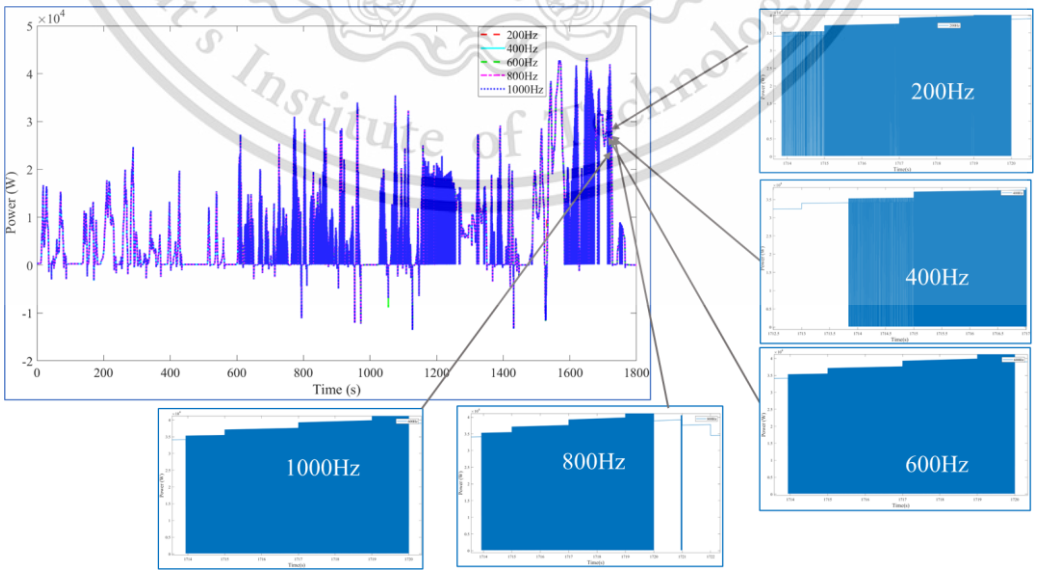

Figure 4.71 Battery power losses variation in different switching frequencies.

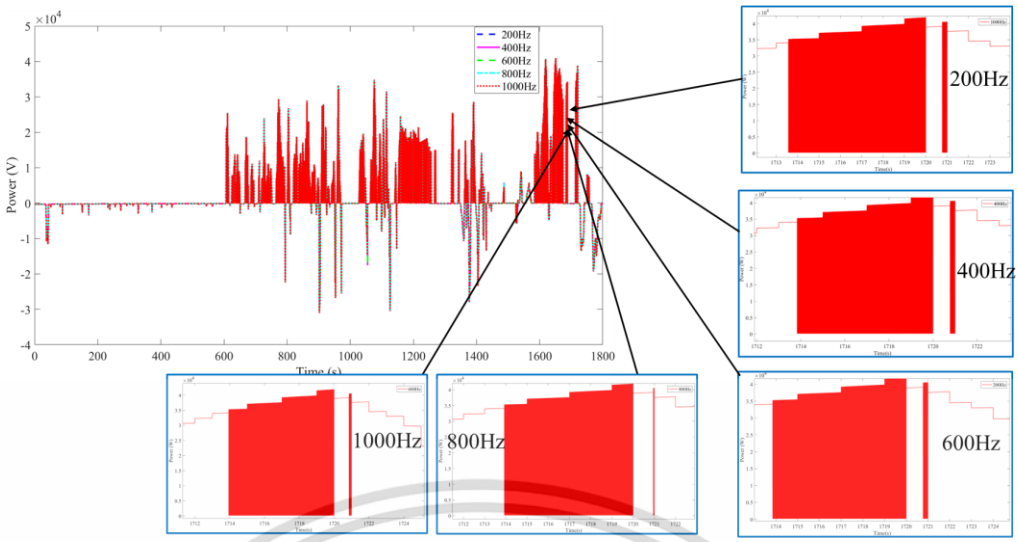

Figure 4.72 Supercapacitor power losses variation in different switching frequencies.

High switching frequencies in a hybrid energy storage system result in increased losses in both the supercapacitors and batteries power. That means using hybrid energy storage system at lower switching frequencies results in good performance and less losses. Optimizing switching frequencies is crucial to minimize these losses and enhance the performance of the hybrid energy storage system.

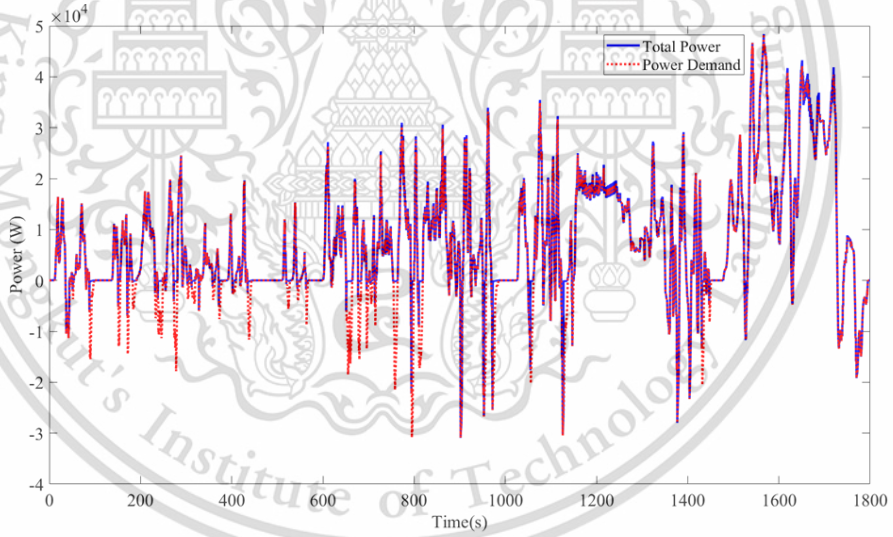

Figure 4.73 Power comparison of total power from HESS and power demand at 600Hz.

According to the results at different switching frequencies, HESS generated output power required by the load by applying pulse discharging method although there is switching losses. In the presence of switching losses, HESS demonstrates its proficiency in generating the required power demand by the load. It was observed that operating Hybrid Energy Storage System with pulse current power sharing method at low switching frequency generated higher output power than at high switching frequencies. Through the results, advantages of the usage of supercapacitors in hybrid energy storage rather than for using only batteries can be seen. Supercapacitors can deliver and absorb energy at a much higher rate than batteries. By handling high power demands and rapid cycling, supercapacitors can reduce the stress on batteries. Moreover, supercapacitors

can efficiently capture and release energy even in short bursts, optimizing the overall energy management of the system.

Chapter 5 Conclusions and future works

In this thesis, two studies were performed. Mainly, for pulse current method in experiments, the performance of the Lithium-ion batteries was analyzed by applying pulse discharging method at different frequencies ranging from 200Hz to 1000Hz. To explore the effects of pulse discharging at various frequencies, constant current discharging is performed and compared the results with pulse discharging. In terms of discharging time, Pulse current discharging generated longer discharging time than constant current discharging. The discharging time at low switching frequency generated longer duration than at high switching frequency. In terms of discharge capacity, pulse current discharging produced higher discharge capacity than constant current discharging. It was observed that lower switching frequencies facilitate achieving higher discharge capacity due to the recovery of energy during rest time of pulse discharging method. In terms of discharge energy, pulse current discharging method produced higher discharge capacity than constant current discharging.

For pulse current method in hybrid energy storage system, high switching frequencies developed losses in some areas of battery power. It was observed that lower switching frequencies facilitate achieving higher power from battery power. The Hybrid Energy Storage System demonstrated the capability to generate power in accordance with the dynamic power demands by the load. Applying the pulse current power-sharing method enables the achievement of required power. It was observed that operating Hybrid Energy Storage System with pulse current power sharing method at low switching frequency generated higher output power than at high switching frequencies.

As for the future works, this development of simulation model can be considered and further developed for discharging two batteries pack with high different voltages in electric vehicles.

REFERENCES

[1] Dr. A. S. Et.al, "Electric Vehicle Battery Modelling and Simulation Using MATLAB-Simulink," *Turkish Journal of Computer and Mathematics Education (TURCOMAT)*, vol. 12, no. 3, 2021.

[2] B. V. K. Raja, I. Raja, and R. Kavvampally, "Advancements in Battery Technologies of Electric Vehicle," in *Journal of Physics: Conference Series*, 2021, vol. 2129, no. 1.

[3] M. Elmahallawy, T. Elfouly, A. Alouani, and A. M. Massoud, "A Comprehensive Review of Lithium-Ion Batteries Modeling, and State of Health and Remaining Useful Lifetime Prediction," *IEEE Access*, vol. 10, 2022.

[4] Z. Cabrane, D. Batool, J. Kim, and K. Yoo, "Design and simulation studies of battery-supercapacitor hybrid energy storage system for improved performances of traction system of solar vehicle," *J Energy Storage*, vol. 32, 2020.

[5] I. Azizi and H. Radjeai, "A new strategy for battery and supercapacitor energy management for an urban electric vehicle," *Electrical Engineering*, vol. 100, no. 2, 2018.

[6] M. E. Şahin and F. Blaabjerg, "A hybrid PV-battery/supercapacitor system and a basic active power control proposal in MATLAB/simulink," *Electronics (Switzerland)*, vol. 9, no. 1, 2020.

[7] D. R. Brafianto, W. Wijono, and T. Nurwati, "Energy Management Applications in Battery and Supercapacitor Hybrid Electric Vehicles Using Fuzzy Logic," in *Proceedings - 11th Electrical Power, Electronics, Communications, Control, and Informatics Seminar, EECCIS 2022*, 2022.

[8] D. Lemian and F. Bode, "Battery-Supercapacitor Energy Storage Systems for Electrical Vehicles: A Review," *Energies*, vol. 15, no. 15. 2022.

[9] S. M. Shin, G. J. Jung, W. J. Lee, C. Y. Kang, and J. P. Wang, "Recovery of electrodic powder from spent lithium ion batteries (LIBs)," *Archives of Metallurgy and Materials*, vol. 60, no. 2, 2015.

[10] M. Ghiji *et al.*, "A review of lithium-ion battery fire suppression," *Energies*, vol. 13, no. 19. 2020.

[11] W. Fang, O. J. Kwon, and C. Y. Wang, "Electrochemical-thermal modeling of automotive Li-ion batteries and experimental validation using a three-electrode cell," *Int J Energy Res*, vol. 34, no. 2, 2010.

[12] L. Lam, P. Bauer, and E. Kelder, "A practical circuit-based model for Li-ion battery cells in electric vehicle applications," in *INTELEC, International Telecommunications Energy Conference (Proceedings)*, 2011.

[13] E. Ezemobi, M. Silvagni, A. Mozaffari, A. Tonoli, and A. Khajepour, "State of Health Estimation of Lithium-Ion Batteries in Electric Vehicles under Dynamic Load Conditions," *Energies (Basel)*, vol. 15, no. 3, 2022.

[14] S. Saxena, Y. Xing, D. Kwon, and M. Pecht, "Accelerated degradation model for C-rate loading of lithium-ion batteries," *International Journal of Electrical Power and Energy Systems*, vol. 107, 2019.

[15] R. E. Tudoroiu, M. Zaheeruddin, S. M. Radu, and N. Tudoroiu, "Real-time implementation of an extended kalman filter and a pi observer for state estimation of rechargeable li-ion batteries in hybrid electric vehicle applications—A case study," *Batteries*, vol. 4, no. 2, 2018.

[16] H. Hemi, N. K. M'Sirdi, A. Naamane, and B. Ikken, "Open circuit voltage of a lithium ion battery model adjusted by data fitting," in *Proceedings of 2018 6th International Renewable and Sustainable Energy Conference, IRSEC 2018*, 2018.

[17] S. S. Madani, E. Schaltz, and S. K. Kær, "An electrical equivalent circuit model of a lithium titanate oxide battery," *Batteries*, vol. 5, no. 1, 2019.

[18] G. Saldaña, J. I. S. Martín, I. Zamora, F. J. Asensio, and O. Oñederra, "Analysis of the current electric battery models for electric vehicle simulation," *Energies (Basel)*, vol. 12, no. 14, 2019.

[19] S. Saxena, Y. Xing, D. Kwon, and M. Pecht, "Accelerated degradation model for C-rate loading of lithium-ion batteries," *International Journal of Electrical Power and Energy Systems*, vol. 107, 2019.

[20] K. Liu, K. Li, Q. Peng, and C. Zhang, "A brief review on key technologies in the battery management system of electric vehicles," *Frontiers of Mechanical Engineering*, vol. 14, no. 1. 2019.

[21] M. Auch, T. Kuthada, S. Giese, and A. Wagner, "Influence of Lithium-Ion-Battery Equivalent Circuit Model Parameter Dependencies and Architectures on the Predicted Heat Generation in Real-Life Drive Cycles," *Batteries*, vol. 9, no. 5, 2023.

[22] X. Huang *et al.*, "A review of pulsed current technique for lithium-ion batteries," *Energies*, vol. 13, no. 10. 2020.

[23] J. M. Amanor-Boadu, A. Guiseppi-Elie, and E. Sánchez-Sinencio, "The impact of pulse charging parameters on the life cycle of lithium-ion polymer batteries," *Energies (Basel)*, vol. 11, no. 8, 2018.

[24] L. Guo, P. Hu, and H. Wei, "Development of supercapacitor hybrid electric vehicle," *J Energy Storage*, vol. 65, 2023.

[25] M. Horn, J. MacLeod, M. Liu, J. Webb, and N. Motta, "Supercapacitors: A new source of power for electric cars?," *Econ Anal Policy*, vol. 61, 2019.

[26] S. Satpathy, S. Debbarma, and B. K. Bhattacharyya, "An integration of the review of electrode's materials and a new gamma function-based charging methodology of supercapacitor for high current applications," in *Materials Today: Proceedings*, 2019, vol. 26.

[27] R. Brooke *et al.*, "Large-scale paper supercapacitors on demand," *J Energy Storage*, vol. 50, 2022.

[28] A. Al-Haj Hussein and I. Batarseh, "A review of charging algorithms for nickel and lithium battery chargers," *IEEE Trans Veh Technol*, vol. 60, no. 3, 2011.

[29] I. Miri, A. Fotouhi, and N. Ewin, "Electric vehicle energy consumption modelling and estimation—A case study," *Int J Energy Res*, vol. 45, no. 1, 2021.

[30] F. Adegbohun, A. von Jouanne, B. Phillips, E. Agamloh, and A. Yokochi, "High performance electric vehicle powertrain modeling, simulation and validation," *Energies (Basel)*, vol. 14, no. 5, 2021.

[31] M. R. M. Hassan, M. A. Mossa, and G. M. Dousoky, "Evaluation of electric dynamic performance of an electric vehicle system using different control techniques," *Electronics (Switzerland)*, vol. 10, no. 21, 2021.

[32] D. Mcdonald, "Electric Vehicle Drive Simulation with MATLAB / Simulink," *Proceedings of the 2012 North-Central Section Conference*, 2012.

[33] T. V. Sarathkumar, M. Poornanand, and A. K. Goswami, "Modelling and simulation of electric vehicle drive through SAEJ227 EUDC cycles," in *2020 IEEE Students' Conference on Engineering and Systems, SCES 2020*, 2020.

[34] C. Sunanda, "Modeling and Performance Analysis of an Electric Vehicle with MATLAB/Simulink," *International Research Journal of Engineering and Technology*, 2008.

[35] S. Chauhan, "Motor Torque Calculations For Electric Vehicle," *INTERNATIONAL JOURNAL OF SCIENTIFIC & TECHNOLOGY RESEARCH*, vol. 4, 2015.

[36] B. Duangsrikaew, J. Mongkoltanatas, C. N. Benyajati, P. Karin, and K. Hanamura, "Battery sizing for electric vehicles based on real driving patterns in Thailand," *World Electric Vehicle Journal*, vol. 10, no. 2, 2019.

[37] V. Kubendran, Y. Mohamed Shuaib, and J. Preetha Roselyn, "Modelling of Vehicle Dynamics and Determination of Energy Demand for Electric Vehicle," in *Journal of Physics: Conference Series*, 2022, vol. 2335, no. 1.

[38] T. Barlow, S. Latham, I. Mccrae, and P. Boulter, "A reference book of driving cycles for use in the measurement of road vehicle emissions," *TRL Published Project Report*, 2009.

[39] Y. Xing, C. Lv, and D. Cao, "Longitudinal Driver Intention Inference," in *Advanced Driver Intention Inference*, 2020.

[40] S. Micari *et al.*, "Effect of WLTP CLASS 3B Driving Cycle on Lithium-Ion Battery for Electric Vehicles," *Energies (Basel)*, vol. 15, no. 18, 2022.

[41] J. Lasocki, "The WLTC vs NEDC: A Case Study on the Impacts of Driving Cycle on Engine Performance and Fuel Consumption," *International Journal of Automotive and Mechanical Engineering*, vol. 18, no. 3, 2021.

[42] K. Sayed, S. Abdel-Khalek, H. M. H. Zakaly, and M. Aref, "Energy Management and Control in Multiple Storage Energy Units (Battery–Supercapacitor) of Fuel Cell Electric Vehicles," *Materials*, vol. 15, no. 24, 2022.

[43] Q. Zhang, W. Deng, S. Zhang, and J. Wu, “A Rule Based Energy Management System of Experimental Battery/Supercapacitor Hybrid Energy Storage System for Electric Vehicles,” *Journal of Control Science and Engineering*, vol. 2016, 2016.

[44] O. Rahman, D. A. Robinson, S. Elphick, and S. Perera, “Power Sharing and Energy Management between Supercapacitor and Battery in a Hybrid Energy System for EVs,” in *Proceedings of 2021 31st Australasian Universities Power Engineering Conference, AUPEC 2021*, 2021.